From the classical analysis of the center of pressure signals to a novel approach: study of rotational components.

Emma Chiaramello

Dipartimento di elettronica e telecomunicazioni

Politecnico di Torino

A thesis submitted for the degree of

PhilosophiæDoctor (PhD) in Biomedical Engineering
XXV Cycle

2013 February

Abstract

The balance control is known to be a complex motor skill, which involves the integration of many types of sensory information. The postural control is achieved by feedback mechanisms based on the body-sway motion detected primarily by visual, vestibular, and proprioceptive sensory systems. Static posturography provides an objective assessment of postural control by characterizing the body sway during upright standing. The Center-of-Pressure (CoP) signal is recorded by a force platform and analyzed according to different techniques. Traditional approaches decompose the CoP signal into antero-posterior (AP) and medio-lateral (ML) time series and extrapolate geometrical, statistical and spectral parameters.

In this dissertation the problem of analyzing CoP signals was faced with two different strategies.

Firstly, I applied geometrical parameters to describe the CoP signals and a multivariate statistical approach to analyze differences in quiet standing between groups of pathological and healthy subjects, in two different studies. A new acquisition protocol was proposed, which adds to frontal open- and closed-eye conditions, conditions in which quiet standing of the subject is evaluated after a fast or a slow head rotation, on the left or on the right side, both with eyes open and closed.

The aim of the first work (accepted to be published in Human Movement Science) was to analyze the postural control of volleyball players and the impact that vision has on it. The main hypothesis of this study was that, since volleyball players use the visual system differently from untrained subjects, the role of vision on postural control should also be different. Volleyball players showed greater CoP ellipses with respect to controls. A multivariate approach to data analysis demonstrated that the two groups

were different when the subjects kept their eyes open, but they were not with visual deprivation. The influence of the athletes expertise and team role on balance performances was also analyzed. Differences in the upright stance of national and regional athletes were found, as well as differences between defensive players and hitters.

The second work (published in Gait & Posture) evaluated differences in postural performances in controls and patients with residual neuro-ophthalmic deficits after a traumatic brain injury. It was possible to evidence significant balance abnormalities in TBI patients with respect to controls. Moreover, by means of a multivariate analysis, I was able to discriminate different levels of residual neuro-ophthalmic impairment.

The second approach was based on the hypothesis that CoP signal contains rotational components. To verify this hypothesis and to extract rotational components from the CoP signal, the rotary spectra analysis - a well known technique developed in the meteorological and oceanographic field in the 70s - was applied. Rotary spectra analysis involves the representation of a two-dimensional signal in the complex plane as a superimposition of ellipses, which can be analyzed in terms of their shape and orientation. Each ellipse is the sum of a counterclockwise (CCW) and a clockwise (CW) rotating phasors, called rotary components. This approach allows to consider both the AP and ML time-series not only as mono-variate signals, but also as components of a complex signal, taking into account both the amplitude of the whole signal, and its phase. The rotary spectra approach permits to separate rotational isofrequential components from non-rotational ones, providing a different approach in understanding of the physiological mechanisms underlying postural control.

The rotary spectra analysis was applied to the CoP signal of a population of healthy subjects. The presence of rotational components in the signal was demonstrated, and useful parameters about the rotational characteristics of the body sway were extracted. An interesting result highlighted by this new approach was that the mode value of the rotary spectra fell in the range 0.14-0.17 rps. The peak that was observed in this frequency

range probably has a physiologically explainable meaning that was never documented before. I hypothesized that rotary spectra peaks obtained in the study of postural control during upright standing are strictly correlated to the bursts of muscle sympathetic nerve activity. This work passed the first stage of review to be published in Motor Control.

Since the CoP signal is not strictly stationary, considering the classical rotary spectra analysis it is possible only to obtain frequency marginals of the signal during the 60s test. To analyze the CoP trajectories as non-stationary random signals, the classical rotary spectra theory was extended to deal with non-stationary signals. In particular, I applied both bilinear Cohen's class Choi-Williams time-frequency distribution and wavelet method to obtain time-frequency analysis of rotating components. This allowed evaluating rotational characteristics of the CoP signal in the time-frequency plane.

As interpretation and classification of a large number of time-frequency distributions could be difficult, time expensive, and highly depending on the researcher, I developed an automatic analysis method. It consists of three main steps: (i) using image processing tools, the main frequency components were identified on the time-frequency plane; (ii) a set of features was extracted; (iii) a clustering algorithm was applied. Applying this method to the distributions calculated by the time-frequency rotary analysis of the CoP signals of a population of healthy subjects, I obtained a fast and repeatable description of each distribution in terms of frequency components. Moreover, a classification in five groups of the distribution was obtained.

In conclusion, both the two followed strategies gave satisfactory results. The proposed protocol and the evaluation of geometrical parameters allowed highlighting differences between groups of pathological and healthy subjects. I proposed a new approach in analyzing CoP signal in terms of rotational components, which gave interesting results on a group of healthy subjects. The technique was extended to time-frequency domain and an automatic analysis method of time-frequency distribution was developed.

To my father

Acknowledgements

I would like to acknowledge Professor Marco Knaflitz, for his patient guidance, encouragement and his precious advices.

My grateful thanks are also extended to Dr. Agostini, Professor Balestra and Professor Molinari for their advices.

A huge thanks to Kristen, Giangiacomo, Beppe, Samanta, Gianmaria, Issey, and all the Biolab group members for their advices and their friendship.

Contents

List of Figures

LIST OF FIGURES

List of Tables

LIST OF TABLES

1

Introduction

Human upright stance is intrinsically unstable. Even when a subject is asked to stand quietly in upright position, his/her body shows small postural oscillations. A small deviation from a perfect upright position results in a torque due to gravity that accelerates the body further away from the upright position. To maintain the upstanding position the destabilizing torque due to gravity must be counterbalanced by a corrective torque exerted by the feet against the support surface [1]. The resultant of these movements is perceived by the subject as a continuous body oscillation around the perfect upright position.

However, maintaining an equilibrium position is essential in all daily activities [2], and balance impariments could lead to high risk of fall and injuries, expecially in the elderly.

This imposes critical demands on the postural control system.

Balance control is known to be a complex motor skill that involves the integration of many types of sensory information to plan and execute flexible movement patterns to achieve different potential postural goals [2]. Regulation of normal posture and balance is achieved by feedback mechanisms based on the body-sway motion detected primarily by visual, vestibular, and proprioceptive sensory systems. Afferent information - visual, vestibular and proprioceptive - about internally or externally generated postural perturbations, need to be gathered, weighted and centrally integrated, to choose the most appropriate postural response. The complex physiological mechanisms underlying these reactions can only be unraveled under carefully controlled experimental conditions, with calibrated control of the environment, standardized bodily perturbations

and use of quantitative outcome measures.

Balance assessment involves different aspects: first of all it is necessary to hypothesize models of the mechanisms underlying postural control regulation, secondly to develop reliable instruments and protocols to quantify balance performances, and finally it is necessary to have analysis and interpretation tools to cope with experimental evidences. All these three aspects have been extensively described in literature.

In this chapter we will synthetically describe the most important models of the postural control and introduce most used quantitative techniques to assess balance.

1.1 Postural control models

The mechanism underlying spontaneous sway are not fully understood, and controversy remains regarding the organization of sensory and motor system contributing to spontaneous sway [3].

According to Morasso at al. [4], the complexity and uniqueness of postural control is due to the following reasons:

- the mechanic plant (the controlled object) is intinsically unstable;
- the controlled variable (the Center of Mass: CoM) is not directly measurable;
- the available sensory receptors operate quite close to their absolute threshold of sensibility;
- stability critically dependent upon delays in the reafferent signals;
- there is a dynamic coupling with other motor subsystems, which is not relevant so much for accuracy as it is for stability itself.

The starting point for every model of postural control during quiet standing is the biomechanical model described by numerous authors in literature (e.g. [1, 3, 4, 5, 6, 7, 8]) as a linearized inverted pendulum.

Fig. 1.1. shows the biomechanical model of quiet standing in the Antero-Posterior (AP) plane. The motion of the body could be assumed to be determined by two forces:

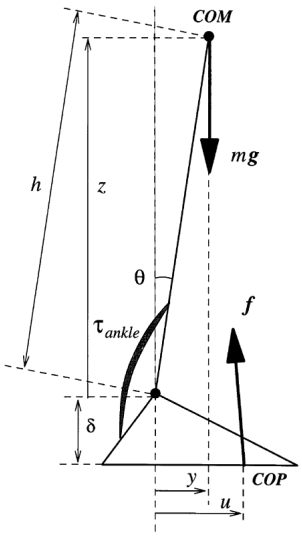

Figure 1.1: Biomechanical model of quiet standing in the Antero-Posterior (AP) direction (from Morasso et al., [4]). The variables *y, z, θ* are horizontal, vertical and angular position of the CoM; u is the horizontal position of the CoP. About the forces: f is the ground reaction force,τ_{ankle} is the total ankle torque due to all the muscles operating around the ankle. *h, δ, m* are constant parameter representing, respectively, the length of the segment from the CoP and the center of the ankle, the distance of the center of the ankle from ground and the subject's mass.

the weight force mg applied in the Center of Mass (CoM) and the ground reaction force, applied to the Center of Pressure (CoP).We can write the canonical equations:

$$f + mg = \frac{\partial mv}{\partial t}. \tag{1.1}$$

$$f \times (CoM - CoP) = \frac{\partial I_t \omega}{\partial t}, \tag{1.2}$$

where m is the total mass of the body, I_t its inertial tensor, v the velocity of the CoM and ω the angular velocity. We can simplify the equation as:

$$f_h \delta + f_v u + \tau_{ankle} = 0, \tag{1.3}$$

where τ_{ankle} is the torque applied by the ankle muscles,f_h and f_v are the horizontal and vertical components of the ground reaction, δ is the vertical displacement of the ankle from the support surface, and u is the horizontal displacement of the CoP from

the ankle. Moreover, we can write:

$$f_v - mg = m\ddot{\approx}0 \tag{1.4}$$

$$f_h = m\ddot{y} \tag{1.5}$$

$$\tau_{ankle} + mgy = \frac{\partial I_a \dot{\theta}}{\partial t} \approx I_a \ddot{\theta} \approx mh^2 k_s \frac{\ddot{y}}{h} = mhk_s \ddot{y} \tag{1.6}$$

y and z are the horizontal and vertical positions of the COM with respect to the ankle; θ is the angle with respect to the vertical line; m is the weight of the body excluding the feet,I_a is the corresponding moment of inertia with respect to the ankle joint, h is the distance of the COM from the ankle, and k_s is a shape factor that depends on the distribution of mass in the body.
Looking at equations 1.3 and 1.4, we can approximate the vertical component to zero; therefore we are able to write

$$u(t) \approx -\frac{1}{mg}\theta_{ankle}, \tag{1.7}$$

that means that CoP signal is a scaled version of the ankle torque.
There are three approximations in the model, that are well satisfied for sway in quiet standing:

- the vertical acceleration of the barycenter is negligible;
- the moment of inertia is constant
- the angular acceleration is proportional to the horizontal acceleration of the COM.

We can now combine the previous obtained equations:

$$\ddot{y} = \frac{g}{hk_s + \delta}(y - u) = k(y - u). \tag{1.8}$$

This means that the CoM-CoP difference is proportional to the acceleration of the CoM. From the point of view of motor control, this equation defines the transfer function of the body plant and thus *y(t)* can be considered as the controlled variable whereas *u(t)* the control variable.

Although the biomechanical model is accepted by all the researchers, there is still a debating about the organization of sensory and motor system contributing to spontaneous sway. The hypothesis that the stabilization of balance during quiet standing is achieved by the intrinsic stiffness of ankle muscles, due to the mechanical properties of the muscles and connective tissue with no neural command, was formulated by Winter et al. [9, 10] on the basis of two arguments: the experimental observation that the oscillation on the support surface of the center of mass (COM) appears to be in phase with the center of pressure (COP) and the theoretical consideration that such phase lock is incompatible with the afferent and efferent delays associated with active control. Morasso and Schieppati [4] demonstrated, on the basis on the model of the inverted pendulum, that the phase relation is a consequence of the dynamic of the model and that is independent from the stabilization system. Moreover, other articles [4, 11, 12, 13] demonstrated that the "stiffness model" is not plausible because of the non-physiological critical value of the necessary stiffness, much higher than values measurable in normal subjects. The importance of a central nervous activation during quiet standing was demonstrated (e.g. by Gatev et al. [14]) observing that electromyographic activity of ankle muscles is modulated in anticipation of postural sway.

An alternative to the "stiffness model" is the widely held view that the corrective torque is generated through the action of a feedback control system [1, 3, 15]. The feedback mechanism involves a time delay due to sensory transduction, transmission, processing, and muscle activation [15].

Finally, a third view observes that feedback mechanisms contribute to postural stabilization, but states that feedback alone in insufficient and that feed-forward predictive mechanisms are required to explain postural control behavior [7]. Mello et al. [16] verified the presence of electromyographic evidences for anticipatory mechanism in body sway control. Also other works suggested the presence of internal models [4, 17], or intermittent control model [6, 18].

1.2 Assessing postural control

The complex physiological mechanisms underlying postural control mechanisms can be unraveled under carefully controlled experimental conditions, with calibrated control of the environment, standardized bodily perturbations and use of quantitative outcome

measures [19]. However, in clinical practice, non-quantitative measures are still used. Horak [2] classified different approaches to the clinical assessment of balance in (i) functional approach, (ii) systems approach and (iii) quantitative methods. Functional assessment tools rate the performance of various tasks requiring balance control in order to identify the functional limitations or capacity to do a task or activity (Tinetti's test, Berg Functional Balance Scale). A system approach to balance assessment tries to identify the set of impaired subcomponents underlying the functional balance limitations in order to focus treatment on those subcomponents. In this work we will focus our attention on quantitative assessment of postural control.

Literature describes a wide range of different posturography techniques [2, 5, 19, 20, 21, 22]. Earlier methods for evaluating balance are summarized in [23]. It is common practice to allocate a particular posturography technique to one of two major categories: *Static* posturography and *Dynamic* posturography [24].

In the static approach the subjects is asked to stay on a flat, horizontal, unperturbed surface with eyes open or closed; the spontaneous sway movements are typically recorded through the trajectory of the CoP (Center of Pressure) on the support surface and the trajectory is parameterized according to different techniques.
In the dynamic approach the spontaneous posture is perturbed by means of different types of typically unpredictable stimuli in order to evaluate the relative contribution of the visual, vestibular, and somatosensory channels in regaining the initial posture. Perturbations of the quiet standing could be due to moving platforms (see fig. 1.2) or to external forces [19].
These two techniques are complementary as they address different aspects of the posture control system and yield independent types of information. Baratto et al. [5] pointed out two main differences among the two techniques:

- In the static case, most sensory channels are activated near or below the physiological threshold, with the exception of the plantar cutaneous receptors; in the dynamic case all the sensory channels are activated above threshold and feed strong reflex actions.

- In the static case, the main source of disturbance (the instability of the body inverted pendulum) is internal and predictable and thus the control system can rely

on some kind of internal anticipatory model; in the dynamic case the disturbance is usually unpredictable and the response is essentially a set of reflexes.

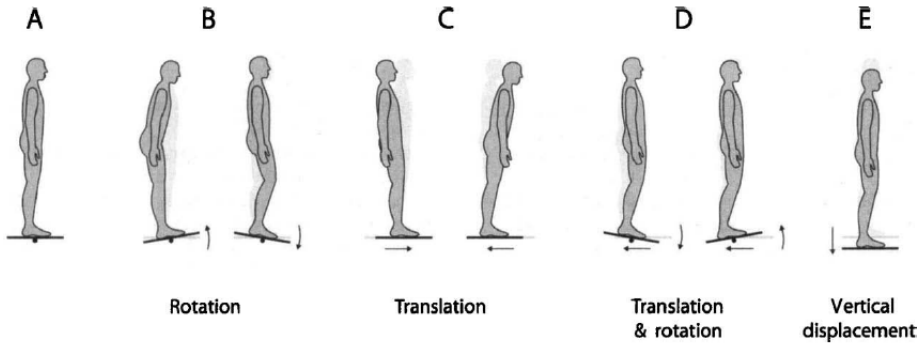

Figure 1.2: Different types of platform movements (from [19]). A: Baseline position. B: Rotational movements of the support surface, usually about the ankle axis as shown here. C: Horizontal translations of the support surface, shown here for the anterior-posterior direction. D: Combinations of simultaneously occurring rotations and translations. E: Purely vertical displacements

.

Table 1.1: Different techniques and outcome measures to objectively assess postural control (modified from Bloem et al. [19]).

	Equipment	Outcome measures
Kinematics	Motion sensors	Segment motion
	Optical motion analysis	3-D spatial representation of body in time
Kinetics	Force platforms	Center of pressure (CoP)
		Torques
		Shear forces and moments
Electromyography	EMG Electrodes	Muscle activity

To objectively assess postural control in static and dynamic conditions, different techniques have been employed [19, 22]. This includes kinetic measures (analysis of forces and joint moments), kinematic measures (analysis of how body parts move) or measures of muscle activity such as electromyography (EMG). Table 1.1 summarizes the different techniques. Kinetics is the most widely applied in quantifying postural control, in both dynamic and static condition. In our discussion we will focus our attention on

kinetics techniques, in particular to the use of force platforms in evaluating postural control in quiet standing, accordingly with the static paradigm.

1.3 Clinical applications

Quantitative posturography has been applied in investigating postural control in healthy subjects, both adults [5, 25, 26, 27] and children [28, 29]. In literature, several papers have addressed the effect of aging on balance performances using posturography [30, 31, 32, 33, 34].

Moreover, posturography has been used in evaluating balance in a wide spread range of pathologies, e.g. in vestibular patients [35], pathologies of the central nervous system, as Parkinson [36, 37, 38, 39], and multiple sclerosis [40],pathologies of the peripheral nervous system as diebetic patients [41, 42, 43], in traumatic brain injury patients [44, 45, 46], in patients after a stroke [47], and many other cases [48, 49, 50].

Another important field of application of the quantitative posturography is in the sport disciplines. The effectiveness of a balance training in preventing serious injuries was demonstrated in various sports [51, 52, 53, 54]. Training allows sport expertise to acquire new abilities in balance control according to the discipline practiced [55, 56]. In literature there are studies investigating postural control in dancers [55, 57, 58], gymnasts [59], judokas [55], soccer [60] and volleyball players [61, 62].

References

[1] R. J. Peterka, "Sensorimotor integration in human postural control.," *J Neurophysiol*, vol. 88, pp. 1097–1118, Sep 2002.

[2] F. B. Horak, "Clinical assessment of balance disorders," *Gait & Posture*, vol. 6, pp. 76–84, 1997.

[3] C. Maurer and R. J. Peterka, "A new interpretation of spontaneous sway measures based on a simple model of human postural control.," *J Neurophysiol*, vol. 93, pp. 189–200, Jan 2005.

[4] P. G. Morasso, L. Baratto, R. Capra, and G. Spada, "Internal models in the control of posture.," *Neural Netw*, vol. 12, pp. 1173–1180, Oct 1999.

[5] L. Baratto, P. Morasso, C. Re, and G. Spada, "A new look at posturographic analysis in the clinical context: sway density vs. other parametrization techniques," *Motor control*, vol. 6, pp. 246–270, 2002.

[6] A. Bottaro, Y. Yasutake, T. Nomura, M. Casadio, and P. Morasso, "Bounded stability of the quiet standing posture: an intermittent control model.," *Hum Mov Sci*, vol. 27, pp. 473–495, Jun 2008.

[7] R. Fitzpatrick, D. Burke, and S. C. Gandevia, "Loop gain of reflexes controlling human standing measured with the use of postural and vestibular disturbances.," *J Neurophysiol*, vol. 76, pp. 3994–4008, Dec 1996.

[8] D. A. Winter, "Human balance and posture control during standing and walking," *Gait & Posture*, vol. 3, pp. 193–214, 1995.

[9] D. A. Winter, A. E. Patla, F. Prince, M. Ishac, and K. Gielo-Perczak, "Stiffness control of balance in quiet standing.," *J Neurophysiol*, vol. 80, pp. 1211–1221, Sep 1998.

[10] D. A. Winter, A. E. Patla, S. Rietdyk, and M. G. Ishac, "Ankle muscle stiffness in the control of balance during quiet standing.," *J Neurophysiol*, vol. 85, pp. 2630–2633, Jun 2001.

REFERENCES

[11] P. G. Morasso and V. Sanguineti, "Ankle muscle stiffness alone cannot stabilize balance during quiet standing.," *J Neurophysiol*, vol. 88, pp. 2157–2162, Oct 2002.

[12] M. Casadio, P. G. Morasso, and V. Sanguineti, "Direct measurement of ankle stiffness during quiet standing: implications for control modelling and clinical application.," *Gait Posture*, vol. 21, pp. 410–424, Jun 2005.

[13] I. D. Loram and M. Lakie, "Direct measurement of human ankle stiffness during quiet standing: the intrinsic mechanical stiffness is insufficient for stability.," *J Physiol*, vol. 545, pp. 1041–1053, Dec 2002.

[14] P. Gatev, S. Thomas, T. Kepple, and M. Hallett, "Feedforward ankle strategy of balance during quiet stance in adults.," *J Physiol*, vol. 514 (Pt 3), pp. 915–928, Feb 1999.

[15] R. J. Peterka, "Postural control model interpretation of stabilogram diffusion analysis," *Biolobical Cybernetics*, vol. 82, pp. 335–343, 2000.

[16] R. G. T. Mello, L. F. Oliveira, and J. Nadal, "Anticipation mechanism in body sway control and effect of muscle fatigue.," *J Electromyogr Kinesiol*, vol. 17, pp. 739–746, Dec 2007.

[17] H. van der Kooij and R. J. Peterka, "Non-linear stimulus-response behavior of the human stance control system is predicted by optimization of a system with sensory and motor noise.," *J Comput Neurosci*, vol. 30, pp. 759–778, Jun 2011.

[18] A. Bottaro, M. Casadio, P. G. Morasso, and V. Sanguineti, "Body sway during quiet standing: is it the residual chattering of an intermittent stabilization process?," *Hum Mov Sci*, vol. 24, pp. 588–615, Aug 2005.

[19] B. R. Bloem, J. E. Visser, and J. H. Allum, *Handbook of clinical neurophysiology*, ch. Posturography, pp. Vol 1: 295–336. Elsevier, 2003.

[20] H. Chaudhry, B. Bukiet, Z. Ji, and T. Findley, "Measurement of balance in computer posturography: Comparison of methods–a brief review.," *J Bodyw Mov Ther*, vol. 15, pp. 82–91, Jan 2011.

[21] A. Nardone and M. Schieppati, "The role of instrumental assessment of balance in clinical decision making.," *Eur J Phys Rehabil Med*, vol. 46, pp. 221–237, Jun 2010.

[22] J. E. Visser, M. G. Carpenter, H. van der Kooij, and B. R. Bloem, "The clinical utility of posturography.," *Clin Neurophysiol*, vol. 119, pp. 2424–2436, Nov 2008.

[23] Y. Terekhov, "Stabilometry as a diagnostic tool in clinical medicine.," *Can Med Assoc J*, vol. 115, pp. 631–633, Oct 1976.

[24] J. Furman, R. Baloh, K. Barin, T. Hain, S. Herdman, H. Kordam, and S. Parker, "Assessment: posturography. report of the therapeutics and technology assessment subcommittee of the american academy of neurology.," *Neurology*, vol. 43, pp. 1261–1264, Jun 1993.

[25] R. J. Doyle, E. T. Hsiao-Wecksler, B. G. Ragan, and K. S. Rosengren, "Generalizability of center of pressure measures of quiet standing.," *Gait Posture*, vol. 25, pp. 166–171, Feb 2007.

[26] L. Chiari, L. Rocchi, and A. Cappello, "Stabilometric parameters are affected by anthropometry and foot placement.," *Clin Biomech (Bristol, Avon)*, vol. 17, no. 9-10, pp. 666–677, 2002.

[27] S. H. Nordahl, T. Aasen, B. M. Dyrkorn, S. Eidsvik, and O. I. Molvaer, "Static stabilometry and repeated testing in a normal population.," *Aviat Space Environ Med*, vol. 71, pp. 889–893, Sep 2000.

[28] M. Schmid, S. Conforto, L. Lopez, P. Renzi, and T. D'Alessio, "The development of postural strategies in children: a factorial design study.," *J Neuroeng Rehabil*, vol. 2, p. 29, 2005.

[29] Y.-S. Hsu, C.-C. Kuan, and Y.-H. Young, "Assessing the development of balance function in children using stabilometry.," *Int J Pediatr Otorhinolaryngol*, vol. 73, pp. 737–740, May 2009.

[30] T. E. Prieto, J. B. Myklebust, R. G. Hoffmann, E. G. Lovett, and B. M. Myklebust, "Measures of postural steadiness: differences between healthy young and elderly adults.," *IEEE Trans Biomed Eng*, vol. 43, pp. 956–966, Sep 1996.

REFERENCES

[31] J. A. Norris, A. P. Marsh, I. J. Smith, R. I. Kohut, and M. E. Miller, "Ability of static and statistical mechanics posturographic measures to distinguish between age and fall risk.," *J Biomech*, vol. 38, pp. 1263–1272, Jun 2005.

[32] T. L. A. Doyle, E. L. Dugan, B. Humphries, and R. U. Newton, "Discriminating between elderly and young using a fractal dimension analysis of centre of pressure.," *Int J Med Sci*, vol. 1, no. 1, pp. 11–20, 2004.

[33] H. Amoud, M. Abadi, D. J. Hewson, V. Michel-Pellegrino, M. Doussot, and J. Duchne, "Fractal time series analysis of postural stability in elderly and control subjects.," *J Neuroeng Rehabil*, vol. 4, p. 12, 2007.

[34] M. G. Carpenter, A. L. Adkin, L. R. Brawley, and J. S. Frank, "Postural, physiological and psychological reactions to challenging balance: does age make a difference?," *Age Ageing*, vol. 35, pp. 298–303, May 2006.

[35] R. W. Baloh, K. M. Jacobson, K. Beykirch, and V. Honrubia, "Static and dynamic posturography in patients with vestibular and cerebellar lesions.," *Arch Neurol*, vol. 55, pp. 649–654, May 1998.

[36] J. W. Blaszczyk and R. Orawiec, "Assessment of postural control in patients with parkinson's disease: sway ratio analysis.," *Hum Mov Sci*, vol. 30, pp. 396–404, Apr 2011.

[37] S. Fioretti, M. Guidi, L. Ladislao, and G. Ghetti, "Analysis and reliability of posturographic parameters in parkinson patients at an early stage.," *Conf Proc IEEE Eng Med Biol Soc*, vol. 1, pp. 651–654, 2004.

[38] C. Maurer, T. Mergner, and R. J. Peterka, "Abnormal resonance behavior of the postural control loop in parkinson's disease.," *Exp Brain Res*, vol. 157, pp. 369–376, Aug 2004.

[39] L. Rocchi, L. Chiari, and F. B. Horak, "Effects of deep brain stimulation and levodopa on postural sway in parkinson's disease.," *J Neurol Neurosurg Psychiatry*, vol. 73, pp. 267–274, Sep 2002.

[40] M. L. Corradini, S. Fioretti, T. Leo, and R. Piperno, "Early recognition of postural disorders in multiple sclerosis through movement analysis: a modeling study.," *IEEE Trans Biomed Eng*, vol. 44, pp. 1029–1038, Nov 1997.

[41] S. Fioretti, M. Scocco, L. Ladislao, G. Ghetti, and R. A. Rabini, "Identification of peripheral neuropathy in type-2 diabetic subjects by static posturography and linear discriminant analysis.," *Gait Posture*, vol. 32, pp. 317–320, Jul 2010.

[42] R. Yamamoto, T. Kinoshita, T. Momoki, T. Arai, A. Okamura, K. Hirao, and H. Sekihara, "Postural sway and diabetic peripheral neuropathy.," *Diabetes Res Clin Pract*, vol. 52, pp. 213–221, Jun 2001.

[43] L. Uccioli, P. G. Giacomini, G. Monticone, A. Magrini, L. Durola, E. Bruno, L. Parisi, S. D. Girolamo, and G. Menzinger, "Body sway in diabetic neuropathy.," *Diabetes Care*, vol. 18, pp. 339–344, Mar 1995.

[44] V. Agostini, E. Chiaramello, C. Bredariol, C. Cavallini, and M. Knaflitz, "Postural control after traumatic brain injury in patients with neuro-ophthalmic deficits.," *Gait Posture*, vol. 34, pp. 248–253, Jun 2011.

[45] A. C. Geurts, G. M. Ribbers, J. A. Knoop, and J. van Limbeek, "Identification of static and dynamic postural instability following traumatic brain injury.," *Arch Phys Med Rehabil*, vol. 77, pp. 639–644, Jul 1996.

[46] L. D. Wade, C. G. Canning, V. Fowler, K. L. Felmingham, and I. J. Baguley, "Changes in postural sway and performance of functional tasks during rehabilitation after traumatic brain injury.," *Arch Phys Med Rehabil*, vol. 78, pp. 1107–1111, Oct 1997.

[47] M. Roerdink, M. D. Haart, A. Daffertshofer, F. Donker, A. C. H. Geurts, and P. J. Beek, "Dynamical structure of center-of-pressure trajectories in patients recovering from stroke," *Exp Brain Res*, vol. 174, p. 256269, 2006.

[48] D. Lafond, A. Champagne, M. Descarreaux, J.-D. Dubois, J. M. Prado, and M. Duarte, "Postural control during prolonged standing in persons with chronic low back pain.," *Gait Posture*, vol. 29, pp. 421–427, Apr 2009.

[49] K. Ishizaki, N. Mori, T. Takeshima, Y. Fukuhara, T. Ijiri, M. Kusumi, K. Yasui, H. Kowa, and K. Nakashima, "Static stabilometry in patients with migraine and tension-type headache during a headache-free period.," *Psychiatry Clin Neurosci*, vol. 56, pp. 85–90, Feb 2002.

[50] C. Rossi, A. Alberti, P. Sarchielli, G. Mazzotta, G. Capocchi, M. Faralli, G. Ricci, E. Molini, and G. Altissimi, "Balance disorders in headache patients: evaluation by computerized static stabilometry.," *Acta Neurol Scand*, vol. 111, pp. 407–413, Jun 2005.

[51] K. Sderman, S. Werner, T. Pietil, B. Engstrm, and H. Alfredson, "Balance board training: prevention of traumatic injuries of the lower extremities in female soccer players? a prospective randomized intervention study.," *Knee Surg Sports Traumatol Arthrosc*, vol. 8, no. 6, pp. 356–363, 2000.

[52] E. Verhagen, A. van der Beek, J. Twisk, L. Bouter, R. Bahr, and W. van Mechelen, "The effect of a proprioceptive balance board training program for the prevention of ankle sprains: a prospective controlled trial.," *Am J Sports Med*, vol. 32, pp. 1385–1393, Sep 2004.

[53] W. Petersen, C. Braun, W. Bock, K. Schmidt, A. Weimann, W. Drescher, E. Eiling, R. Stange, T. Fuchs, J. Hedderich, and T. Zantop, "A controlled prospective case control study of a prevention training program in female team handball players: the german experience.," *Arch Orthop Trauma Surg*, vol. 125, pp. 614–621, Nov 2005.

[54] T. A. McGuine and J. S. Keene, "The effect of a balance training program on the risk of ankle sprains in high school athletes.," *Am J Sports Med*, vol. 34, pp. 1103–1111, Jul 2006.

[55] P. Perrin, D. Deviterne, F. Hugel, and C. Perrot, "Judo, better than dance, develops sensorimotor adaptabilities involved in balance control.," *Gait Posture*, vol. 15, pp. 187–194, Apr 2002.

[56] P. G. Gerbino, E. D. Griffin, and D. Zurakowski, "Comparison of standing balance between female collegiate dancers and soccer players.," *Gait Posture*, vol. 26, pp. 501–507, Oct 2007.

[57] E. Golomer, J. Crmieux, P. Dupui, B. Isableu, and T. Ohlmann, "Visual contribution to self-induced body sway frequencies and visual perception of male professional dancers.," *Neurosci Lett*, vol. 267, pp. 189–192, Jun 1999.

[58] J. M. Schmit, D. I. Regis, and M. A. Riley, "Dynamic patterns of postural sway in ballet dancers and track athletes.," *Exp Brain Res*, vol. 163, pp. 370–378, Jun 2005.

[59] N. Vuillerme, N. Teasdale, and V. Nougier, "The effect of expertise in gymnastics on proprioceptive sensory integration in human subjects.," *Neurosci Lett*, vol. 311, pp. 73–76, Sep 2001.

[60] E. Biec and M. Kuczynski, "Postural control in 13-year-old soccer players.," *Eur J Appl Physiol*, vol. 110, pp. 703–708, Nov 2010.

[61] M. Kuczynski, Z. Rektor, and D. Borzucka, "Postural control in quiet stance in the second league male volleyball players," *Human movement*, vol. 10(1), pp. 12–15, 2009.

[62] B. Dai, C. J. Sorensen, and J. C. Gillette, "The effects of postseason break on stabilometric performance in female volleyball players.," *Sports Biomech*, vol. 9, pp. 115–122, Jun 2010.

REFERENCES

2

Static posturography

In this chapter I will focuse on static posturography as a quantitative technique aimed at characterizing the body sway during quiet standing. In static posturography the trajectories of the Centre of Pressure (CoP) on a plane surface are recorded by means of a force platform. The CoP is used as a measure of postural stability, and it is recorded both in antero-posterior (AP) and medio-lateral (ML) components.

In literature an important effort was done to methodologically improve acquisition settings to assess postural performances in quiet standing. Therefore I will briefly describe a typical experimental set up and the most used acquisition protocols.

Many approaches have been used to cope with CoP signal. Traditional parameters are extracted from the CoP trajectories under the assumption that the CoP is a stationary time series. They provide geometrical and statistical description of the signal, in time and frequency domain [1, 2]. An alternative method for analyzing CoP signal was described in [3], modeling the signal as a fractal Brownian motion. Moreover, also the chaotic approach was proposed to look inside the dynamic properties of the signal [4]. A description of the most widely used signal processing approaches to cope with the CoP signal will be provided.

2.1 Acquisition setup and protocols

In this section I will briefly describe as a typical acquisition set up instruments used during my experiments, and will analyze the main aspect of the static posturography acquisition protocol according to the literature.

2.1.1 Typical experimental setup

A typical experimental set-up for posturographic studies consists of a force plate and a signal conditioning and acquisition chain to store signals in a computer, which is used for the offline extraction of suitable parameters from the centre of pressure (CoP) trajectories [5]. Force platforms can be equipped with either piezoelectric or strain gauge-type sensors [6].

In my experimental acquisitions I used a Kistler type 9286A force platform, with piezoelectric 3-component force sensors. Table 2.1 shows the force platform technical characteristics, while figure 2.1 shows its dimensions. The resulting analogue data are amplified and and converted into digital data by means of Step32 Junction box and the Step32 PCI card. The acquisition software is Step32.

Table 2.1: Force platform Kistler type 9286A: technical characteristics.

Measuring range	F_x, F_y	kN	-2.5...2.5
	F_z	kN	0...10
Linearity		%FSO	$< \pm$ 0.5
Crosstalk	$F_x \leftrightarrow F_y$	%	$< \pm$ 1.5
	F_x, $F_y \leftrightarrow F_z$	%	$< \pm$2.0
	$F_z \leftrightarrow F_x$, F_y	%	$< \pm$0.5
Overload	F_x,F_y	kN	-3/3
	F_z	kN	0/12
Hysteresis		%FSO	$\pm$ 0.5
Rigidity	x-axle	/μm	$\approx$12
	y-axle	N/μm	$\approx$12
	z-axle	/μm	$\approx$12

The subject is usually asked to stand as quiet as possible of the platform surface, in a quiet environment and for a few seconds (details of the acquisition protocol will be discuss in the next pages). Figure 2.2 shows the picture of a subject during a stabilometric test.

From each acquisition, the system records eight output signals: four of them are a

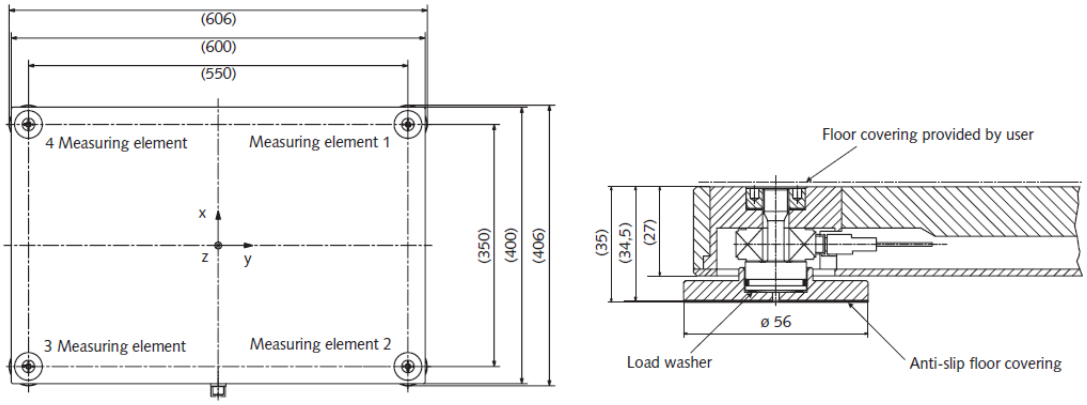

Figure 2.1: Dimension of the Kistler force platform type 9286A (from the force platform data sheet)

.

linear combination of the horizontal forces in the xy plane (we assume x as the antero-posterior axes and y as the medio-lateral axes, with respect to the subject), while the others are the vertical components revealed by each piezoelectric sensor.

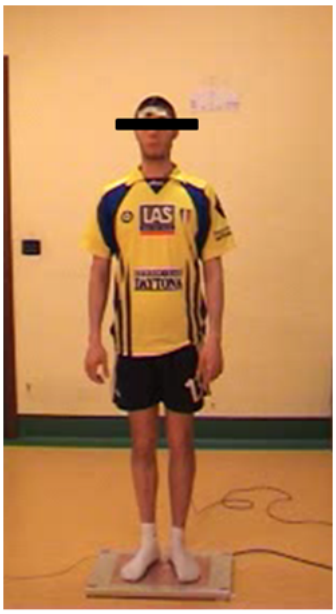

Figure 2.2: Static posturography: experimental set up

.

Many papers in literature describes acquisition set up similar to the previous pre-

sented one [2, 7, 8, 9, 10, 11, 12].
Some authors investigated the reliability ans accuracy of force platform in measuring the CoP position. More specifically, Rogind et al. [7] compared two different commercial systems to assess balance, concluding that both of them are reliable and reproducible. Middleton et al. [12] assessed the accuracy of piezoelectric force platform in determining the CoP position, and their conclusion was that errors were substantially larger when force was applied through a single point than when the force was distributed between two blocks, to simulate double stance. In order to face the problem of drift in piezoelectric force platform, Quagliarella et al. [6] proposed a method for numerical compensation.

2.1.2 Methodological approaches and protocols

Past studies of postural control during quiet standing have employed a wide range of procedures to quantify postural control [9], using different approaches concerning the duration of the acquisition trial, sampling and cut-off frequencies, subject position, number of repetition and duration of the time interval between repeated tasks, visual condition, surface condition, and methods for data processing. Due to these differences it is quite difficult to compare results of different studies.
To overcome this limit, a large number of paper in literature examined different aspects of the static posturography acquisition protocol in terms of repeatability and reliability.

Experimental condition The large majority of studies have been conducted in quiet environment, with controlled lighting, temperature and noise level, in order to avoid to stimulate the subject with uncontrolled visual and auditory stimuli [2, 5, 13].

A factor usually not taken into due consideration but likely to influence the postural exam is the instruction given to the subject before the test: Zok et al. [14] investigated how a different instructions could influence postural performances of a group of healthy subjects. Their results suggested that different instructions given to the subjects influence the outcome of the test, and should be standardized.

Visual condition The most usual protocol for testing postural control in quiet standing consists of two trials, one with open eyes gazing at a visual target and one with closed eyes. Many studies described effect of visual input on outcome measures (e.g.

[13, 15]). Kapoula [16] investigated effects of distance and gaze position on postural performances in young and old healthy subjects.

Feet position Static posturography could be carried on both in single and in double stance. In literature there are both studies in which feet placement have been standardized [2, 17] and studies in which the subjects were asked to choose the more comfortable feet position [18] on the platform surface. However, feet placement during posturographic test have been demonstrated to have a relevant effect on CoP parameters [18, 19], therefore it should be standardized [8].

Test duration Some studies in literature investigated the impact of sample duration on the magnitude and reliability of CoP measures in time and frequency domains [9, 11, 20]. All of them found that the test duration influences reliability and validity of CoP parameters. Carpenter et al. [9] investigated test duration from 15 to 120 seconds, while in an other work [20] longer duration, upon to 300 seconds was proposed. Ruhe et al. [8] in their literature review work suggested a 90 seconds test duration, in order to achieve a good CoP parameters reliability.

Sampling and cut-off frequency In literature, sampling rates from 10 to 200 Hz have been reported [2, 5, 8, 13, 21, 22, 23, 24].
It has been shown that COP measures and its reliabilities vary depending on both the acquisition and cut-off frequency chosen [5, 8, 22]. More specifically, Schmidt et al. [5] investigated influence on the outcome measures of the values chosen for the cut-off frequency of anti-aliasing filters, the sampling rate and the dynamic range of analogue-to-digital (A/D) converters. They focused on the cut-off frequency and suggested a value of 10 Hz.

Raymakers et al. [22] observed that sampling frequency could have a big effect on the traditional calculated CoP parameters. In chapter 4 I will focus on the sampling frequency effect on geometrical CoP parameters.

Number of repetitions In order to enhance reliability of the center of pressure measures, several authors proposed to repeat the posturographic test in identical conditions for many times (from 3 to 10) [8, 23, 24]. Increasing the number or repetition, results

appeared to be more reliable. However, it has also been demonstrated that repeated tests lead to a learning effect [15, 21], and that this effect is enhanced when the time interval between the trials is shorter. Moreover, repeating many tests could be difficult in assessing postural control in pathological or aged subjects; therefore Ruhe et al. [8] proposed to average 3-5 trials to obtain reliable data.

2.2 The CoP signal

From the signals recorded from the force platform, it is possible to obtain both forces and moments exchanged between the subject and the force platform surface and the Centre of Pressure orthogonal components CoP_x and CoP_y.

In the previous described experimental setting, this can be done as:

$Fx = Fx_{12} + Fx_{34}$	force in the antero-posterior direction
$Fy = Fy_{14} + Fy_{23}$	force in the medio-lateral direction
$Fz = Fz_1 + Fz_2 + Fz_3 + Fz_4$	vertical component
$Mx = b * (Fz_1 + Fz_2 - Fz_3 - Fz_4)$	moment around x axes
$My = a * (-Fz_1 + Fz_2 + Fz_3 - Fz_4)$	moment around y axes
$Mz = b * (-Fx_{12} + Fx_{34}) + a * (Fy_{14} - Fy_{23})$	moment around z axes
$CoP_x = (Fx * a_{z0} - My)/Fz$	CoP: antero-posterior component
$CoP_y = (Fy * a_{z0} + Mx)/Fz$	CoP: medio-lateral component

(a and b are specific numerical compensation for the used force platform).
A plot of the time-varying coordinates of the CoP in the xy as shown in figure 2.3 is known as *stabilogram* or *sway path* [4].

Several techniques have been proposed to analyze the CoP signal, usually decomposing it into the antero-posterior (AP) and medio-lateral (ML) time-series. Many of the previous studies considered the CoP time series from the geometrical and statistical points of view, in the time and frequency domains [1, 2, 13, 18, 25]. To analyse the dynamic characteristics of CoP signals, Collins et al. [3] proposed a method based on fractional Brownian motion. Moreover, an alternative model based on chaos theory was proposed [4, 26].
For each of these approaches there is a different underlying model for the CoP signal.

In this section we will describe the main CoP signal models and analysis methods.

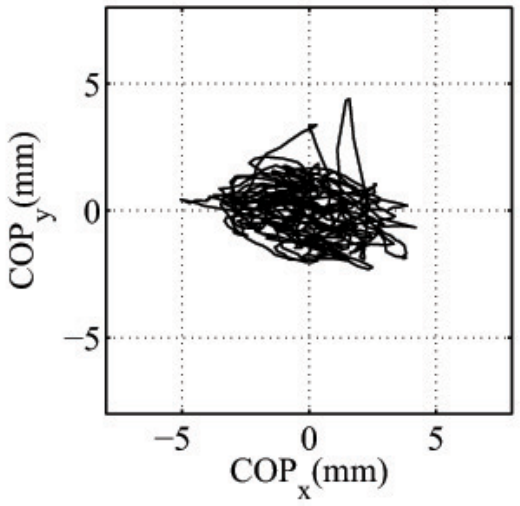

Figure 2.3: Representative CoP signal

.

2.2.1 Global posturographic parameters

This approach is the most largely used in literature, e.g. in [1, 2, 13, 18, 25]. It consists in analyzing CoP trajectories both in time and frequency domain, from geometrical and statistic point of view. The underlying hypothesis, motivated by the variability and random appearance of the posturograms, is that posturograms are simple stationary stochastic processes that express the noise in the posture control system. Therefore, these parameters have an integral nature and their purpose is to estimate the size of the noise [2].

The CoP signal is analyzed both in its orthogonal components CoP_x and CoP_y, and in its bidimensional aspects. AP and ML time-series are, respectively, the Antero-Posterior and the Medio-Lateral coordinates of the displacement of the CoP on the platform surface, while Resultant time-series (R) is defined as vector distance from the center of the platform to each CoP position. Many parameters have been defined according to this approach [1]; we will focuse our attention on the most common ones.

Time domain The main time domain defined parameters are:

- Sway Path Lenght: it is defined as the length of CoP during the whole trial. Unit of measurement: mm.

$$SwayPathLength = \sum_{n=1}^{N-1} [(AP[n+1] - AP[n])^2 + (ML[n+1] - ML[n])^2]. \quad (2.1)$$

- Sway Area: it is an estimation of the surface area included in the stabilogram. Many different formulations are described in literature to assess this parameter. Prieto et al. [1] reported the following:

  - Confidence Circle Area (Area-CC): it is defined as the area of a circle equal to the one-sided 95% confidence limit distribution of Resultant Distance (RD) timeseries. It describes the CoP as the area of the circle that has the 95% of probability to contain the sway path, hypothesizing that CoP positions are distributed according to a normal bivariate probability distribution. Unit of measurement: mm^2

  - Confidence Ellipse Area (Area-CE): it is defined as the area of an ellipse equal to the one-sided 95% confidence limit distribution of the Resultant Distance (RD) timeseries. It describes the CoP as the area of the ellipse that has the 95% of probability to contain the sway path, hypothesizing that CoP positions are distributed according to a normal bivariate probability distribution. Unit of measurement: mm^2.

  - Sway Area: estimates the area enclosed by the CoP path per unit of time. It is not based on a statistical approach, but it is approximated by summing the area of the triangles formed by two consecutive points of the CoP path and the centre of the platform. Unit of measurement: mm^2/s

$$SwayArea = \frac{1}{2T} \sum_{n=1}^{N-1} |AP[n+1] * ML[n] - AP[n] * ML[n+1]|. \quad (2.2)$$

- Mean Velocity: It is defined as the length of CoP during the whole trial normalized on the time duration of the acquisition. It is analogally to the Sway Path length. Unit of measurement: mm/s.

- Root Mean Square: It is defined as the root mean square value of the AP, ML and R time-series. Unit of measurement: mm.

$$RmsR = \sqrt{\frac{1}{N-1}\sum_{n=1}^{N}(R[n] - \bar{R})^2}. \tag{2.3}$$

- Major Axis: Length of the major axis of the smallest ellipse containing the CoP. Unit of measurement: mm.

- Minor Axis: Length of the minor axis of the smallest ellipse containing the CoP. Unit of measurement: mm.

- Eccentricity: Eccentricity of the smallest ellipse containing the CoP. Unit of measurement: adimentional.

Frequency domain The frequency domain parameters are based on the power spectral analyis of CoP time-series. The main parameters are:

- The total power (TP), defined as the integrated area of the power spectrum[1]. Unit of measurement: mm^2.

- The centroidal frequency, defined as the frequency at which the spectral power is concentrated[1]. Unit of measurement: Hz.

- The frequency dispersion, which is a uniteless measure of the variability in the frequency content of the power spectral density [1].

- Frequency bands containing a fraction of the area under the amplitude spectrum of the CoP signal, respectevely 70% (f70), 80% (f80), 85% (f85), 90% (f90), 95% (f95) of the total power [2]. Moreover, Prieto et al. [1] defined also the parameter "Median Frequency", as the frequency below which the 95% of the total power is present. Unit of measurement: Hz.

All the above described frequency domain parameters could be evaluated both considering the CoP orthogonal components in the antero-posterior and medio-lateral directions and the resultant time-series.

It is important to notice that the described parameters consider the AP and ML components as separate signals. Even when considering the resultant distance time-series, only information form the Euclidean norm is taken into account, while phase characteristics are completely discarded [27].

2.2.2 Diffusion plots

Collins and De Luca [3, 28, 29] approached the problem of characterizing stabilograms in a different way from the above described ones, in order to consider the dynamic characteristic of stabilograms. They hypothesized that the output of the human postural control system under quiet standing conditions can be modeled as a system of bounded, correlated random walks.

In [28] using surrogate analysis, it was demonstrated that the postural control task should not be modeled as a chaotic process, and that it is better represented as a stochastic one. In particular, the hypothesis of fractional Brownian random walk was formulated to analyze CoP trajectories.

The general driving principle of statistical mechanics is that although the outcome of an individual random event is unpredictable, it is still possible to obtain definite expressions for the probabilities of various aspects of a stochastic process or mechanism. A classic example of a statistical mechanical phenomenon is Brownian motion. The simplest case of Brownian motion is the random movement of a single particle along a straight line. This model is known as a one-dimensional random walk. The mean square displacement $\langle \Delta x^2 \rangle$ of a one-dimensional random walk was related to the time interval Δt by the expression:

$$\langle \Delta x^2 \rangle = 2D\Delta t, \tag{2.4}$$

where D is the diffusion coefficient, an average measure of the stochastic activity of the random walker. The *fractional Brownian random walk* is a family of Gaussian stochastic processes, it is an extension of the classical Brownian motion. The difference between classical and fractional Brownian motion is the characteristic for which in fractional Brownian motion past increments in a particle's displacement are correlated with future increments, while in the classical Brownian motion they are independent.

For fractional Brownian random walks:

$$\left\langle \Delta x^2 \right\rangle = \Delta t^{2H}, \tag{2.5}$$

where the scaling exponent H is a real number in the range (0,1). For $H = \frac{1}{2}$ the motion is a classical random walk (as seen in eq.2.4). The scaling exponent H can be determined from the slope of the log-log plot of the mean square displacement versus Δt. The correlation function is given by the expression:

$$C = 2(2^{2H-1} - 1). \tag{2.6}$$

For $H > \frac{1}{2}$ the stochastic is positively correlated, therefore a fractional Brownian particle moving in a particular direction for some t_0 will continue in the same direction for $t > t_0$. This type of behavior is called *persistence*. The opposite situation occurs for $H < \frac{1}{2}$, when past and future increments are negatively correlated. This type of behavior is called *anti-persistence*.

Diffusion plot of CoP Trajectories. Collins and De Luca applied the fractional Brownian random walk model to CoP trajectories, analyzing both their AP and ML components as one-dimensional motion and the whole CoP signal as a two-dimensional motion [3, 29]. The displacement analysis was carried out by computing the square of the displacements between all pairs of points separated in time by a specified time interval Δt (Fig. 2.4a). A plot of mean square COP displacement versus time interval Δt will be referred to as a stabilogram-diffusion plot (Fig. 2.4b).

Diffusion coefficients D (equation 2.4) were calculated from the slopes of the resultant linear-linear plots of mean square COP displacement versus time interval curves. Similarly, scaling exponents H (equation 2.5) were computed from the resultant log-log plots of such curves. Diffusion plots were calculated for AP and ML components of stabilogram and for the whole CoP signal. In each diffusion plot two different regions were identified, a short-term and a long-term region (as shown in figure 2.4). These regions were separated by a transition period where the slope of the stabilogram-diffusion plot changed considerably. Diffusion coefficients and scaling exponents were calculated for each region. Moreover, an estimate for each critical point was determined as the intersection point of the straight lines fitted to the two regions of the linear-linear version of each stabilogram-diffusion plot.

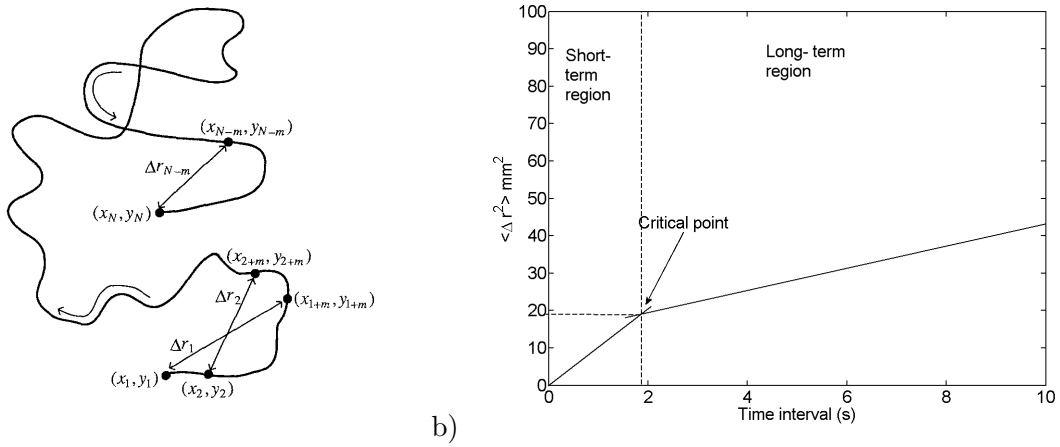

Figure 2.4: a) Method for calculating mean square planar displacement $\langle \Delta r^2 \rangle$ for a CoP trajectory. b) Schematic representation of the Stabilogram-Diffusion plot (from [3]).

Observing the two separate region of the diffusion plot, Collins and De Luca suggested the presence of at least two control mechanisms in postural control. More specifically, they hypothesized the presence of an open-loop control mechanism in short-term intervals (which have a higher level of stochastic activity) and a second closed-loop control mechanism used over long-term intervals.

Summarizing, diffusion plots parameters defined by Collins and De Luca from the described stabilogram diffusion plots are:

- Diffusion coefficients D (mm^2/s), calculated on short-term and long-term region of each linear-linear scaled diffusion plot.
- Scaling components H, calculated on short-term and long-term region of each log-log scaled diffusion plot.
- Critical point coordinates (time intervals (s) and mean square displacements (mm^2)), calculated on each linear-linear scaled diffusion plot.

2.2.3 Sway density plot

This analysis approach was firstly proposed by Baratto et al. in [2]. The underlying idea [30] is that feed forward control is the prevalent mechanism in the postural

stabilization process, thus breaking down the control process into a sequence of anticipatory motor commands. The hypothesis underlying the sway density plot formulation is that two main type of control strategies take part to the postural control process. More specifically, these strategies are (i) the intrinsic feedback due to the mechanical properties of ankle muscles, characterizing the persistent component of the CoP signal, and (ii) the anticipatory muscle activations determined by an internal model of the inverted pendulum. The last strategy has a feed forward nature and aims at stopping the current fall, therefore has a anti-persistence behavior. This distinction between components with persistence and anti-persistence behavior is a common point with the diffusion plot analysis [3].

Starting from these assumptions on the postural model, Sway Density Plot (SDP) or Curves (SDC) are defined as the time-dependent curves constructed counting, for each time instant, the number of consecutive samples of the CoP trajectories that fall inside a circle of given radius. The sample count is divided by the sampling rate, yielding a time dimension for the ordinate axis. In other words, the SDP is a time-versus-time curve, showing the evolution over time of the stay time of the posturographic trace inside a moving circle of radius R [31].
Figure 2.5a exemplify the sway density plot definition. A typical SDP, as shown in figure 2.5b exhibits a regular alternation of peaks and valleys:

- peaks correspond to time instants in which the ankle torque and the associated motor commands are relative stable;
- valley corresponds to time instants in which the ankle torque rapidly shifts from one stable value to another.

After identifying the peaks on the SDP, the following parameters were computed [2, 31]:

- Time interval T (s) between peaks (related to the rate of production of postural commands): mean value (MT) and standard deviation (σT).
- Distance D (s) between peaks (related to the amplitude of postural commands): mean value (MD) and standard deviation (σD).
- Peaks values P (s): mean value (MP) and standard deviation (σS).

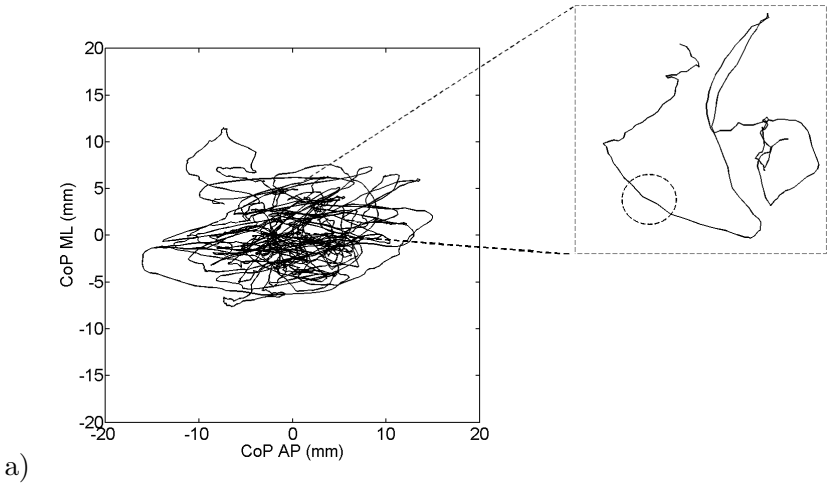

a)

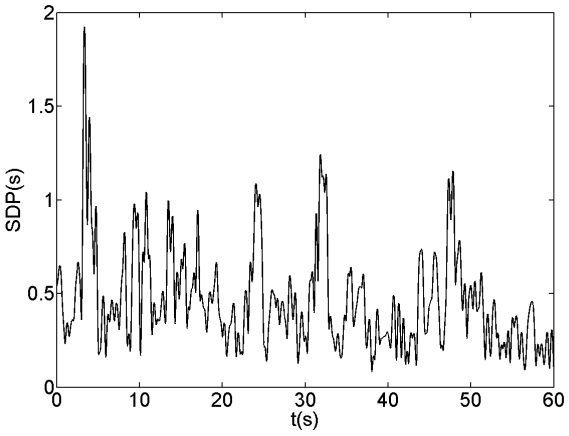

b)

Figure 2.5: a) Example of stabilogram: from each point of the CoP trajectories, SDP are computed counting the number of consecutive point contained in the probe circle of radius R centered in that point b) Sway density plot.

- After computing σT, σD and σP, their population means were calculated, obtaining 3 more parameters ST (s), SD (mm) and SP(s).

2.2.4 Nonlinear analysis: Chaos approach

Nonlinear analysis offers a way to characterize qualitative changes in the dynamics of postural control system [26]. Methods based on nonlinear analysis techniques allow to reconstruct the dynamics of a system starting from a single time series. A characteristic that this kind of analysis can reveal is the chaotic behaviour of signals

generated by deterministic nonlinear systems. A deterministic nonlinear system is defined as chaotic when it shows a positive largest Lyapunov exponent (LLE), or with an attractor with fractal characteristics. Nonlinear analysis have often been used to characterize physiological signals [32, 33, 34].

The first nonlinear approach to CoP signal was described in [4] by Yamada, who verified the chaotic behaviour of stabilograms. After this first paper, many authors analyzed CoP trajectories as chaotic signals [26, 35, 36, 37, 38, 39, 40, 41]. We will briefly summerize nonlinear analysis approach and describe the computed stabilometric parameters.

The main idea is that under generic conditions the attractor A of a dynamical system D (in our case the postural system) of which we know the time-series (CoP time-series) can be embedded into a vector space V of a suitable dimension m using a lag τ. The analysis starts from the original data y(t) from which it is possible to calculate new vectors $\bar{Y}(t)$ belonging to the embedded space formed from time-delayed version of y(t).

$$\bar{Y}(t) = [y(t), y(t+\tau), y(t+2\tau), ..., y(t+(m-1)\tau)], \tag{2.7}$$

where $\bar{Y}(t)$ is the m-dimensional state vector, τ is the time delay and m is the embedding dimension. The optimal choice for the parameters τ and m is estimated, respectively, with the mutual information function I(τ) and the false nearest method (both described in [26]).

Once done this state-space reconstruction, it is possible to compute the most relevant properties of the system like the fractal dimension, or correlation dimension, D_2 and the maximum for the Lyapunov exponent of the attractor A. The computation method si well explained in [26, 37]. In numerous articles a preliminary surrogate data test has been presented, to verify the deterministic nature of time series [4, 26, 40]. Summarizing, the calculates parameters using the described approach are:

- the correlation dimension D_2 which is a simple measure of the possibly fractal size of the attractor and also a geometrical measure of complexity;
- the largest Lyapunov exponent as a measure of chaos, which indicates how sensitive the system is to initial conditions.

An alternative way of nonlinear analysis is proposed in [38], implementing on postural sway a method proposed by Higuchi [42]. This method, in contrast to an attractor' s fractal dimension, does not require preliminary reconstruction of the system's phase space but can be directly applied to experimental data. The calculated fractal dimension D_f denotes the fractal dimension of the signal' s time series itself and should not be confused with the previously described attractor s fractal dimension measured in the system' s phase space. The fractal dimension was interpreted as a measure of the complexity of posturographic signal. This method was applied by Doyle in [39].

2.2.5 Other approaches

Many other parameters have been described in literature, but they are not widely used in posturography.
Blaszczyk in [43] introduced the "Sway ratio" parameter, obtained as the CoP-to-CoM path length ratio. This parameter was formulated in order to take in account both the CoP and CoM characteristics.

Following the Collins and De Luca proposal of analyzing the CoP trajectories as fractional Brownian motion [3], many different approaches for the analysis of CoP dynamics have been described. Bardet [44] proposed a multiscale fractional Brownian motion to investigate postural control. One approach is based on the quantification of the complexity of COP time series in terms of their irregularity. Newell [45] used the approximate entropy to characterize the dynamical structure of human postural sway. The aim was to investigate the effect of motor development and aging on the complexity of COP trajectories during quiet standing. The results were consistent with the hypothesis of a reduction of the degrees of freedom of the system with aging. Sabatini [46] combined different algorithms using entropy measures of signal complexity, to extract a complexity index and investigated the effect of visual perception. Roerdink et al. [41] published a study on the dynamical structures of COP trajectories in patients recovering from stroke. Ramdani et al [47] described a sample entropy algorithm to characterize the irregularity of the CoP trajectories through the analysis of the velocity variable.
An other described approach consists of modeling CoP trajectories using Markov chains [48, 49]. Following this approach, a discrete Markov chain model was used to extract

dynamical information from CoP signals; in [49], the Invariant Density Analysis (IDA), based on the Markov chain calculated on the CoP trajectories, was proposed.

It has been demonstrated that CoP trajectories are non-stationary signals [50, 51]. Different methods have been applied to CoP trajectories to evaluate time varying characteristics: short time Fourier transform (STFT) [52], methods based on bilinear distributions [53, 54], evolutionary spectrum theory [55, 56], wavelet decomposition [57]. In this thesis the non-stationarity of the CoP signals will be afforded in chapter 3 and 5. An alternative approach based on the Hilbert-Huang transformation was described in [58, 59], both using univariate and bivariate empirical mode decomposition.

A really interesting approach was described by Bravi and Sabatini in [27]. They observed that it is a commonplace to analyze orthogonal components AP and ML of the CoP trajectories separately. The proposal was to consider the real and imaginary parts of a complex-valued signal in terms of AP and ML components of the postural sway. Using this representation is possible to exploit information both from the amplitude and the phase of the CoP signal. The authors introduced a hyper complex approach in modeling postural sway, processing four-dimensional representation obtained from the complex-valued CoP signal.

Starting from the complex-valued representation of CoP trajectories, I proposed another approach in postural signals processing, based on the rotary spectra analysis [60, 61]. This method will be exhaustively described in chapter 3.

2.3 Conclusions

A typical experimental set-up for static posturography and critical aspects in designing posturographic experiments have been described.

The presented approaches to cope with the CoP signal led to many different typologies of parameters. Although most of them have been developed from a model of the signal, no widespread consensus has emerged so far about the clinical meaningful application of such methods [2].

In the next chapter a new analysis method will be introduced, based on the application of the rotary spectra analysis technique to the CoP signal.

References

[1] T. E. Prieto, J. B. Myklebust, R. G. Hoffmann, E. G. Lovett, and B. M. Myklebust, "Measures of postural steadiness: differences between healthy young and elderly adults.," *IEEE Trans Biomed Eng*, vol. 43, pp. 956–966, Sep 1996.

[2] L. Baratto, P. G. Morasso, C. Re, and G. Spada, "A new look at posturographic analysis in the clinical context: sway-density versus other parameterization techniques.," *Motor Control*, vol. 6, pp. 246–270, Jul 2002.

[3] J. J. Collins and C. J. DeLuca, "Open-loop and closed-loop control of posture: a random-walk analysis of center-of-pressure trajectories.," *Exp Brain Res*, vol. 95, no. 2, pp. 308–318, 1993.

[4] N. Yamada, "Chaotic swaying of the upright posture," *Human Movement Science*, vol. 14, pp. 711–726, 1995.

[5] M. Schmid, S. Conforto, V. Camomilla, A. Cappozzo, and T. D'Alessio, "The sensitivity of posturographic parameters to acquisition settings.," *Med Eng Phys*, vol. 24, pp. 623–631, Nov 2002.

[6] L. Quagliarella, N. Sasanelli, and V. Monaco, "Drift in posturography systems equipped with a piezoelectric force platform: analysis and numerical compensation," *IEEE Transactions on instrumentation and measurement*, vol. 57(5), pp. 997–1003, 2008.

[7] H. Rogind, H. Simonsen, P. Era, and H. Bliddal, "Comparison of kistler 9861a force platform and chattecx balance system for measurement of postural sway: correlation and test-retest reliability.," *Scand J Med Sci Sports*, vol. 13, pp. 106–114, Apr 2003.

[8] A. Ruhe, R. Fejer, and B. Walker, "The test-retest reliability of centre of pressure measures in bipedal static task conditions–a systematic review of the literature.," *Gait Posture*, vol. 32, pp. 436–445, Oct 2010.

[9] M. G. Carpenter, J. S. Frank, D. A. Winter, and G. W. Peysar, "Sampling duration effects on centre of pressure summary measures.," *Gait Posture*, vol. 13, pp. 35–40, Feb 2001.

[10] C. Bauer, I. Grger, R. Rupprecht, and K. G. Gassmann, "Intrasession reliability of force platform parameters in community-dwelling older adults.," *Arch Phys Med Rehabil*, vol. 89, pp. 1977–1982, Oct 2008.

[11] K. L. Clair and C. Riach, "Postural stability measures: what to measure and for how long.," *Clin Biomech (Bristol, Avon)*, vol. 11, pp. 176–178, Apr 1996.

[12] J. Middleton, P. Sinclair, and R. Patton, "Accuracy of centre of pressure measurement using a piezoelectric force platform.," *Clin Biomech (Bristol, Avon)*, vol. 14, pp. 357–360, Jun 1999.

[13] V. Agostini, E. Chiaramello, C. Bredariol, C. Cavallini, and M. Knaflitz, "Postural control after traumatic brain injury in patients with neuro-ophthalmic deficits.," *Gait Posture*, vol. 34, pp. 248–253, Jun 2011.

[14] M. Zok, C. Mazz, and A. Cappozzo, "Should the instructions issued to the subject in traditional static posturography be standardised?," *Med Eng Phys*, vol. 30, pp. 913–916, Sep 2008.

[15] J. Tarantola, A. Nardone, E. Tacchini, and M. Schieppati, "Human stance stability improves with the repetition of the task: effect of foot position and visual condition.," *Neurosci Lett*, vol. 228, pp. 75–78, Jun 1997.

[16] Z. Kapoula and T.-T. L, "Effects of distance and gaze position on postural stability in young and old subjects.," *Exp Brain Res*, vol. 173, pp. 438–445, Aug 2006.

[17] W. McIlroy and B. Maki, "Preferred placement of the feet during quiet stance: development of a standardized foot placement for balance testing," *Clinical Biomechanics*, vol. 12(1), p. 6670, 1997.

[18] L. Chiari, L. Rocchi, and A. Cappello, "Stabilometric parameters are affected by anthropometry and foot placement.," *Clin Biomech (Bristol, Avon)*, vol. 17, no. 9-10, pp. 666–677, 2002.

[19] A. Mouzat, M. Dabonneville, and P. Bertrand, "The effect of feet position on orthostatic posture in a female sample group," *Neuroscience Letters*, vol. 365, p. 7982, 2004.

[20] H. van der Kooij, A. D. Campbell, and M. G. Carpenter, "Sampling duration effects on centre of pressure descriptive measures.," *Gait Posture*, vol. 34, pp. 19–24, May 2011.

[21] S. H. Nordahl, T. Aasen, B. M. Dyrkorn, S. Eidsvik, and O. I. Molvaer, "Static stabilometry and repeated testing in a normal population.," *Aviat Space Environ Med*, vol. 71, pp. 889–893, Sep 2000.

[22] J. A. Raymakers, M. M. Samson, and H. J. J. Verhaar, "The assessment of body sway and the choice of the stability parameter(s).," *Gait Posture*, vol. 21, pp. 48–58, Jan 2005.

[23] N. Pinsault and N. Vuillerme, "Test-retest reliability of centre of foot pressure measures to assess postural control during unperturbed stance.," *Med Eng Phys*, vol. 31, pp. 276–286, Mar 2009.

[24] M. Salavati, M. R. Hadian, M. Mazaheri, H. Negahban, I. Ebrahimi, S. Talebian, A. H. Jafari, M. A. Sanjari, S. M. Sohani, and M. Parnianpour, "Test-retest reliability [corrected] of center of pressure measures of postural stability during quiet standing in a group with musculoskeletal disorders consisting of low back pain, anterior cruciate ligament injury and functional ankle instability.," *Gait Posture*, vol. 29, pp. 460–464, Apr 2009.

[25] L. Rocchi, L. Chiari, and A. Cappello, "Feature selection of stabilometric parameters based on principal component analysis.," *Med Biol Eng Comput*, vol. 42, pp. 71–79, Jan 2004.

[26] L. Ladislao and S. Fioretti, "Nonlinear analysis of posturographic data," *Med Biol Eng Comput*, vol. 45, pp. 679–688, 2007.

[27] A. Bravi and A. M. Sabatini, "A multidimensional approach to postural sway modeling," in *Medical Measurements and Applications Proceedings (MeMeA), 2010 IEEE International Workshop on*, 2010.

[28] J. J. Collins and C. J. DeLuca, "The effects of visual input on open-loop and closed-loop postural control mechanisms.," *Exp Brain Res*, vol. 103, no. 1, pp. 151–163, 1995.

[29] J. J. Collins, C. J. D. Luca, A. Burrows, and L. A. Lipsitz, "Age-related changes in open-loop and closed-loop postural control mechanisms.," *Exp Brain Res*, vol. 104, no. 3, pp. 480–492, 1995.

[30] P. G. Morasso, L. Baratto, R. Capra, and G. Spada, "Internal models in the control of posture.," *Neural Netw*, vol. 12, pp. 1173–1180, Oct 1999.

[31] M. Jacono, M. Casadio, P. G. Morasso, and V. Sanguineti, "The sway-density curve and the underlying postural stabilization process.," *Motor Control*, vol. 8, pp. 292–311, Jul 2004.

[32] P. C. Ivanov, L. A. Amaral, A. L. Goldberger, S. Havlin, M. G. Rosenblum, Z. R. Struzik, and H. E. Stanley, "Multifractality in human heartbeat dynamics.," *Nature*, vol. 399, pp. 461–465, Jun 1999.

[33] A. L. Goldberger, L. A. N. Amaral, J. M. Hausdorff, P. C. Ivanov, C.-K. Peng, and H. E. Stanley, "Fractal dynamics in physiology: alterations with disease and aging.," *Proc Natl Acad Sci U S A*, vol. 99 Suppl 1, pp. 2466–2472, Feb 2002.

[34] A. Eke, P. Hermn, J. B. Bassingthwaighte, G. M. Raymond, D. B. Percival, M. Cannon, I. Balla, and C. Ikrnyi, "Physiological time series: distinguishing fractal noises from motions.," *Pflugers Arch*, vol. 439, pp. 403–415, Feb 2000.

[35] A. Murata and H. Iwase, "Chaotic analysis of body sway," in *Conf Proc IEEE Eng Med Biol Soc, Vol 20, No 3*, 1998.

[36] S. Fioretti, M. Guidi, L. Ladislao, and G. Ghetti, "Analysis and reliability of posturographic parameters in parkinson patients at an early stage.," *Conf Proc IEEE Eng Med Biol Soc*, vol. 1, pp. 651–654, 2004.

[37] P. Pascolo, F. Barazza, and R. Carniel, "Considerations on the application of the chaos paradigm to describe the postural sway," *Chaos, Solitons and Fractals*, vol. 27, pp. 1339–1346, 2006.

[38] J. W. Blaszczyk and W. Klonowski, "Postural stability and fractal dynamics.," *Acta Neurobiol Exp (Wars)*, vol. 61, no. 2, pp. 105–112, 2001.

[39] T. L. A. Doyle, E. L. Dugan, B. Humphries, and R. U. Newton, "Discriminating between elderly and young using a fractal dimension analysis of centre of pressure.," *Int J Med Sci*, vol. 1, no. 1, pp. 11–20, 2004.

[40] J. B. Myklebust, T. Prieto, and B. Myklebust, "Evaluation of nonlinear dynamics in postural steadiness time series.," *Ann Biomed Eng*, vol. 23, no. 6, pp. 711–719, 1995.

[41] M. Roerdink, M. D. Haart, A. Daffertshofer, F. Donker, A. C. H. Geurts, and P. J. Beek, "Dynamical structure of center-of-pressure trajectories in patients recovering from stroke," *Exp Brain Res*, vol. 174, p. 256269, 2006.

[42] T. Higuchi, "Approach to an irregular time series on the basis of the fractal theory," *Physica D: Nonlinear Phenomena*, vol. 31(2), pp. 277–283, 1988.

[43] J. W. Blaszczyk, "Sway ratio - a new measure for quantifying postural stability.," *Acta Neurobiol Exp (Wars)*, vol. 68, no. 1, pp. 51–57, 2008.

[44] J.-M. Bardet and P. Bertrand, "Identification of the multiscale fractional brownian motion with biomechanical applications," *JOURNAL OF TIME SERIES ANALYSIS*, vol. 28(1), p. 152, 2007.

[45] K. M. Newell, *Applications of nonlinear dynamics to developmental process modeling*, ch. Degrees of freedom and the development of postural center of pressure profiles., p. 63/84. Lawrence Erlbaum Associates Publishers, 1998.

[46] A. M. Sabatini, "Analysis of postural sway using entropy measures of signal complexity," *Med Biol Eng Comput*, vol. 38, pp. 617–624, 2000.

[47] S. Ramdani, B. Seigle, J. Lagarde, F. Bouchara, and P. L. Bernard, "On the use of sample entropy to analyze human postural sway data.," *Med Eng Phys*, vol. 31, pp. 1023–1031, Oct 2009.

[48] J. Rasku, M. Juhola, T. Tossavainen, I. Pyykko, and E. Toppila, "Modelling stabilograms with hidden markov models.," *J Med Eng Technol*, vol. 32, no. 4, pp. 273–283, 2008.

[49] P. Hur, K. A. Shorter, P. G. Mehta, and E. T. Hsiao-Wecksler, "Invariant density analysis: modeling and analysis of the postural control system using markov chains.," *IEEE Trans Biomed Eng*, vol. 59, pp. 1094–1100, Apr 2012.

[50] J. P. Carroll and W. Freedman, "Nonstationary properties of postural sway.," *J Biomech*, vol. 26, no. 4-5, pp. 409–416, 1993.

[51] K. Newell, S. Slobounov, B. Slobounova, and P. Molenaar, "Short-term nonstationarity and the development of postural control," *Gait Posture*, vol. 6, pp. 56–62, 1997.

[52] S. Conforto, T. DAlessio, and V. C. andA Cappozzo, "Time-frequency analysis of postural signals," in *Abstracts from the 1st SIAMOC Congress, Ancona, Italy*, 2001.

[53] P. J. Loughlin and M. S. Redfern, "Spectral characteristics of visually induced postural sway in healthy elderly and healthy young subjects.," *IEEE Trans Neural Syst Rehabil Eng*, vol. 9, pp. 24–30, Mar 2001.

[54] Y.-J. Shin, D. Gobert, S.-H. Sung, E. J. Powers, and J. B. Park, "Application of cross time-frequency analysis to postural sway behavior: the effects of aging and visual systems.," *IEEE Trans Biomed Eng*, vol. 52, pp. 859–868, May 2005.

[55] T. Schumann, M. S. Redfern, J. M. Furman, A. el Jaroudi, and L. F. Chaparro, "Time-frequency analysis of postural sway.," *J Biomech*, vol. 28, pp. 603–607, May 1995.

[56] M. Ferdjallah, G. F. Harris, and J. J. Wertsch, "Instantaneous postural stability characterization using time-frequency analysis.," *Gait Posture*, vol. 10, pp. 129–134, Oct 1999.

[57] J. R. Chagdes, S. Rietdyk, J. M. Haddad, H. N. Zelaznik, A. Raman, C. K. Rhea, and T. A. Silver, "Multiple timescales in postural dynamics associated with vision and a secondary task are revealed by wavelet analysis.," *Exp Brain Res*, vol. 197, pp. 297–310, Aug 2009.

[58] H. Amoud, M. Abadi, D. J. Hewson, V. Michel-Pellegrino, M. Doussot, and J. Duchne, "Fractal time series analysis of postural stability in elderly and control subjects.," *J Neuroeng Rehabil*, vol. 4, p. 12, 2007.

[59] H. Amoud, H. Snoussi, D. Hewson, and J. Duchene, "Univariate and bivariate empiricalmode decomposition for postural stability analysis," *EURASIP Journal on Advances in Signal Processing*, 2008.

[60] E. Chiaramello, M. Knaflitz, and V. Agostini, "Rotary spectra analysis applied to static stabilometry.," *Conf Proc IEEE Eng Med Biol Soc*, vol. 2011, pp. 4939–4952, 2011.

[61] E. Chiaramello, V. Agostini, and M. Knaflitz, "Rotational components in centre of pressure signals," in *III Congresso del Gruppo Nazionale di Bioingegneria (GNB 2012)*, Patron, 2012.

3

Rotary spectra analysis

Many interesting time series are intrinsically bivariate. If the two variables represent the same physical quantity, such as a position or a velocity, or may be normalized in some meaningful way, then it is natural to think of the time series as tracing out an ellipse. Some examples of signals of this type include: planetary orbits, two-dimensional oscillators, measurements of currents or wind, electromagnetic polarization, and the three orthogonal planes of seismic motion. [1]

Among these different examples it is possible to consider also the CoP signal as a bivariate time-series, allowing to analyzing it from a different point of view. The underlying rationale in this approach is the hypothesis that the CoP signal contains rotational components.

To extract the rotational components from CoP signal I applied rotary spectra analysis, a well known technique developed in the meteorological and oceanographic fields by Gonella [2] and Mooers [3] as a method to cope with bidimensional time series. In particular, this method was used for the interpretation of geophysical data exhibiting inherent rotational characteristics [4]. This problem has been well explained by Mooers in [3]: *"Physical oceanographers are increasingly confronted with the necessity of analyzing time series of horizontal velocity. For time series of velocity which have sampled simultaneously at two or more spatial points, a statistical measure of the coherence and phase versus frequency is often desired."*

Rotary spectra analysis involves the representation of a two-dimensional signal in the complex plane as a superimposition of ellipses, which can be analyzed in terms of their shape and orientation. Each ellipse is the sum of a counterclockwise (CCW) and a clockwise (CW) rotating phasors, called rotary components. From a mathematical

point of view, each ellipse is the widely linear minimum mean-squared error approximation of the signal from its rotary components at a given frequency f [5]. From a practical point of view, the analysis of ellipse and rotary components properties carries information about the underlying physics. This approach allows to separate rotational iso-frequential components from non-rotational ones.

The advantages in analyzing time-series - when showing rotational components - in terms of polarized components are: (i) it is possible to analyze both the Cartesian components in the frequency domain, not only considering their vector sum in the plane (ii) the calculation of coherence and phase for the polarized components is invariant under the coordination rotation [3].

The developed method was applied not only in analyzing oceanographic data, but also in optics [6], astronomy [7], electromagnetics and communications [8].

To the best of our knowledge, the rotary spectral analysis was never applied in biomedical signal processing.

In this chapter the description of the mathematical formulation of the rotary spectra will be provided, both in stationary and non-stationary cases.

3.1 Stationary case

In this section I will analyze the rotary spectra analysis applied to a bivariate time series which real-valued time series $x(t)$ and $y(t)$ are stationary stochastic processes. The analysis will be carried out considering the complex-valued time series $w(t) = x(t) + jy(t)$ [9].

The basic steps in rotary spectra analysis are:

- A two dimensional vector can be represented as a complex-valued function of time
- The complex-valued vector can de decomposed, for each frequency, into two counter-rotating components
- Two-sided spectra and one cross-spectrum can be calculated

The rotary spectral analysis involves the representation of a random time series in complex form and its subsequent decomposition into two polarized counter-rotating components in the frequency domain. In this representation A^-, A^+, and θ^-, θ^+, are amplitudes and phases of the clockwise (CW) and counter-clockwise (CCW) rotating

components, respectively. The CCW component is considered to be rotating with positive angular frequency ($\omega \geq 0$) and the CW component with negative angular frequency ($\omega \leq 0$).

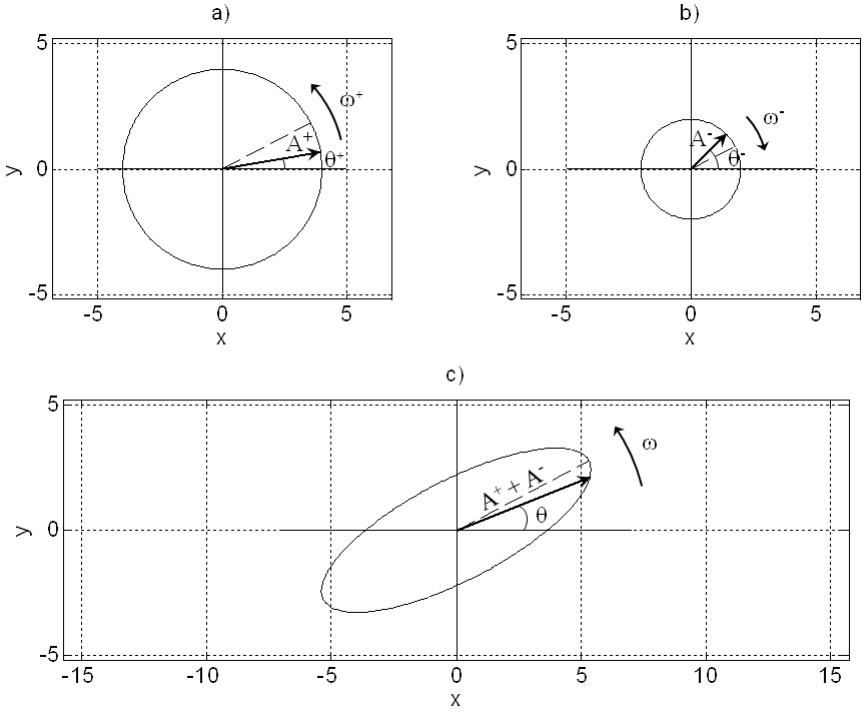

Figure 3.1: a) Counter-clockwise component ω^+, with amplitude A^+ and initial phase θ^+. b) Clockwise component ω^- with amplitude A^- and initial phase θ^-. c) Ellipse formed by the vector addition of two counter-rotating vectors, with major axis $|A^+ + A^-|$ tilted at an angle $\frac{\theta^+ + \theta^-}{2}$ counter-clockwise. In this case the prevalent verse of rotation is the counter-clockwise one.

The eccentricity ϵ of the ellipse is determined by the relative amplitudes of the two components. Motions at frequency ω are circularly polarized if one of the two components is zero; motions are rectilinear if both circularly polarized components have the same magnitude. In these cases, the shape of the ellipse degenerates into a circle or into a line, respectively [5].
The combined vector - obtained from the vector sum of the two oppositely rotating circular components - traces out an ellipse over one complete cycle, as shown in figure 3.1.

In the next paragraphs mathematical details about the method will be described.

3.1.1 Rotary component analysis

A bi-dimensional time series with components x(t) and y(t) can be represented in Cartesian coordinates as a complex function:

$$w(t) = x(t) + jy(t) \tag{3.1}$$

This representation allows to consider also the information arising from the phase of the complex time series and not only amplitude of the single real-valued time series [5].

We assume that the component x(t) and y(t) are continuous, stationary stochastic processes with zero mean values, and that they have Fourier integral representation [3]. The vector w(t) can be written in Fourier series form

$$\begin{aligned} w(t) &= \overline{x(t)} + \sum_{k=1}^{N} X_k cos(\omega_k t - \phi_k) + j\left[\overline{y(t)} + \sum_{k=1}^{N} Y_k cos(\omega_k t - \psi_k)\right] = \\ &= \left[\overline{x(t)} + j\overline{y(t)}\right] + \sum_{k=1}^{N} \left[X_k cos(\omega_k t - \phi_k) + jY_k cos(\omega_k t - \psi_k)\right] \end{aligned} \tag{3.2}$$

where $\overline{x(t)} + j\overline{y(t)}$ is the mean value, $\omega_k = 2\pi f_k, f_k = \frac{k}{N\Delta t}, k = 1, ..., N$ is the angular frequency, $t = n\Delta t$ is the time, n is the length of each time series in samples, $N = nf_{sampling}$, and and (X_k, Y_k) and (ϕ_k, ψ_k) are the amplitudes and phases, respectively, of the Fourier constituents - for each frequency - of the real and imaginary components.

Subtracting the mean value and expanding the trigonometric functions, we find:

$$\begin{aligned} w'(t) &= w(t) - \overline{w(t)} = \\ &= \sum_{k=1}^{N} \left[X_{1k} cos(\omega_k t) + X_{2k} sin(\omega_k t)\right] + j\left[Y_{1k} cos(\omega_k t) + Y_{2k} sin(\omega_k t)\right], \end{aligned} \tag{3.3}$$

where

$$\begin{aligned} X_{1k} &= X_k cos\phi_k \quad X_{2k} = X_k sin\phi_k \\ Y_{1k} &= Y_k cos\psi_k \quad Y_{2k} = Y_k sin\psi_k. \end{aligned} \tag{3.4}$$

It is possible to separate each k^{th} frequency component of the series in the sum of

counter-clockwise and clockwise components

$$w_k(t) = w_k^+(t) + w_k^-(t) = A_k^+ e^{j\theta_k^+} e^{j\omega_k t} + A_k^- e^{j\theta_k^-} e^{j\omega_k t} = \\ = e^{\frac{j(\theta_k^+ + \theta_k^-)}{2}} \left\{ \left[A_k^+ + A_k^-\right] cos(\frac{j(\theta_k^+ + \theta_k^-)}{2} + \omega_k t) + j\left[A_k^+ - A_k^-\right] sin(\frac{j(\theta_k^+ + \theta_k^-)}{2} + \omega_k t) \right\}, \tag{3.5}$$

where the amplitudes of the CCW and CW rotary components are:

$$\begin{aligned} A_k^+ &= \frac{1}{2}\left[(X_{1k} + Y_{2k})^2 + (X_{2k} - Y_{1k})^2\right]^{\frac{1}{2}} \\ A_k^- &= \frac{1}{2}\left[(X_{1k} - Y_{2k})^2 + (X_{2k} + Y_{1k})^2\right]^{\frac{1}{2}} \end{aligned} \tag{3.6}$$

and the corresponding phase angle for time t=0 are:

$$\begin{aligned} \theta_k^+ &= tan^{-1}\left[\frac{(Y_{1k} - X_{2k})}{(X_{1k} + Y_{2k})}\right] \\ \theta_k^- &= tan^{-1}\left[\frac{(Y_{1k} + X_{2k})}{(X_{1k} - Y_{2k})}\right]. \end{aligned} \tag{3.7}$$

For each frequency value, the components of the equation 3.5 form an ellipse on the complex plane, with semi-major axis $L_M =\mid A_k^+ + A_k^- \mid$, semi-minor axis $L_m =\mid A_k^+ - A_k^- \mid$, and eccentricity $\epsilon_k = \frac{2\sqrt[2]{A_k^+ A_k^-}}{A_k^+ + A_k^-}$. The ellipse is tilted at an angle $\frac{1}{2}(\theta_k^+ + \theta_k^-)$ from the x-axis in counter-clockwise direction. The vector resulting from the composition of the rotating vectors at that frequency value is along the major axis of the ellipse at time $t = \frac{\theta^+ - \theta^-}{4\pi f_k}$, when the two rotating vectors are overlapped.

The one-sided spectra for the two oppositely rotaring components for frequencies $f_k = \frac{\omega}{2\pi}$ are:

$$\begin{aligned} S(f_k^+) &= (A_k^+)^2, \quad f_k = 0, ..., \frac{1}{2\Delta t} \\ S(f_k^-) &= (A_k^-)^2, \quad f_k = -\frac{1}{2\Delta t}, ..., 0. \end{aligned} \tag{3.8}$$

Division by the signal time duration T transforms the energy spectral density of equation 3.8 into the power spectral density:

$$\begin{aligned} S(f_k^+) &= \frac{(A_k^+)^2}{N\Delta t}, \quad f_k = 0, ..., \frac{1}{2\Delta t} \\ S(f_k^-) &= \frac{(A_k^-)^2}{N\Delta t}, \quad f_k = -\frac{1}{2\Delta t}, ..., 0. \end{aligned} \tag{3.9}$$

As reported by both Gonella [2] and Mooers [3], it is possible to represent the spectral energy $S^+(f)$ and $S^-(f)$ for the two oppositely rotating components in terms of the Cartesian components.

$$\begin{aligned} S(f_k^+) &= (A_k^+)^2 = \frac{1}{2}\left[S_{xx}(f_k) + S_{yy}(f_k) + 2Q_{xy}(f_k)\right] \quad f_k \geq 0 \\ S(f_k^-) &= (A_k^-)^2 = \frac{1}{2}\left[S_{xx}(f_k) + S_{yy}(f_k) - 2Q_{xy}(f_k)\right] \quad f_k \leq 0 \end{aligned} \tag{3.10}$$

where

$$\begin{aligned} S_{xx}(f_k) &= \frac{1}{2}(X_{1k}^2 + X_{2k}^2) \\ S_{yy}(f_k) &= \frac{1}{2}(Y_{1k}^2 + Y_{2k}^2) \end{aligned} \tag{3.11}$$

are the autospectra of the x(t) and y(t) cartesian components. The cross-spectra of the cartesian components x(t) and y(t) is defined as:

$$\begin{aligned} &S_{xy}(f_k) = \frac{1}{2}X^*(f_k)Y(f_k) = \frac{1}{2}X_kY_ke^{j(\phi_k - \psi_k)} = \\ &= \frac{1}{2}\left\{X_kY_kcos(\phi_k - \psi_k) + jX_kY_ksin(\phi_k - \psi_k)\right\} = \\ &= \frac{1}{2}\left\{X_kY_k(cos\phi_kcos\psi_k + sin\phi_ksin\psi_k) + jX_kY_k(sin\phi_kcos\psi_k - cos\phi_ksin\psi_k)\right\} = \\ &= \frac{1}{2}(X_{1k}Y_{1k} + X_{2k}Y_{2k}) - j\frac{1}{2}(X_{1k}Y_{2k} - X_{2k}Y_{1k}) = \\ &= C_{xy}(f_k) - jQ_{xy}(f_k), \end{aligned} \tag{3.12}$$

and

$$Q_{xy}(f_k) = (X_{1k}Y_{2k} - X_{2k}Y_{1k}) \tag{3.13}$$

is the quadrature of the spectrum.

Gonella [2] defined two other parameters to characterize the rotating components of a time series, the mean orientation of the ellipse:

$$\psi(f_k) = \frac{1}{2}tan^{-1}\left[\frac{2S_{xy}(f_k)}{S_{xx}(f_k) - S_{yy}(f_k)}\right], \tag{3.14}$$

and the "stability of ellipse":

$$\begin{aligned} \mu(f_k) &= \frac{\langle A^+A^-\rangle}{\sqrt[2]{(S^+(f_k) - S^-(f_k))}} = \\ &= \frac{1}{2}\frac{\mid S_{xx}(f_k) - S_{yy}(f_k) + jS_{xy}(f_k) \mid}{\sqrt[2]{(S^+(f_k) - S^-(f_k))}}. \end{aligned} \tag{3.15}$$

This parameter is defined similarly to the coherence function between the clockwise and counter-clockwise rotating components.

Another useful property parameter to describe a motion in terms of rotating components is the *rotary coefficient*, to study if there is a prevalence of the CW component over the CCW component, or vice versa, defined as:

$$r(f_k) = \frac{S_k^+(f_k) - S_k^-(f_k)}{S_k^+(f_k) + S_k^-(f_k)}, \tag{3.16}$$

which ranges from r = -1 for clockwise motion, to r = 0 for unidirectional motion, and to r = 1 for counter-clockwise motion. It provides an objective means of quantifying the rotation associated with the asymmetry of the spectrum and is directly related to the expected ellipse shape, at each frequency [10]. The rotary coefficient is defined for each specific frequency. In [9] a description of the statistical properties of the rotary coefficient were given, deriving a confidence interval for the rotary coefficient values.

If one is interested in obtaining a single value that describes the prevalence of one component over the other, a different parameter - condensing the overall information - must be introduced. To this purpose I define the Integrated Rotary Coefficient:

$$IRC = \sum_{k=1}^{N} \rho(f_k) \tag{3.17}$$

Examples

In order to clarify the above described rotary spectra analysis, I applied rotary decomposition to simple motions in the plane. I would like to highlight how rotary spectra analysis allows to extrapolate rotation components from a motion in the plane, selecting in this way motions which Cartesian components are iso-frequential.

Figure 3.2 shows a CCW circular motion, figure 3.3 a rectilinear motion, figure 3.4 a random motion, and figure 3.5 the superimposition of a CCW circular motion and a random motion. Since we are treating complex signals, the spectra are not symmetric. In the representation of the CW spectral component I have folded the negative frequency axis around f = 0 and plotted it on the positive frequency axis.

Figure 3.2(a) shows the CCW circular trajectory w(t) in the xy plane. Both Cartesian components are sinusoidal, with angular frequency ω equal to 1 rotation per second (rps) and the amplitude equal to 1 mm. In figures 3.2(b) and 3.2(c) the CCW and CW rotary spectral components are reported, respectively.

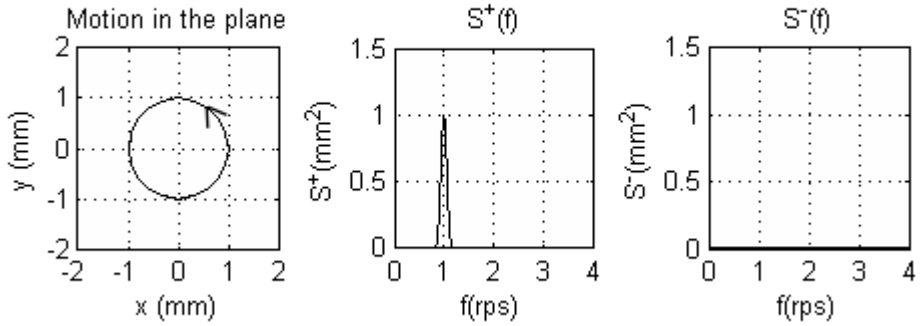

Figure 3.2: Counter-clockwise circular motion in the plane xy and its rotary spectral decomposition.

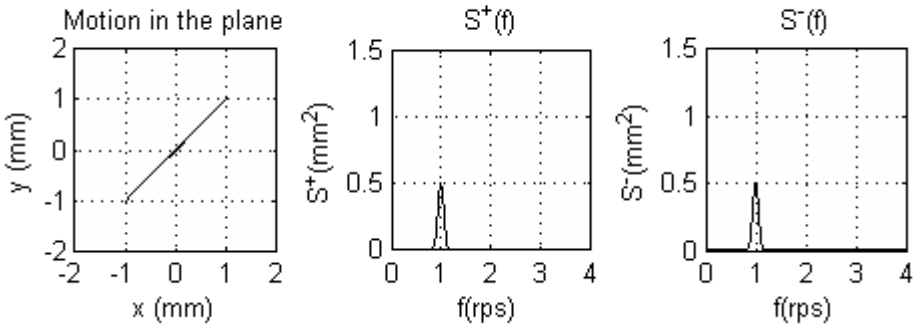

Figure 3.3: Rectilinear motion in the plane xy and its rotary spectral decomposition.

Figure 3.3(a) shows the rectilinear trajectory w(t) in the xy plane, whose Cartesian components have the same oscillation frequency equal to ω equal to 1 rotation per second (rps). Figures 3.3(b) and 3.3(c) show the rotary spectra corresponding to the CCW and CW components, respectively. Both CCW and CW components show a peak with amplitude equal to 0.5 mm^2 at 1 rps.

Figure 3.4(a) shows the trajectory w(t) in the xy plane, whose completely uncorrelated Cartesian components x(t) and y(t) were modeled as Gaussian process with zero-mean and variance $\sigma^2 = 1$. They have been filtered with a shaping band-pass filter with low cutoff frequency equal to 0.05 Hz and high cutoff frequency equal to 4 Hz, to mimic the CoP signal bandwidth. Figures 3.4(b) and 3.4(c) show the rotary

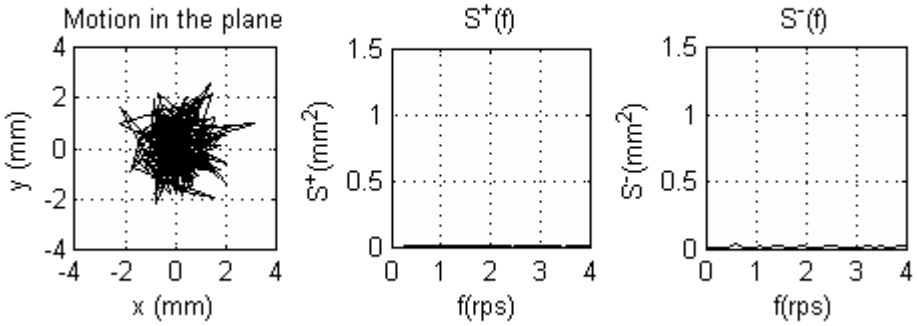

Figure 3.4: Random motion in the plane xy and its rotary spectral decomposition.

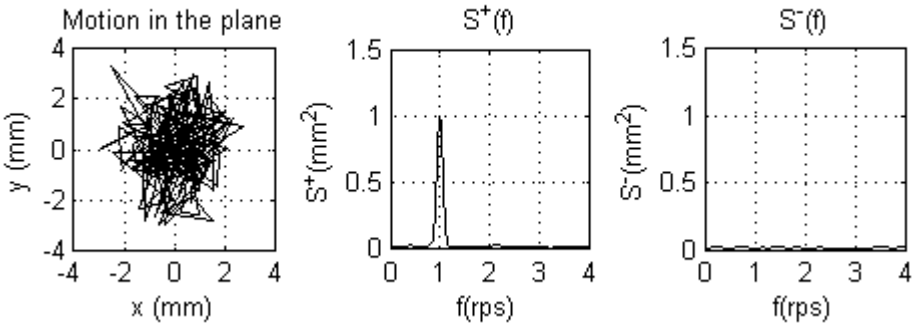

Figure 3.5: Superimposition of a CCW circular motion and random motion: trajectory in xy plane and rotary spectra components.

spectra corresponding to the CCW and CW components, respectively. As expected, no rotating components is detected, since the motion is completely random.

Figure 3.5(a) shows the trajectory in the xy plane due to the superimposition of the CCW circular motion and the random motion previously analyzed. The characteristics of the CCW circular motion are angular frequency ω equal to 1 rps and amplitude equal to 1 mm. Figure 3.5(a) appears very similar to the previously described figure 3.4(a), as looking at the trajectory in the plane we are not able to distinguish the CCW circular from the random motion. Applying the rotary spectra analysis, I am able to extract the CCW circular component, as shown in figures 3.5(b) and 3.5(c).

3.1.2 Rotary cross spectral analysis

Having summarized the rotary vector analysis for a single time series, now I want to consider the coherence and the cross-spectral properties for two time series. The purpose is to determine the similarity between the two time series in terms of their circularly polarized components. For two vector series, two one-sided autospectra and two one-sided cross-spectra can be computed for the rotary components. Mooers [3] formulated these as two two-sided rotary autospectra called, respectively, the *Inner cross-spectrum* and *Outer cross-spectrum.* This terminology originating from the resemblance of the inner and outer rotary autocovariance functions derived from the autospectra to the inner (dot) and outer (cross) products in mathematics. As the spectra are complex, they have both amplitude and phase. Hence, coherence and phase spectra can be computed, just as with the cross-spectra of two scalar time series.

Inner functions describe co-rotating components, while outer functions describe counter-rotating components. I could, of course, use standard Cartesian components for this task. Unfortunately, the Cartesian vectors and their derived relationships generally are dependent on the selected orientation of the coordinate system.

The advantages of the rotary type of analysis are: (i) the coherence analysis is independent of the coordinate system (i.e. is coordinate invariant); and (ii) the results encompass the coherence and phase of oppositely rotating, as well as like-rotating components, for motions that may be highly nonrectilinear. Because the counter-rotating components have circular symmetry, invariance under coordinate rotation follows for coherence.

I consider two vector time series :

$$w_1(t) = u_1(t) + jv_1(t) \qquad \text{and} \qquad w_2(t) = u_2(t) + jv_2(t)$$

with Fourier transform $W_1(f_k)$ and $W_2(f_k)$, where

$$W_j(f_k) = \begin{cases} A_j^+ e^{-j\theta_j^+} \text{ if } \quad f_k \geq 0 \\ \\ A_j^- e^{-j\theta_j^-} \text{ if } \quad f_k \leq 0. \end{cases} \qquad j = 1, 2 \tag{3.18}$$

The inner cross spectrum $S_{w_n w_m}(\omega)$ provides an estimation of the joint energy content of the two times series for rotating components rotating in the same direction

$$S_{w_n w_m}(\omega) = \begin{cases} A_n^+(\omega) A_m^+(\omega) e^{-j(\theta_n^+ - \theta_m^+)} & \text{if} \quad \omega \geq 0 \\ \\ A_n^-(\omega) A_m^-(\omega) e^{-j(\theta_n^- - \theta_m^-)} & \text{if} \quad \omega \leq 0 \end{cases} \tag{3.19}$$

For n = m the inner spectrum is the power spectrum of the counter-clockwise series for positive frequencies and the power spectrum of the clockwise series for negative frequencies.

$$S_{w_n w_n}(\omega) = \begin{cases} \mid A_n^+(\omega) \mid^2 & \text{if} \quad (\omega) \geq 0 \\ \\ \mid A_n^-(\omega) \mid^2 & \text{if} \quad (\omega) \leq 0 \end{cases} \tag{3.20}$$

In terms of cartesian components, this is equivalent to equation 3.10.

Is it possible to define the square coeherence function related to the inner cross-spectrum.

$$\gamma_{12}^2(\omega) = \begin{cases} \frac{\left\langle \left[A_1^+ A_2^+ cos(\phi_1^+ - \phi_2^+)\right]^2 \right\rangle + \left\langle \left[A_1^+ A_2^+ sin(\phi_1^+ - \phi_2^+)\right]^2 \right\rangle}{\left\langle (A_1^+)^2 \right\rangle \left\langle (A_2^+)^2 \right\rangle} \text{ if } \omega \geq 0 \\ \\ \frac{\left\langle \left[A_1^- A_2^- cos(\phi_1^- - \phi_2^-)\right]^2 \right\rangle + \left\langle \left[A_1^- A_2^- sin(\phi_1^- - \phi_2^-)\right]^2 \right\rangle}{\left\langle (A_1^-)^2 \right\rangle \left\langle (A_2^-)^2 \right\rangle} \text{ if } \omega \leq 0 \end{cases} \tag{3.21}$$

The square coeherence function range is $0 \leq \gamma_{12}^2(\omega) \leq 1$ Is it possible to define the phase function related to the inner cross-spectrum.

$$\delta_{12}(\omega) = \begin{cases} tan^{-1}\left(\frac{\left\langle \left[A_1^+ A_2^+ sin(\phi_1^+ - \phi_2^+)\right] \right\rangle}{\left\langle \left[A_1^+ A_2^+ cos(\phi_1^+ - \phi_2^+)\right] \right\rangle}\right) \text{ if } \omega \geq 0 \\ \\ tan^{-1}\left(\frac{\left\langle \left[-A_1^- A_2^- sin(\phi_1^- - \phi_2^-)\right] \right\rangle}{\left\langle \left[A_1^- A_2^- cos(\phi_1^- - \phi_2^-)\right] \right\rangle}\right) \text{ if } \omega \leq 0 \end{cases} \tag{3.22}$$

The outer cross spectrum $Y_{w_n w_m}(\omega)$ provides an estimate of the joint energy content of the two times series for opposite rotating components.

$$Y_{w_n w_m}(\omega) = \begin{cases} A_n^-(\omega) A_m^+(\omega) e^{-j(\theta_m^+ - \theta_n^-)} & \text{if } \omega \geq 0 \\ \\ A_n^+(\omega) A_m^-(\omega) e^{j(\theta_n^+ - \theta_m^-)} & \text{if } \omega \leq 0 \end{cases} \tag{3.23}$$

For n = m, in a single case series

$$Y_{w_n w_n}(\omega) = A_n^-(\omega) A_n^+(\omega) e^{j(\theta_n^+ - \theta_n^-)} \quad (\omega) \geq 0 \tag{3.24}$$

$Y_{w_n w_n}((\omega))$ is simmetric about $\omega = 0$. However it is complex valued. In equation 3.15 the numerator corresponds to the outer-cross spectrum in the case of a single time series $Y_{w_n w_n}$. In fact, in terms of cartesian components, the outer cross spectrum is defined as:

$$Y_{w_n w_n}(\omega) = \frac{1}{2} \left[S_{xx}(f_k) - S_{yy}(f_k) + j S_{xy}(f_k) \right] \tag{3.25}$$

Is it possible to define the square coeherence function related to the outer cross-spectrum.

$$\lambda_{12}^2(\omega) = \begin{cases} \frac{\left\langle A_1^- A_2^+ \right\rangle^2 \left[\left\langle cos(\phi_2^+ - \phi_1^-) \right\rangle^2 + \left\langle sin(\phi_2^+ - \phi_1^-) \right\rangle^2 \right]}{\left\langle (A_2^+)^2 \right\rangle \left\langle (A_1^-)^2 \right\rangle} \text{ if } \omega \geq 0 \\ \\ \frac{\left\langle A_1^- A_2^+ \right\rangle^2 \left[\left\langle cos(\phi_1^+ - \phi_2^-) \right\rangle^2 + \left\langle sin(\phi_1^+ - \phi_2^-) \right\rangle^2 \right]}{\left\langle (A_1^+)^2 \right\rangle \left\langle (A_2^-)^2 \right\rangle} \text{ if } \omega \leq 0 \end{cases} \tag{3.26}$$

The square coeherence function range is $0 \leq \lambda_{12}^2(\omega) \leq 1$

Is it possible to define the phase function related to the outer cross-spectrum.

$$\psi_{12}(\omega) = \begin{cases} tan^{-1}\left(\frac{\left\langle \left[A_1^- A_2^+ sin(\phi_1^- - \phi_2^+) \right] \right\rangle}{\left\langle \left[A_1^- A_2^+ cos(\phi_1^- - \phi_2^+) \right] \right\rangle} \right) \text{ if } \omega \geq 0 \\ \\ tan^{-1}\left(\frac{\left\langle \left[A_1^+ A_2^- sin(\phi_2^- - \phi_1^+) \right] \right\rangle}{\left\langle \left[A_1^+ A_2^- cos(\phi_2^- - \phi_1^+) \right] \right\rangle} \right) \text{ if } \omega \leq 0 \end{cases} \tag{3.27}$$

The cross-spectral rotary analysis was applied in [11], in order to examine wind data obtained in different weather station.

3.2 Non-stationary case

The described analysis method is designed for stationary time-series, therefore it is not able to evaluate time-varying characteristics of bivariate time-series.

In literature have been described several effort in development of a time-frequency rotary spectra analysis to deal with non-stationary bi-variate signals in different research fields. Many works described extension of rotary spectra and polarization analysis to non-stationary signals focused on wavelet transform [1, 12, 13, 14, 15], Short Time Fourier Transform [16, 17], and bilinear transforms, in particular Rihaczek transform [10].

The first result was described by Crew [16]. The technique of analyzing time varying rotary spectra basically involved computing and plotting the rotary spectrum for one segment of a two components vector time-series, and then repeating this for segments centered successively later in time. In particular, hourly series of the vector components of the wind were generated and clock-averaged to form three-hourly mean series of the geographical vector components.

Another approach, based on wavelet decomposition, was proposed by Liu and Miller [12]. They used the complex-valued modulated Gaussian wavelet known as the Morlet wavelet transform to obtain time-frequency characteristics of rotary components in oceanographic data.

The wavelet approach was later applied also by Lilly and Gastard [1] in proposing a method for evaluating the properties of a time-varying elliptical signal. This work is focused on the geometrical properties of the polarization ellipse, and not on the time-frequency representation of the rotating components.

In [10] the bilinear Cohen's class Rihaczek time-frequency distribution was applied to deal with non-stationary bivariate signals. This approach provides, in each instant, a local ellipse in the complex plane which is the best local approximation of the signal from a given frequency component. The ellipse is characterized in terms of its shape, orientation, and degree of polarization.

In this chapter the problem of analyzing a non-stationary bivariate time-series in terms of rotary components using bilinear Cohen's class Choi-Williams time-frequency distribution. Moreover, a wavelet approach to the problem will be described.

3.2.1 Time-frequency analysis

The approach I propose is based on the Cohen Class of time-frequency representations [18], a largely used method in dealing with non-stationary biomedical signals [19, 20, 21, 22, 23, 24]. In the following I will briefly describe the properties of the time-frequency transforms of the Cohen Class. Finally, the extension of the rotary spectra analysis to non-stationary problems using the Choi-Williams time-frequency transform will be described.

The Cohen Class consists of all the bilinear time-frequency representations that are time and frequency shift invariant [18]. This characteristic is of paramount importance when the purpose is to correlate the time-frequency representation of a signal with the underlying physical or physiological phenomena [20].

All the time-frequency transforms belonging to the Cohen Class can be expressed in the following form:

$$TF(t,f) = \int_{-\infty}^{+\infty}\int_{-\infty}^{+\infty}\int_{-\infty}^{+\infty} x(t'+\frac{\tau}{2})x^*(t'-\frac{\tau}{2})g(\theta,\tau)e^{-j2\pi\theta(t'-t)}e^{-j2\pi f\tau}d\theta dt' d\tau, \tag{3.28}$$

where TF(t,f) is the time-frequency distribution, x(t) is the analytic signal obtained from the series of the signal samples, x*(t) is its complex conjugate, t is time, f is frequency, τ is time-lag, θ is frequency-lag, and $g(\theta,\tau)$ is referred to as the *kernel* of the transform. The kernel characteristics are strictly related to the distribution properties. Equation 3.28 leads to the definition of four different domains: the temporal correlation (t,τ), the spectral correlation (θ,f), the ambiguity (θ,τ), and the time-frequency (t,f). The starting point for this formulation is the definition of the instantaneous autocorrelation function in which the time dependence is maintained, in order to avoid not respecting the Wiener-Kintchine theorem:

$$R_{xx}(t,\tau) = x(t+\frac{\tau}{2})x*(t-\frac{\tau}{2}). \tag{3.29}$$

In this way, $R_{xx}(t,\tau)$ is still a correlation measure as in the stationary case, the only difference is that this measure now becomes time dependent.

Applying the Fourier transform directly to $R_{xx}(t,\tau)$, to pass from the temporal correlation (t,τ) to the time-frequency domain (t,f), I obtain the definition of the *Wigner-*

Ville time-frequency transform:

$$WV_{xx}(t,f) = F_{\tau\to f}R_{xx}(t,\tau) = \int_{-\infty}^{+\infty} x(t'+\frac{\tau}{2})x*(t'-\frac{\tau}{2})e^{-j2\pi f\tau}d\tau \tag{3.30}$$

Wigner-Ville transform is one of the most popular transform of the Cohen Class. It can be obtained from equation 3.28 by defining the kernel $g(\theta,\tau)=1$.

While the WignerVille transform has several desirable properties when applied to deterministic signals constituted by a single component, it is not well-suited for application to multicomponent signals [25]. In fact, calculating the Wigner-Ville transform of a multi-component signal, two types of terms are obtained: the *auto-components*, which are due to each subcomponent of the signal, and the *inference terms*. These inference terms are due to the products among the frequency components of the signal, caused by the bi-linear formulation of the transform. The inference terms looks like non-zero values of the distribution in the points in the time-frequency domain where the signal is zero. These interference terms may not be easily distinguished from authentic signal components, therefore the interpretation of distributions obtained from multicomponent signals is difficult [20]. To attenuate the interference terms without significantly affecting the auto-terms of the time-frequency distribution, a filtering function needs to be applied.

The application of a filtering function in the ambiguity domain was firstly proposed by Choi and Williams [26]. The ambiguity function is defined as the inverse Fourier transform of $R_{xx}(t,\tau)$ (equation 3.29), with respect to the first variable:

$$AF(\theta,\tau) = F^{-1}_{t\to\theta}\left[R_{xx}(t,\tau)\right] = \int_{-\infty}^{+\infty} x(t'+\frac{\tau}{2})x*(t'-\frac{\tau}{2})e^{j2\pi\theta t}dt \tag{3.31}$$

The ambiguity function corresponding to a signal constituted by several frequency components, shows that the signal autoterms located on the θ axis, while the interference terms are located outside the θ axis, in correspondence of the distance of the centroids of the auto-terms in the time-frequency domain. The kernel is designed in the ambiguity domain to specifically attenuate the interference components simply multiplying it for the ambiguity function. Therefore, equation 3.28 has been obtained with a Fourier transform of the kernel by ambiguity function product.

$$TF(t,f) = F_{\tau\to f}\left\{F_{\theta\to t}\left[AF(\theta,\tau)g(\theta,\tau)\right]\right\} \tag{3.32}$$

The properties of the kernel are strictly connected to the properties of the final TF transformation. The Choi-Williams transform belongs to the Cohen Class and is defined by following the kernel:

$$g_{CW}(\theta,\tau) = e^{-(2\pi\theta\tau)^2/\sigma} \tag{3.33}$$

The parameter σ allows control of the selectivity of the 2D-exponential filter in the ambiguity domain. Choi-Williams distribution has been largely employed in biomedical signal processing [20, 27, 28, 29, 30, 31].

In analogous way, it is possible to define the bilinear cross-transform of the Cohen-class as:

$$XTF(t,f) = \int_{-\infty}^{+\infty}\int_{-\infty}^{+\infty}\int_{-\infty}^{+\infty} x(t'+\frac{\tau}{2})y*(t'-\frac{\tau}{2})g(\theta,\tau)e^{-j2\pi\theta(t'-t)}e^{-j2\pi f\tau}d\theta dt' d\tau, \tag{3.34}$$

where x(t) and y(t) are the two time-series to analyze. The cross time-frequency distribution inherits all the properties of the correspondent time-frequency distribution (same kernel), except for the characteristics of never being real valued.

Time-frequency analysis applied to rotary spectra

To extend the rotary spectra analysis to the non-stationary case, the Choi-Williams time frequency distributions of the two Cartesian time series x(t) and y(t) and the cross time-frequency distribution between x(t) and y(t), always according Choi-Williams method, are calculated. The obtained time-frequency spectra are combined to calculate the rotating components as reported above in equation 3.10. The time-varying rotating spectra can be re-written as:

$$\begin{aligned} S(t,f_k^+) &= (A^+(t,f_k))^2 = \frac{1}{2}\left[S_{xx}(t,f_k)+S_{yy}(t,f_k)+2Q_{xy}(t,f_k)\right] \quad f_k \geq 0 \\ S(t,f_k^-) &= (A^-(t,f_k))^2 = \frac{1}{2}\left[S_{xx}(t,f_k)+S_{yy}(t,f_k)-2Q_{xy}(t,f_k)\right] \quad f_k \leq 0 \end{aligned} \tag{3.35}$$

where $S_{xx}(t,f)$ and $S_{yy}(t,f)$ are the time-varying auto-spectra of x(t) and y(t) and $Q_{xy}(t,f)$ is the quadrature of the time-frequency cross-spectrum between the two components.

3.2.2 Wavelet analysis

The wavelet analysis is another useful method to deal with non-stationarity of signals. In this section I will briefly describe its application to rotary spectra method from a theoretical point of view for completeness, even if I will not apply it in analyzing the CoP signals.

The wavelet transform is a signal decomposition on a set of basis functions, obtained by dilatations, contractions, and shifts of a original function, the wavelet prototype. A very basic distinction between wavelet transforms and Fourier methods, is that while the basis functions of the latter consist of a function of constant width translated in time, the former has a frequency-dependent width. Wavelet analysis methods have been widely used in biomedical signal processing, e.g. [32, 33, 34, 35, 36].

The function to be used as a choice of wavelet prototype of "mother wavelet" could be either real or complex, but has to respect two requirements:

- having zero mean value $\int_{-\infty}^{+\infty} \psi(t)dt = 0$
- having square norm equal to 1 $\int_{-\infty}^{+\infty} |\psi(t)|^2 dt = 1$

Given a time series x(t), its continuous wavelet transform CWT is defined as

$$CWT_x(a,b) = \frac{1}{\sqrt{a}} \int_{-\infty}^{+\infty} x(t)\psi^* \left(\frac{t-b}{a} \right) dt, \tag{3.36}$$

where * denotes complex conjugation, a represents the scaling factor and b represents the shift in time. Time t and the time-scale parameters vary continuously. When the scale factor a becomes large, the basis function $\psi_{a,b}(t)$ become a stretched version of the prototype, which is useful for the analysis of low-frequency components of the signal. On the other hand, when the scale factor is small, the basis function will be contracted, which is useful for the analysis of high-frequency components. The wavelet prototype behaves has a bandpass function (the factor $\frac{1}{\sqrt{a}}$ in equation 3.36 ensures energy preservation).

The discrete wavelet transform (DWT) can be obtained by discretization of the time-scale parameters a and b. One possible way to do so is to sample the time-scale parameters on a "dyadic" grid (basis 2) in the time-scale plane for the wavelet and scaling parameters.

In both continous and discrete cases, the wavelet power is defined as $|WT_x(a,b)|^2$ [37]. The complex argument of $|CWT_x(a,b)|^2$ can be interpreted as the local phase. The cross wavelet transform (XWT) of two time series x(t) and y(t) is defined as

$$WT_{xy} = WT_x WT_y^*, \tag{3.37}$$

where * denotes complex conjugation. This definition will be useful in applying wavelet analysis to rotary spectra.

Wavelet method applied to rotary spectra

Wavelet approach has been largely used in order to extend rotary spectra analysis to the non-stationary case [1, 12, 13, 14, 15].

The mother wavelet used was the Gaussian Morlet wavelet:

$$\psi_(t) = (e^{jmt} - e^{-m^2/2})e^{-t^2/2}, \tag{3.38}$$

where m is dimensionless frequency and t is dimensionless time. Analogously to the time-frequency distribution approach, we applied wavelet analysis to the terms of equation 3.10, in order to obtain the rotating components.

3.3 Conclusions

In this chapter a method to analyze bivariate time-series in terms of rotational components was described fro the theoretical point of view. The rotary spectra approach allows to separate rotational iso-frequential components from non-rotational ones. The method involves the representation of a two-dimensional signal in the complex plane as a superimposition of ellipses, which can be analyzed in terms of their shape and orientation. Each ellipse is the sum of a counterclockwise (CCW) and a clockwise (CW) rotating phasors, called rotary components.

Main advantages in applying this method are: (i) it is possible to analyze both the Cartesian components in the frequency domain, not only considering their vector sum in the plane (ii) the calculation of coherence and phase for the polarized components is invariant under the coordination rotation [3].

The rotary spectra approach was described both in the stationary and non-stationary cases. In particular, time-frequency analysis of rotating components was carried on both

applying bilinear Cohen's class Choi-Williams time-frequency distribution and wavelet method.

The describe method will be applied to the CoP signal in the chapter 5, demonstrating the presence of rotational components, and extracting information about the rotational characteristics of the body sway.

References

[1] J. M. Lilly and J. Gascard, "Wavelet ridge diagnosis of time-varying elliptical signals with application to an oceanic eddy," *Nonlin. Processes Geophys.*, vol. 13, p. 467483, 2006.

[2] J. Gonella, "A rotary-component method for analyzing meteorological and oceanographic vector time series," *Deep-Sea Res*, vol. 19, pp. 833–846, 1972.

[3] N. K. Mooers, "A technique for the cross spectrum analysis of pairs of complex-values time series, with emphasis on properties of polarized components and rotational invariants.," *Deep-Sea Res*, vol. 20, pp. 1129–1141, 1973.

[4] W. J. Emery and R. E. Thomson, *Data Analysis Methods in Physical Oceanography*. Pergamon, 1998.

[5] P. J. Schreier and L. L. Scharf, *Statistical Signal Processing of Complex-Value Data*. Cambridge University Press., 2010.

[6] M. Born and E. Wolf, *Principles of Optics*. Cambridge University Press, 1999.

[7] J. F. Simmons and B. G. Stewart, "Point and interval estimation of the true unbiased degree of linear polarization in the presence of low signal-to-noise ratios," *Astron. Astrophy*, vol. 142(1), pp. 100–106, 1985.

[8] L. Anttila, M. Valkama, and M. Renfors, "Circularity-based i/q imbalance compensation in wideband direct-conversion receivers," *IEEE Trans. Vehicular Techn*, vol. 57(4), pp. 2099–2113, 2008.

[9] S. Chandna and A. Walden, "Statistical properties of the estimator of the rotary coefficient.," *IEEE Trans. Signal Process*, vol. 59(3), pp. 1298–1303, 2011.

[10] P. J. Schreier, "Polarization ellipse analysis of non-stationary random signals," *IEEE Trans. Signal Process*, vol. 56, p. 43304339, 2008.

[11] D. Livingstone and T. C. Royer, "Eddy propagation determined from rotary spectra," *Deep-Sea Research*, vol. 27A, pp. 823–835, 1980.

[12] P. Liu and G. Miller, "Wavelet transforms and ocean current data analysis," *Journal of the atmospheric and oceanic technology*, vol. 13, pp. 1090–1099, 1996.

[13] J. M. Lilly and J. Park, "Multiwavelet spectral and polarization analysis," *Geophys. J. Int.*, vol. 122, p. 10011021, 1995.

[14] S. Olhede and A. T. Walden, "Polarization phase relationships via multiple morse wavelets. i. fundamentals," *Proc. Roy. Soc. London A, Mat.*, vol. 459, p. 413444, 2003.

[15] S. Olhede and A. T. Walden, "Polarization phase relationships via multiple morse wavelets. ii. data analysis," *Proc. Roy. Soc. London A, Mat.*, vol. 459, p. 641657, 2003.

[16] H. Crew and N. Plutchak, "Time varying rotary spectra," *Journal of the oceanographical society of Japan*, vol. 30, pp. 61–66, 1974.

[17] A. Roueff, J. Chanussot, and J. I. Mars, "Estimation of polarization parameters using time-frequency representations and its application to waves separation," *Signal Process*, vol. 86(12), p. 37143731, 2006.

[18] L. Cohen, "Time-frequency distribution: a review. ;:," *Proc of IEEE*, vol. 77, p. 94181, 1989.

[19] P. Novak and V. Novak, "Time/frequency mapping of the heart rate, blood pressure and respiratory signals.," *Med Biol Eng Comput*, vol. 31, pp. 103–110, Mar 1993.

[20] M. Knaflitz and P. Bonato, "Time-frequency methods applied to muscle fatigue assessment during dynamic contractions.," *J Electromyogr Kinesiol*, vol. 9, pp. 337–350, Oct 1999.

[21] Z. Y. Lin and J. D. Chen, "Time-frequency representation of the electrogastrogram–application of the exponential distribution.," *IEEE Trans Biomed Eng*, vol. 41, pp. 267–275, Mar 1994.

[22] Z.-G. Zhang, J.-L. Yang, S.-C. Chan, K. D.-K. Luk, and Y. Hu, "Time-frequency component analysis of somatosensory evoked potentials in rats.," *Biomed Eng Online*, vol. 8, p. 4, 2009.

[23] G. Tognola, F. Grandori, and P. Ravazzani, "Time-frequency distribution methods for the analysis of click-evoked otoacoustic emissions.," *Technol Health Care*, vol. 6, pp. 159–175, Sep 1998.

[24] F. Clari, M. Vallverd, J. Riba, S. Romero, M. J. Barbanoj, and P. Caminal, "Characterization of the cerebral activity by time-frequency representation of evoked eeg potentials.," *Physiol Meas*, vol. 32, pp. 1327–1346, Aug 2011.

[25] M. Akay, *Time frequency and wavelets in biomedical signal processing*. IEEE press, 1998.

[26] H. Choi and W. Williams, "Improved time-frequency representation of multicomponent signals using exponential kernels," *IEEE Trans on Acoust Speech and Signal Processing*, vol. 37, p. 86271, 1989.

[27] H. L. Chan, H. H. Huang, and J. L. Lin, "Time-frequency analysis of heart rate variability during transient segments.," *Ann Biomed Eng*, vol. 29, pp. 983–996, Nov 2001.

[28] W. Liboni, F. Molinari, G. Allais, O. Mana, E. Negri, G. Bussone, G. D'Andrea, and C. Benedetto, "Spectral changes of near-infrared spectroscopy signals in migraineurs with aura reveal an impaired carbon dioxide-regulatory mechanism.," *Neurol Sci*, vol. 30 Suppl 1, pp. S105–S107, May 2009.

[29] E. Roy, P. Abraham, S. Montrsor, and J. L. Saumet, "Comparison of time-frequency estimators for peripheral embolus detection.," *Ultrasound Med Biol*, vol. 26, pp. 419–423, Mar 2000.

[30] Y. Wang and P. J. Fish, "Comparison of doppler signal analysis techniques for velocity waveform, turbulence and vortex measurement: a simulation study.," *Ultrasound Med Biol*, vol. 22, no. 5, pp. 635–649, 1996.

[31] H. I. Choi, W. J. Williams, and H. Zaveri, "Analysis of event related potentials: time-frequency energy distribution.," *Biomed Sci Instrum*, vol. 23, pp. 251–258, 1987.

[32] M. Akay, "Wavelets in biomedical engineering.," *Ann Biomed Eng*, vol. 23, no. 5, pp. 531–542, 1995.

[33] Z. Hou and T. S. Koh, "Wavelet shrinkage prefiltering for brain tissue segmentation.," *Conf Proc IEEE Eng Med Biol Soc*, vol. 2, pp. 1604–1606, 2005.

[34] I. D. Dinov, J. W. Boscardin, M. S. Mega, E. L. Sowell, and A. W. Toga, "A wavelet-based statistical analysis of fmri data: I. motivation and data distribution modeling.," *Neuroinformatics*, vol. 3, no. 4, pp. 319–342, 2005.

[35] M. David, M. Hirsch, J. Karin, E. Toledo, and S. Akselrod, "An estimate of fetal autonomic state by time-frequency analysis of fetal heart rate variability.," *J Appl Physiol*, vol. 102, pp. 1057–1064, Mar 2007.

[36] J. R. Chagdes, S. Rietdyk, J. M. Haddad, H. N. Zelaznik, A. Raman, C. K. Rhea, and T. A. Silver, "Multiple timescales in postural dynamics associated with vision and a secondary task are revealed by wavelet analysis.," *Exp Brain Res*, vol. 197, pp. 297–310, Aug 2009.

[37] A. Grinsted, J. C. Moore, and S. Jevrejeva, "Application of the cross wavelet transform and wavelet coherence to geophysical time series," *Nonlinear Processes in Geophysics (2004)*, vol. 11, p. 561566, 2004.

4

Applications of geometrical parameters

This chapter reports main findings obtained applying geometrical parameters to the study of the CoP signal.

Describing CoP signal with these parameters, introduced in chapter 2, an important relationship between some geometrical parameters and sampling frequency was observed.

Two studies of application of geometrical parameters to study different groups of subjects will be reported in this chapter. In both studies, a new acquisition protocol is proposed, which adds to frontal open- and closed-eye conditions, conditions in which quiet standing of the subject is evaluated after a fast or a slow head rotation, on the left or on the right side, both with eyes open and closed. After evaluating geometrical parameters both on healhty and pathological subjects, a multivariate statistical approach will be used to differenciate between groups.

The aim of the first work [1] was to analyze the postural control of volleyball players and the impact that vision has on it. A multivariate approach to data analysis demonstrated that the two groups were different when the subjects kept their eyes open, but they were not with visual deprivation. The influence of the athletes expertise and team role on balance performances was also analyzed.

The second work [2] evaluated differences in postural performances in controls and patients with residual neuro-ophthalmic deficits after a traumatic brain injury. It was possible to evidence significant balance abnormalities in TBI patients with respect

to controls. Moreover, I was able to discriminate different postural performances in patients with different levels of residual neuro-ophthalmic impairment.

4.1 Influence of the sampling frequency of geometrical parameters

Few studies focused on the influence of the choice of the sampling frequency on posturographic parameters [3, 4]. Schmid et al. [3] observed the influence of the acquisition settings on posturographic parameters, focusing on the choice of the cut-off frequency values. They observed that the robustness of parameters to the cut-off frequency variations is different, depending on the parameters mathematical definition. Raymakers's work [4] did not focus on the problem, but just observed that some geometrical parameters were influenced by different values of sampling frequencies.

I this section I will report some observations about the influence of the frequency sampling on geometrical parameters.

Force platform signals were registered out by using a cutoff frequency of 25 Hz for the acquisition filter, and a sampling frequency of 2000 samples/s. The choice of the acquisition bandwidth is over-dimensioned, compared with the typical values used in posturography, but it allows to down-sample the signal with different values, to simulate different sampling frequencies.

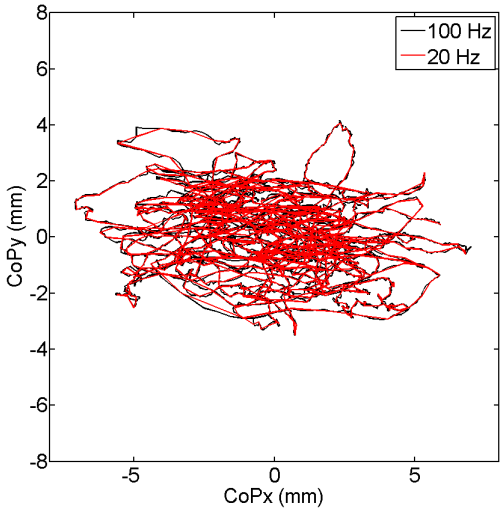

Figure 4.1: CoP trajectories with different sampling frequencies

Figure 4.1 shows CoP trajectories of the force platform for two different sampling frequencies. The trajectory of the CoP appears more complex when more intermediate CoP points are recorded and the trajectory measured will therefore appear to be longer (and indeed more accurate) when calculated from higher sampling frequencies registrations [3]. Figure 4.2 shows the trend of some parameters for different values of sampling frequencies, from 1 Hz to 200 Hz. It is possible to observe that Mean Velocity and Sway Area are the most influenced parameters. Their values increase in a significant way if the frequency sampling is higher.

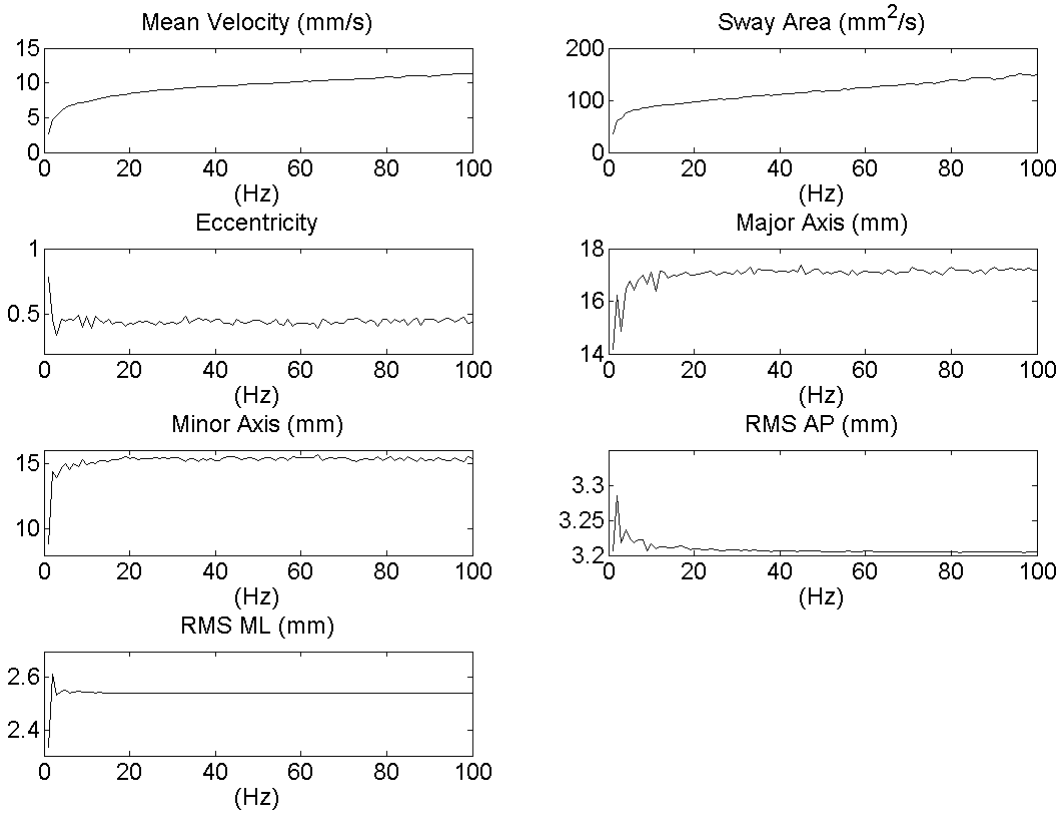

Figure 4.2: Influence of the sampling frequency on geometrical parameters

Geometrical parameters describing the smallest ellipse containing the CoP trajectories (major and minor axes, and eccentricity) do not show great dependencies from the sampling frequency values, as they oscillate in a narrow range of values, but without showing increments or decrements. RMS AP and RMS ML do not to depend from sampling frequency values. This is not surprising, due to their mathematical definition

(see 2).

A common aspect that all the calculated parameter show is a great dependence from sampling rate at low frequencies. Therefore, neglecting information by choosing a low sampling frequency may reduce accuracy and thereby discriminating capability [4].

Table 4.1 shows mean values ± standard deviation of the geometrical parameters calculated on a population of 42 healthy subjects. The results have been reported for both sampling frequencies of 20, 50 and 100 Hz. The parameters mean velocity and sway area show higher values with higher sampling frequencies, and these increasing are statistical significant ($p \leq 0.05$).

Table 4.1: Mean values ± standard deviation of geometrical parameters vs.sampling frequency. * Significant difference between different sampling values ($p \leq 0.05$)

Sampling frequency	20 Hz	50 Hz	100 Hz
Mean Velocity (mm/s)	7.9±2.2*	9.0±2.3 *	10.6±2.43*
Sway Area (mm^2/s)	90.5±46.3*	110.2±55.1*	139.9±68.5*
Eccentricity	0.7±0.1	0.7±0.1	0.7±0.1
Major Axis (mm)	18.5±4.9	18.6±4.9	18.6±4.9
Minor Axis (mm)	11.8 ±3.6	11.9±3.6	11.9±3.6
RMS AP (mm)	3.4±1.1	3.4 ±1.1	3.4±1.1
RMS ML (mm)	2.7± 0.9	2.8±0.9	2.7±0.9

In conclusion, comparison of results of studies performed with different sampling frequencies is not possible. A future work will inevitably be required to investigate another question, about up to what frequency are the CoP displacement signals to be considered as information-carrying.

4.2 Postural control in volleyball players[1]

It is known that volleyball players show better dynamic visual acuity than non-athletes. The aim of this work was to analyze the postural control of volleyball players and the impact that vision has on it. The main hypothesis of this study is that, since volleyball players use the visual system differently from untrained subjects, the role of vision on postural control should also be different. The center of pressure (CoP) in bipedal quiet stance was measured in 46 athletes from national and regional Italian teams and 42 non-athlete controls. Each subject was tested in 10 different conditions, 5 with their eyes open and 5 with their eyes closed. Volleyball players showed greater CoP ellipses with respect to controls in 8 conditions over 10. A multivariate approach to data analysis demonstrated that the two groups were different when the subjects kept their eyes open, but they were not with visual deprivation. The influence of the athlete's expertise and team role on balance performances was also analyzed. Differences in the upright stance of national and regional athletes were found, as well as differences between defensive players and hitters.

4.2.1 Introduction

A skilled control of postural stability is fundamental in many of the actions performed by volleyball athletes. The effectiveness in serving, receiving, setting, or digging the ball is affected by the athletes ability to control their dynamic balance. Volleyball players are asked to adapt their posture very quickly to promptly react to each game situation. A rapid restoration of the body balance after an equilibrium disturbance is crucial. In fact, trying to handle the ball having a poor postural stability results in far less accurate actions. Coaches are aware of the importance of balance training to improve the team's performances. Furthermore, the effectiveness of balance training in preventing serious injuries was demonstrated in various sports [5, 6, 7, 8].

The control of upright posture depends on the integration of information arising from visual, vestibular, and proprioceptive systems [9]. Since many physiological aspects contribute to determine balance performances, evaluating postural control quantitatively may be a challenging task.

[1] This study is described also in [1], a paper accepted to be published in Human Movement Science.

Static posturography provides an objective evaluation of postural control performances by characterizing the body sway during upright standing [9, 10, 11]. This technique is based on the study of the Center of Pressure (CoP) trajectory of a subject in quiet standing on a force platform.

Training allows sportspeople to acquire new abilities in balance control according to the discipline practiced [12, 13, 14]. Postural control investigation in athletes could provide insight into the development of specific postural strategies required by a particular sport. In literature there are studies investigating postural control in dancers [12, 13, 14, 15, 16], gymnasts [17], judokas [14], soccer [18] and volleyball players [19, 20].

In specific sports, practice may modify the influence of the visual input on balance performances. As an example, [15] found that male professional dancers were significantly more stable and less dependent on vision for postural control than untrained subjects. They suggest that professional dance training strengthens the accuracy of proprioceptive inputs and shifts sensorimotor dominance from vision to proprioception.

Athletes practicing volleyball have a constant involvement of the visual system. This is certainly true in many team sports, but volleyball players especially are constantly making ocular movements. Thinking about the position of the eyes that is kept by the players when playing defense (sumsumversion), one realizes how a proper functioning of ocular motility is fundamental to adequately react to the attack of the opposite team. The constant movement of the ball in the game field implies a training of the eye muscles. This ocular training might have an impact in postural control.

In literature there are many studies pointing out the relationship between the performances of athletes in specific disciplines and their visual skills [15, 21, 22, 23]. In fast ball-sports, dynamic visual acuity of athletes is known to be superior to that of non-athletes [24]. In volleyball, it was demonstrated that female players show a better facility of accommodation and more saccadic eye movements than the non-playing control group [21]. Another study, on a male group of volleyball players, demonstrated that expert players perform fewer fixations of longer duration, concentrating on the starting and ending points of the ball trajectory, while non-athletes tend to follow the whole trajectory [23]. The cited works established that vision in volleyball players

differs from that of untrained subjects. Furthermore, [25] reported that saccadic eye movements might modify postural control in keeping the upright standing position.

The main hypothesis of this study is that, since volleyball players use the visual system differently from untrained subjects, the role of vision on postural control should also be different.

The second hypothesis is that the posture of athletes is influenced by their level of expertise and/or by their team role.

4.2.2 Materials and Methods

Subjects

Forty-six volleyball players were recruited from different Italian teams: nine of them were recruited from national professional teams (Italian championship B2 series) and the others from regional semi-professional teams. All of them regularly practiced volleyball. The national athletes were involved in training sessions 3-4 times per week, while the semi-professional players trained 2-3 times per week. Each training session lasted two hours. A weekly match completed the athletes' training. The group was composed of athletes trained to play in different positions. There were 15 outside hitters, 16 central hitters, 2 opposite hitters, 9 setters, and 4 liberos. The different positions were uniformly distributed among athletes of different levels. In particular, among the nine athletes recruited from national teams there were 3 setters, 3 outside hitters and 3 central hitters. To study postural differences of athletes specialized in different roles, I chose to divide hitters (attackers) from other roles (defenders). In the hitters group I included outside, central, and opposite hitters, while in the other roles group I included setters and liberos.

The control group consisted of 42 healthy subjects recruited from the students of the University of Torino, Italy. Table 4.2 reports gender, age and anthropometric characteristics of both groups. Both athletes and controls underwent orthoptic and neuro-ophthalmologic examination at Clinica Oculistica dell' Universit di Torino (Torino, Italy), prior to the posturographic test, to evaluate the visual system. They were examined for visual acuity, autorefractometry and subjective refraction for the determination of the refractive error, strabismus (cover test), fusional amplitudes at far and near distances (prism bar) and ocular motility (optokinetic nystagmus, smooth pursuit and saccades). All the subjects presenting refractive errors reached a normal

visual acuity with correction. The outcome of the examination is summarized in the second part of Table 4.2.

The local ethical committee approved the experimental protocol and all participants gave their written informed consent to be included in the study.

Table 4.2: Description of the two populations: volleyball players and controls

		Volleball players (N = 46)		Controls (N = 42)	
Anthropometric characteristics					
Gender		26 males	20 females	16 males	26 females
Age(years)	mean±std	25.9±6.2	22.9±2.9	25.2±5.4	22.4±2.8
	range	19-37	19-29	19-39	18-28
Height (cm)	mean±std	185.6±7.7	170.8±7.9	179.1±6.9	166.9±5.3
	range	163200	155184	169-196	155-175
Weight (kg)	mean±std	79.2±8.1	62.4±8.5	75.1±9.1	57.4±6.9
	range	5993	4675	55-94	44-72
Orthoptic and neuro-ophthalmologic examination					
No visual correction		57.1%		30.9%	
Visual correction:					
miopia		36.9%		54.7%	
hypermetropia		4.3%		7.1%	
astigmatism		4.3%		11.9%	
Orthophoria		39.1%		33.3%	
Saccades in the range of normality		78.3%		52.4%	

Acquisition protocol

To highlight the specific abilities of each subject in various conditions that stimulate the visual and vestibular systems, I applied an acquisition protocol already used in a previous work [2]. This protocol adds to the traditional frontal open and closed-eye conditions [4, 10, 26], conditions in which the subject is evaluated after a fast or slow head rotation, to the left or to the right side, both with eyes open and closed.

Subjects were asked to stand quietly in upright position, with arms at their sides, over a Kistler 9286A force platform. The inter-malleolar distance was fixed at 4 cm and the feet opening angle was 30. The acquisition protocol consisted of a single trial in 10 different conditions, five with the subject's eyes open (looking at a visual target) and five with their eyes closed. The head positions were: frontal and head rotated left/right after a slow/fast head rotation. At the operator's order, the subject reached the requested head position and maintained it until the end of the acquisition. Specifically, the 10 conditions were: (1) open eyes frontal (OEF), (2) closed eyes frontal (CEF), (3) open eyes and head rotated after a slow left rotation (OELs), (4) closed eyes and head rotated after a slow left rotation (CELs), (5) open eyes and head rotated after a slow right rotation (OERs), (6) closed eyes and head rotated after a slow right rotation (CERs), (7) open eyes and head rotated after a fast left rotation (OELf), (8) closed eyes and head rotated after a fast left rotation (CELf), (9) open eyes and head rotated after a fast right rotation (OERf), (10) open eyes and head rotated after a fast right rotation (CERf).

A biaxial accelerometer fixed to the forehead of the subject allowed us to determine when the requested head position was reached. The accelerometric signal was acquired synchronously with the platform signals with the system Step32 (DemItalia, Italy). The sampling frequency was 2 kHz and the signals were then down-sampled to 20 Hz. Each recording started just before the operator's order and lasted 70 seconds. Then, an epoch of 60 s was extracted for the subsequent analysis, starting when the head position became steady, i.e. discarding the few seconds that the subject used to rotate their head after the operator's order.

The sequence of acquisitions was randomized to avoid data being biased by learning and/or fatigue effects [27]. Every two acquisitions the subject rested one minute, moving away from the platform.

Data analysis

Visual skills. I applied a χ^2-test for the comparison of two proportions (independent samples) to assess the differences between visual skills of volleyball players and controls. I considered 2 x 2 contingency tables (1 degree of freedom) to evaluate group difference for: a) visual acuity, b) saccades in the range of normality and c) orthophoria (see Table 4.2).

CoP parameters. I calculated, for each condition, the major geometrical and time-domain parameters based on the CoP [2, 4, 10, 26]. The definition of the 7 CoP parameters considered is reported in Table 4.3. To avoid data being biased because of anthropometric characteristics [28] I normalized the parameter values with respect to the subjects' body height when the correlation between each parameter and subjects' body height was statistically significant ($p \leq 0.05$). After normalization, I calculated for each group the mean and standard deviation of each CoP parameter/condition, and compared the two populations by means of a two-sample t-test. Moreover, within each group, I tested open-eye vs. closed-eye conditions, to assess the visual contribution in postural control.

MANOVA analysis. I obtained a total of 70 dependent variables (DVs): 10 conditions 7 parameters. Looking at one parameter/condition at a time, it is necessary to understand which parameter/condition can differentiate the two groups (see previous paragraph), but it may be limiting. In fact, a variable that is useless by itself may be useful with others [29]. Therefore, I was interested in taking into account the inter-relations among CoP parameters in the different conditions. To this purpose I applied a multivariate analysis of variance (MANOVA) approach [30, 31, 32].

I applied a 1-factor MANOVA to compare:

(a) volleyball players and controls. DVs: 10 conditions (OEF, OELs, OERs, OELf, OERf, CEF, CELs, CERs, CELf, CERf) x 7 parameters

(b) volleyball players and controls, in eyes-open conditions. DVs: 5 conditions (OEF, OELs, OERs,OELf, OERf) x 7 parameters

(c) volleyball players and controls, in eyes-closed conditions. DVs: 5 conditions (CEF, CELs, CERs, CELf, CERf) x 7 parameters

(d) players of different expertise (national, regional) and controls. DVs: 10 conditions x 7 parameters

(e) players with different team roles (hitters, other roles) and controls. DVs: 10 conditions x 7 parameters.

Table 4.3: Postural sway parameters

Parameter	Dimension	Description	Definition
Mean Velocity	mm/s	Length of CoP divided by the acquisition time T	$\sum_{n=1}^{N-1}[(AP[n+1]-AP[n])^2+$ $+(ML[n+1]-ML[n])^2]$
Sway Area	mm^2/s	Area of the surface enclosed by the CoP path per unit of time	$\frac{1}{2T}\sum_{n=1}^{N-1}\lvert AP[n+1]*ML[n]+$ $-AP[n]*ML[n+1]\rvert$
RMS AP	mm	Root Mean Square of the Antero-Posterior (AP) time series	$\sqrt{\frac{1}{N-1}\sum_{n=1}^{N}(AP[n]-\bar{AP})^2}$
RMS ML	mm	Root Mean Square of the Medio-Lateral (ML) time series	$\sqrt{\frac{1}{N-1}\sum_{n=1}^{N}(ML[n]-\bar{ML})^2}$
Major Axis	mm	Length of the major axis of the smallest ellipse containing the CoP	2a
Minor Axis	mm	Length of the minor axis of the smallest ellipse containing the CoP	2b
Eccentricity	adimentional	Eccenctricity of the smallest ellipse containing the CoP	$e=\sqrt{1-\frac{b^2}{a^2}}$

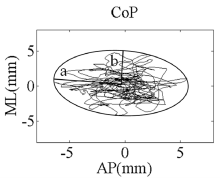

The MANOVA approach considered provided both a graphical representation of data (multivariate descriptive statistics) by means of canonical variate analysis (CVA), and a multivariate inferential test (Wilk's λ) [31]. This allowed to associate a pictorial representation of data with rigorous p-values. In CVA, the canonical variables C are linear combinations of the original variables, chosen to maximize the separation among groups. Specifically, the first canonical variable C1 is the linear combination of the original variables that has the maximum separation among groups. This means that among all possible linear combinations, the first canonical variable is the one with the most significant F-statistics in a 1-way analysis of variance. The second canonical

variable C2 has the maximum separation being orthogonal to C1, and so on.

4.2.3 Results

First I present the results of the orthoptic and neuro-ophthalmologic examination, secondly the t-test for each single postural parameter/condition (Fig. 4.3), and then the MANOVA analysis (Figs. 4.4-4.5).

Visual skills. The χ^2-test evidenced that volleyball players showed better visual acuity ($p = 0.016$) and more normal saccades ($p = 0.011$) than controls. The orthophoria was not different between the groups.

CoP parameters. Figure 4.3 shows the mean and standard deviation of each parameter for athletes and controls in the 10 conditions. Statistically significant differences between groups are indicated with an asterisk ($p \leq 0.05$). The Mean Velocity was not significantly different between groups, but volleyball athletes always showed higher values than controls. The Sway Area differentiated the two groups only in a few test conditions. The Major and Minor Axis, RMS AP and RMS ML showed significant differences in the majority of the conditions. Eccentricity did not differentiate the two groups. Furthermore, considering each group separately, we compared open eyes vs. closed eyes performances. The Mean Velocity showed significant differences in all test conditions, for both groups. For the other parameters, statistically significant differences between eyes open and eyes closed tests were observed only in a few test conditions.

MANOVA analysis. Figure 4.4 shows multivariate data from athletes and controls plotted against the first two canonical variables C1 and C2. Fig. 4.4(a) reports the comparison of athletes and controls based on the complete set of 10 conditions (5 with eyes open and 5 with eyes closed). In order to evaluate the effect of the visual system, Figs. 4.4(b) and 4.4(c) consider the eyes open and eyes closed acquisitions separately. In these plots (Fig. 4.4(a)-(c)), the two groups are slightly separated in the canonical variables plane. They were not significantly different according to Wilk's λ MANOVA test ($p=0.26$) when all the 10 conditions were considered together (Fig. 4.4(a)). On the contrary, the two groups were found to be significantly different in the

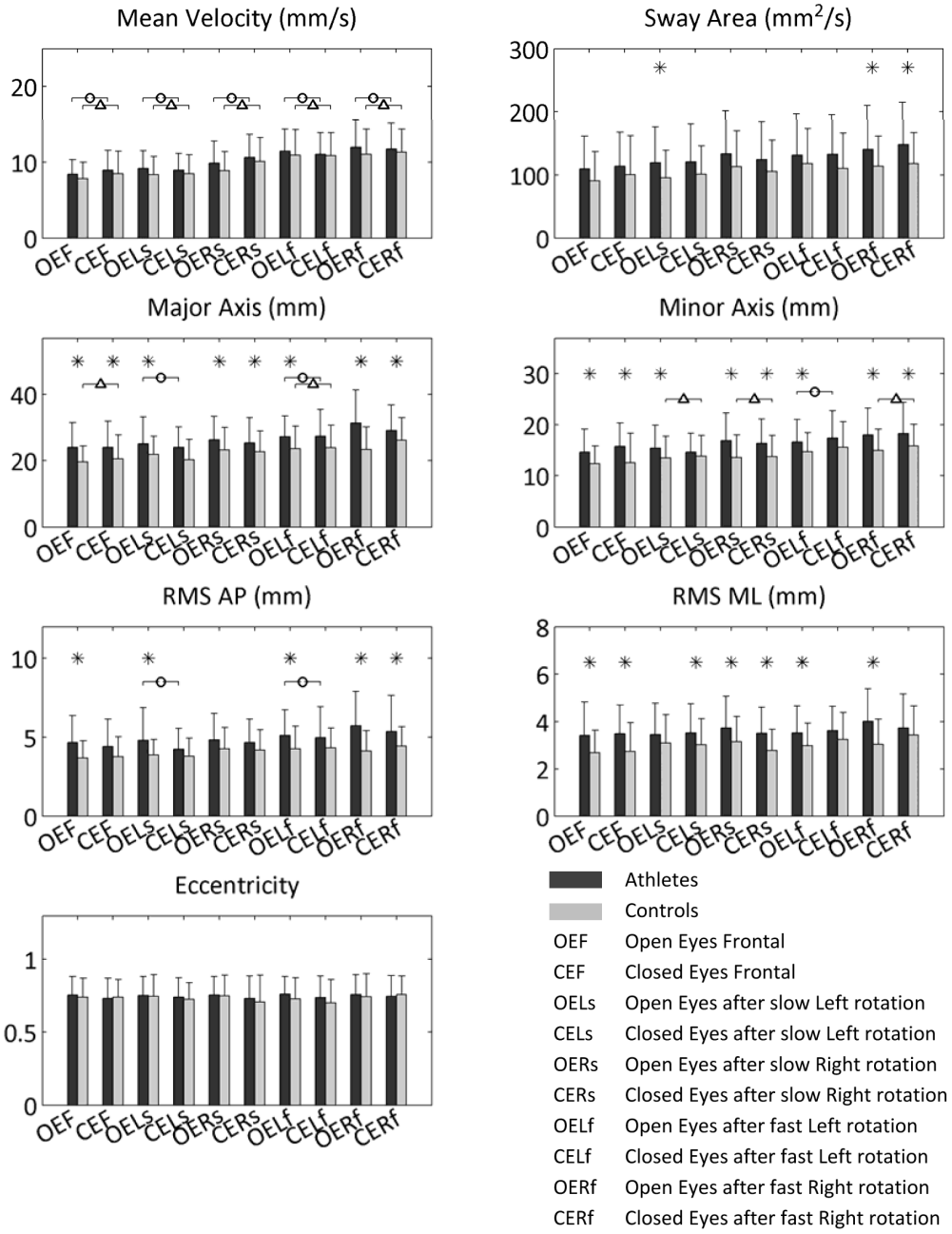

Figure 4.3: Comparison of posturographic parameters between volleyball athletes and controls: mean values and standard deviation are shown for each parameter and each trial condition listed in the legend. * Significant difference between athletes and controls ($p \leq 0.05$); $^{\triangle}$ significant difference, in controls, between eyes open and closed ($p \leq 0.05$); $^{\circ}$ significant difference, in volleyball athletes, between eyes open and closed ($p \leq 0.05$).

open-eyes conditions (p = 0.05) (Fig. 4.4(b)), while visual deprivation did not allow to differentiate the two groups (p = 0.20)(fig4.2(c)).

In Fig. 4.5 I considered separately athletes coming from national and regional teams and playing different team roles. Figure 4.5(a) reports multivariate data relative to athletes at a national level, athletes at a regional level, and controls. The three groups are well separated in the canonical variables plane (Wilk's λ test: p = 0.001). More specifically, volleyball players recruited from national teams are far apart from the other two groups, while the regional group is only slightly apart from controls. Note that the national group is separated from the regional and control group along the first canonical variable C1, while it is only the second canonical variable C2 that separates the regional group from controls. Fig. 4.5(b) reports multivariate data relative to volleyball athletes playing as hitters, playing as other roles, and non-athlete controls. The three groups are separated in the canonical variables plane and the MANOVA test was very close to being statistically significant (p = 0.058). Note that the group constituted by setters and liberos is the one that is the most distant from the other two groups.

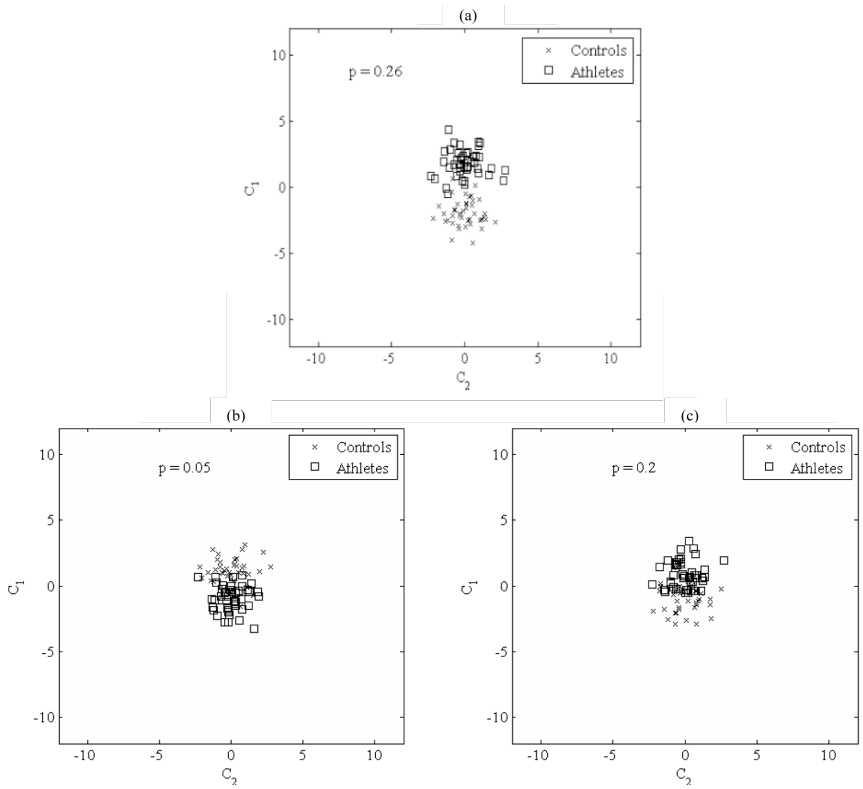

Figure 4.4: Athletes and controls: scatter plots of the first (C1) vs. the second (C2) canonical variable. (a) All 10 conditions. (b) Open-eye conditions (OEF, OELs, OERs, OELf, OERf). (c) Closed-eye conditions (CEF, CELs, CERs, CELf, CERf).

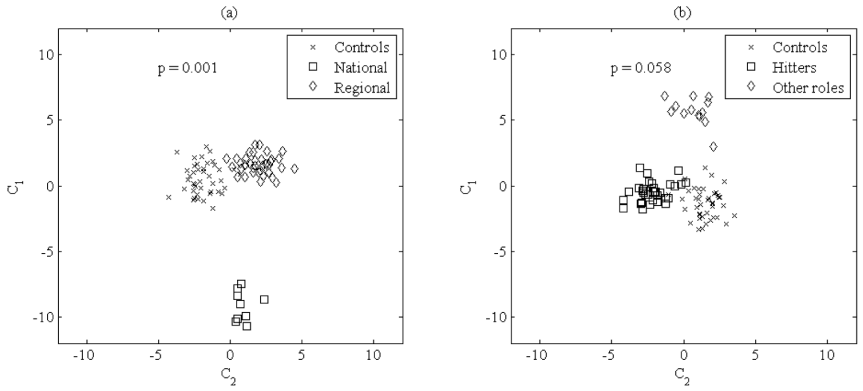

Figure 4.5: Athletes and controls: scatter plots of the first (C1) vs. the second (C2) canonical variable. Different (a) training expertise, and (b) team roles are considered, while all the 10 trials are taken into account.

4.2.4 Discussion

In literature there are few studies examining balance performances in volleyball players. Most of these studies focus on the effect of proprioceptive balance training in reducing the risk of ankle sprains among volleyball athletes [5, 8], but they do not assess balance performances with quantitative tests. Only one study [19] is directly comparable to this one, at least in some aspects. My work analyzes the visual skills of athletes and non-athletes, in order to better understand the postural differences between the groups and then delves deeper into these differences taking into account the level and the playing position of the athletes.

Influence of visual skills on balance performances It is well known that visual skills play an important role in open eyes balance control [9], while closed eyes standing does not depend on vision.

Results of the orthoptic examination show that refractive errors are more numerous in controls than in athletes, but during the balance test all the subjects had refractive correction and reached normal visual acuity. Hence, from a (static) visual acuity point of view, volleyball players cannot be considered different from controls.

However, when a moving target is considered, 'dynamic' visual acuity of athletes is definitely superior to that of controls (see e.g. [24].

It was demonstrated that female volleyball athletes show better facility of accommodation and saccadic eye movements (SEM) than the non-playing control group [21]. Similarly, in our population volleyball players showed adequate SEM in 78.3% of cases, while this was found in only 52.4% of controls. Moreover, it was reported that in a game situation, expert volleyball players adopt a different gazing strategy than non-expert players [23].

Using a multivariate approach I found that the 5 open-eye conditions allow to distinguish athletes from controls ($p = 0.05$), while, considering closed-eye conditions, the difference between groups is not statistically significant ($p = 0.20$). This shows that ocular training of volleyball players has an influence not only in a game situation, as already demonstrated [23], but also in static balance control. Emery [33] indicated measures of dynamic standing as the proper tool in investigating athlete postural control. My findings suggest that also stabilometric tests in bipedal static conditions could be a useful tool in the evaluation of postural performances of volleyball athletes.

Differences between volleyball players and controls Kuczyski et al. [19] analyze the balance performances of 23 volleyball players recruited from the Polish male second league. This study reports that players have lower CoP variability in the ML direction and lower CoP range than controls in both AP and ML directions. The CoP mean velocityof athletes was higher than that of controls. My results are in partial agreement with Kuczyski's study. In fact, I found that the mean velocity of the CoP resultant in OEF shows greater values for volleyball players than for controls, but in my study this difference is not statistically significant ($p = 0.19$). Differently from Kuczyski et al. [19], I found that RMS AP and RMS ML have greater values in athletes than in controls, although these differences are not always statistically significant.

These discrepancies between my study and Kuczyski's work may be explained by different factors: a) the authors of the cited study considered only male athletes, while I considered both females and males, b) they considered only 1 condition (eyes open frontal), while I considered 10 conditions (5 with eyes open and 5 with eyes closed) following the indications suggested by Ruhe et al. [11], c) their test lasted only 20 s, while my test lasted 60 s (which should guarantee a better reliability of the results, as suggested by Doyle et al. [34] and by Ruhe et al. [11]). Moreover, Kuczyski did not apply the standardization of CoP parameters with respect to the anthropometric characteristics and this can bias the data [11, 28].

In the literature, a greater CoP trajectory is usually interpreted as lower stability (e.g. [26]). Nevertheless, there are various studies demonstrating a greater sway ellipse of athletes with respect to non-athletes, which may be read as a paradox. As an example, a study on young male athletes practicing canoeing and kayaking reports larger CoP mean amplitudes and sway velocity for the athletes [35]. Another study reports that synchronized ice skaters unexpectedly showed less 'balance' than controls in upright stance on a rigid force platform [36]. I believe that caution is needed in the interpretation of larger sway ellipses as indicators of a poorer balance of athletes with respect to non-athletes. Similarly to what was found in the cited studies, my work demonstrated that volleyball players show greater values of RMS AP, RMS ML, Major and Minor Axis with respect to controls. I hypothesize that this is due to the attitude that these athletes develop in order to quickly react to each game situation moving rapidly from a static position. This is consistent with the hypothesis of a different model of sensory integration in the postural stability of athletes [35].

Different athlete expertise and team roles Considering the information arising from the 10-condition protocol, I demonstrated that it is possible to separate volleyball players of national level from athletes of regional level and controls. The data presented suggest that the level of expertise of the players influences their postural control in static conditions: the higher the training level, the more remarkable the difference between athlete and non-athlete performances. Jafarzadehpur et al. [21] investigated the visual skills of volleyball players with different levels of expertise: beginner, intermediate, and advanced players. They observed better visual performance in advanced players than in the others. This can be an indirect confirmation of my findings, since the visual system and sensory-motor coordination are mutually interrelated.

In an analogous way, I observed that athletes trained in different team roles (hitters, setters and liberos) have different balance performances. Hitters are usually trained to respond to a single playing scheme and may have longer reaction times than defenders. In fact, they have to react quickly only if the ball is received in the wrong way. Their specific skill is elevation. They express their coordination and balance abilities especially when they jump in the air to make contact with the ball. On the contrary, setters rapidly move toward the moving ball and quickly decide which scheme is better to apply, choosing to which attacker they should deliver the ball. Setters must always have very short reaction times. Liberos are exclusively defensive players. They are usually the players on the court with the quickest reaction time and best passing skills. In literature, anthropometric differences are described among hitters, setters and liberos [37]. However, since I normalized our data with respect to height, these differences should not significantly influence our findings. I hypothesize that the postural differences observed among different team roles are due to the specific training undergone by these athletes rather than to their body structure.

4.2.5 Conclusion

In this study I investigated the postural control of volleyball players in bipedal static conditions. I demonstrated that athletes differ from non-athletes in the open-eyes conditions. More specifically, the sway ellipse and other CoP parameters were larger for athletes. This might be erroneously interpreted as volleyball showing worse balance performances. I hypothesized that this result could be explained as an adaptation of

athletes to a postural scheme that integrates the visual system differently with respect to untrained subjects.

Furthermore, Ie demonstrated that national level athletes differed from regional level ones in upright stance. This difference may be due to the different intensity levels of their training and/or to the subjective aptitude of the athletes. I also observed a different postural stability of defensive players with respect to hitters. Ie hypothesized that this difference is mainly due to their quicker reaction times.

The protocol presented in this work might be useful to assess the efficacy of intensive sport training programs involving the integration of proprioceptive and visual systems and/or to select elite players with an aptitude for a specific playing role.

4.3 Postural control in patients after traumatic brain injury[1]

Postural instability is a common and devastating consequence of traumatic brain injury (TBI). The majority of TBI patients also suffer from neuro-ophthalmic deficits that can be an important contributing element to their sensation of vertigo and dizziness. Static posturography aims at the objective evaluation of patient balance impairment, but is usually affected by large inter- and intra-subject variability. Here I propose a protocol based on 10 randomized trials stimulating in different ways the visual and vestibular systems. Due to its completeness, my protocol highlights the specific residual difficulties of each patient in the various conditions. In this way, it was possible to evidence significant balance abnormalities in TBI patients with respect to controls. Moreover, by means of a multivariate analysis I was able to discriminate different levels of residual neuro-ophthalmic impairment.

4.3.1 Introduction

Traumatic brain injury (TBI) is an important cause of disability at all ages [38]. In the USA the annual incidence of emergency department visits and hospital admission are respectively 403 per 100,000 and 85 per 100,000 [39]. The mean annual incidence rate of hospitalized and fatal TBI for Europe is 235 per 100,000 [40]. Approximately 80% of injuries are classified as mild, 10% as moderate, and 10% as severe [40]. Severity is usually described by the Glasgow Coma Scale (GCS) [41], and is evaluated when the patient enters the emergency department. However, GCS may change during hospitalization and it does not describe the nature and the entity of the residual impairments. One of the most common complaints among TBI patients is postural instability and balance impairment [42, 43].

Neuro-ophthalmic deficits commonly follow TBI, since the afferent and efferent pathways are vulnerable to traumatic injury. Commonly described categories of oculomotor dysfunctions are anomalies of accommodation, version, vergence (nonstrabismic, as well as strabismic), photosensitivity, visual field integrity, and ocular health [44]. Authors indicate different percentages of neuroophthalmic impairments following TBI, ranging from 39% to 90%, as described in [45, 46, 47, 48].

[1] This study is described also in [2].

Neuro-ophthalmic deficits may have important consequences on balance, since postural control integrates information from the visual, vestibular, and somatosensory systems.

Subjective complaints of dizziness that occur in the absence of objective clinical signs are difficult to assess [49, 50]. Static stabilometry may provide an objective evaluation of postural instability [4, 9, 26, 51, 52] by characterizing the performance of the postural control system during quiet standing.

This technique is based on the study of the trajectories of the Center of Pressure (CoP) on the support surface. CoP trajectories are recorded by a force platform and analyzed using different techniques and extracting different kinds of parameters [4, 26, 52]. A possible limit of static stabilometry was highlighted by Ref. [51, 53] due to the high inter-subject and intra-subject variability that many studies report.

Previous studies [49, 50, 54, 55, 56, 57, 58, 59] addressed the problem of quantifying the consequences of TBI on balance assessment using static stabilometry. None of the studies published in the past specifically considered a group of TBI patients with a significant residual visual impairment.

Studies on static posturography are usually based on an acquisition protocol consisting of two trials, with open and closed eyes, respectively, to take into account the role of the visual system.

My study differs from the previous ones in two aspects. First, I consider a group of TBI patients with residual neuro-ophthalmic deficits. Secondly, this study is based on a more complete acquisition protocol that adds to frontal open- and closed-eye trials, trials in which quiet standing of the subject is evaluated after a fast or a slow head rotation. In this way, it is possible to highlight the specific difficulties of each patient in various conditions that stimulate the visual and vestibular systems.

The aim of this study is to present a more complete acquisition protocol that allows to evaluate balance impairments in TBI patients and to demonstrate that such protocol can discriminate between controls and patients. Furthermore, I demonstrate that the presented protocol can also distinguish patients with different levels of visual impairment.

4.3.2 Material and methods

Subjects

TBI patients were recruited from the outpatients of the Clinica Oculistica C. Sperino, Ospedale Oftalmico (Torino), Italy, where they were referred for a neuroophthalmologic examination. On an average, 73% of approximately 70 TBI patients that were referred to Clinica Sperino in a year had neuro-ophthalmic impairments. The assessment of the severity of trauma was based on patients history and medical records obtained from the Post-traumatic Rehabilitation Center of Caraglio (Cuneo, Italy) where they were treated after the injury. My greater sample was formed by 50 subjects. The inclusion criteria were the typology of brain injury, its localization, and the presence of visual impairment only at the time of the test. We considered patients whose injuries were localized in the frontal, fronto-temporal, and fronto-temporo-parietal lobe, to select subjects with a high probability of suffering from neuro-ophthalmic deficits caused by the trauma. I excluded patients who showed residual sensorimotor or vestibular impairments. Thus, 13 TBI patients out of 50 were included in this study. These were four females (age 2841 years, mean 34.5 ± 6.0 years; height 160170 cm, mean 163.0 ± 4.8 cm; weight 53 85 kg, mean 62.5 ± 15.1 kg) and nine males (age 2263 years, mean 33.7 ± 13.9 years; height 170186 cm, mean 181.0 ± 3.4 cm; weight 7090 kg, mean 79.0 ± 6.4 kg). Table 1 shows patients characteristics.

The control group consisted of 43 healthy subjects, 26 females and 17 males, matched for age, height and body mass index, with no orthopedic, neurological or visual problems.

Both TBI patients and controls underwent a neuro-ophthalmologic examination prior to the test to evaluate the visual system.They were examined for pupillary reflex, smooth pursuit, saccades and optokinetic nystagmus. The last column of Table 1 reports the clinical evaluation of the residual visual impairment at the time of the balance test. In all patients abnormal saccades were observed. In five patients global deficits of the eyes version were found. These patients were classified as severe in the last column of Table 1. Three patients showed both saccades and smooth pursuit anomalies and were classified as moderate. Patients in which only abnormal saccades were observed were classified as mild. All the subjects belonging to the control group did not show any neuro-ophthalmologic abnormality.

The experimental protocol was approved by the local ethical committee and all participants gave their written informed consent to the study.

Table 4.4: Postural sway parameters

Patient	Age (years)	Gender (M/F)	GCS score[a]	CT/MRI (months)	Time[b]	Cause	Residual damage[c]
1	26	M	15	Negative	37	Violence	Mild
2	62	M	14	Positive	130	Traffic accident	Moderate
3	25	M	4	Positive	35	Fall from scaffolding	Severe
4	41	F	8	Positive	42	Traffic accident	Severe
5	28	M	8	Positive	95	Traffic accident	Severe
6	31	M	6	Positive	71	Traffic accident	Severe
7	22	M	Not av.	Positive	55	Traffic accident	Mild
8	28	F	9	Positive	64	Fall from horse	Severe
9	31	F	8	Positive	38	Traffic accident	Mild
10	38	F	6	Positive	66	Traffic accident	Moderate
11	38	M	6	Positive	143	Traffic accident	Mild
12	21	M	14	Positive	15	Traffic accident	Mild
13	50	M	14	Positive	17	Fall from scaffolding	Moderate

[a]Lowest Glasgow Coma Scale score after hospitalization.
[b]Time elapsed from head trauma.
[c] Assessed from the clinical neuro-ophthalmic evaluation of the patients prior to the balance test.

Acquisition protocol

Subjects were asked to stand quietly, in upright position, over a Kistler 9286A force platform. The inter-malleolar distance was fixed at 4 cm and the feet opening angle was 308. The acquisition protocol consisted of 10 different trial conditions, five with eyes open (looking at a visual target) and five with eyes closed. The head positions were: (1) frontal: open eyes frontal (OEF), closed eyes frontal (CEF), (2) head rotated after a slow left rotation: open eyes left slow (OELs), closed eyes left slow (CELs), (3) head rotated after a slow right rotation: open eyes right slow (OERs), closed eyes right slow (CERs), (4) head rotated after a fast left rotation: open eyes left fast (OELf), closed eyes left fast (CELf), (5) head rotated after a fast right rotation: open eyes

right fast (OERf), closed eyes right fast (CERf). At the operator order, the subject reached the requested head position and then the signal acquisition started. A biaxial accelerometer fixed on the forehead of the subject was employed for monitoring the head rotation. Each recording started at the end of the head rotation and lasted for 60 s.

The sequence of trials was randomized to avoid learning and/or fatigue effects [27]. For every two trials the subject rested for 1 min moving away from the platform.

The platform signal was recorded with a sampling frequency of 2 kHz and then down-sampled to 50 Hz. The acquisition system was Step32 (DemItalia, Italy).

Data analysis

I calculated the major geometrical and time-domain parameters based on the CoP trajectory [26, 52]. Table 4.3 describes the set of parameters we considered.

First, I compared TBI and controls for each trial condition and CoP parameter by means of a two-sample t-test, after verifying the gaussianity of the distributions.

Moreover, I was interested taking into account the inter-relations among CoP parameters in the different trials, using the global information arising from the complete protocol: for each subject I have a total of 70 dependent variables (10 trials x 7 parameter values). To this purpose, I applied a multivariate analysis of variance (MANOVA) approach [30, 31, 32]. I reduced the number of CoP parameters considered, preserving those containing non redundant information and discarding parameters highly correlated among them or with high within-group variability. To select the reduced set of parameters I used Wilks Lambda statistic (λ) [31]. λ is an index of the parameters discrimination capability. It is defined as the ratio between the within-groups generalized variability and the total generalized variability, the latter being the sum of the within-groups and between groups generalized variability. This index takes values between zero and one, lower λ-values indicating a better discrimination among groups.

The procedure I adopted is the following. As a first step, I calculated λ for each parameter separately and sorted the parameters in λ ascending order. I kept the parameter with lower λ-value. Then I considered all the possible combinations of two parameters, recalculated the corresponding λ-values and sorted them in ascending order, keeping the combination with lower λL-value. The process was carried out iteratively adding one parameter at a time, each time recalculating the λ-value and

choosing the combination of parameters showing the lowest λ-value. The parameter selection stopped when, adding more parameters, λ did not significantly decrease [31].

After the selection of the reduced set of CoP parameters I summarized the information arising from the 10-trial protocol applying a canonical variate analysis (CVA) [31]. The canonical variables C are linear combinations of the original variables, chosen to maximize the separation among groups. Specifically, the first canonical variable C1 is the linear combination of the original variables that has the maximum separation among groups. This means that among all possible linear combinations, it is the one with the most significant F statistic in a one-way analysis of variance. The second canonical variable C2 has the maximum separation while being orthogonal to C1, and so on. I represented the two populations of TBI and controls in the plane of the first two canonical variables.

4.3.3 Results

Figure 4.6 shows, for each parameter, mean and standard deviation of TBI patients and controls in the 10 typologies of acquisition. Differences between groups which are statistically significant (two-sample t-test, $p \leq 0.05$) are indicated with an asterisk. Major and minor axis and the RMS values show significant differences in all of the trials. Mean velocity highlights significant differences between TBI and controls mainly in trials after head rotation (slow or fast). On the contrary, mean velocity is not significantly different in trials with a frontal head position, both with eyes open and closed. Sway area and eccentricity do not differentiate the two groups. I also tested open eyes vs. closed eyes performances: significant differences are indicated with triangles in controls and with circles in TBI patients. In controls, differences were observed in all the test conditions for the mean velocity. For the other parameters, statistically significant differences were observed only in a few test conditions. In TBI patients there were significant differences between open eyes and closed eyes trials only in a single test condition (mean velocity, OERf vs. CERf).

Figure 4.7 shows the values of λ on which we based the parameter selection. The single parameter that better differentiates the two populations is minor axis ($\lambda = 0.42$), the best combination of two parameters is minor and major axes $\lambda = 0.31$), that of three parameter is minor axis, major axis, and RMS AP ($\lambda = 0.15$), that of four parameters is minor axis, major axis, RMS AP, and eccentricity ($\lambda = 0.076$), and, finally, that of

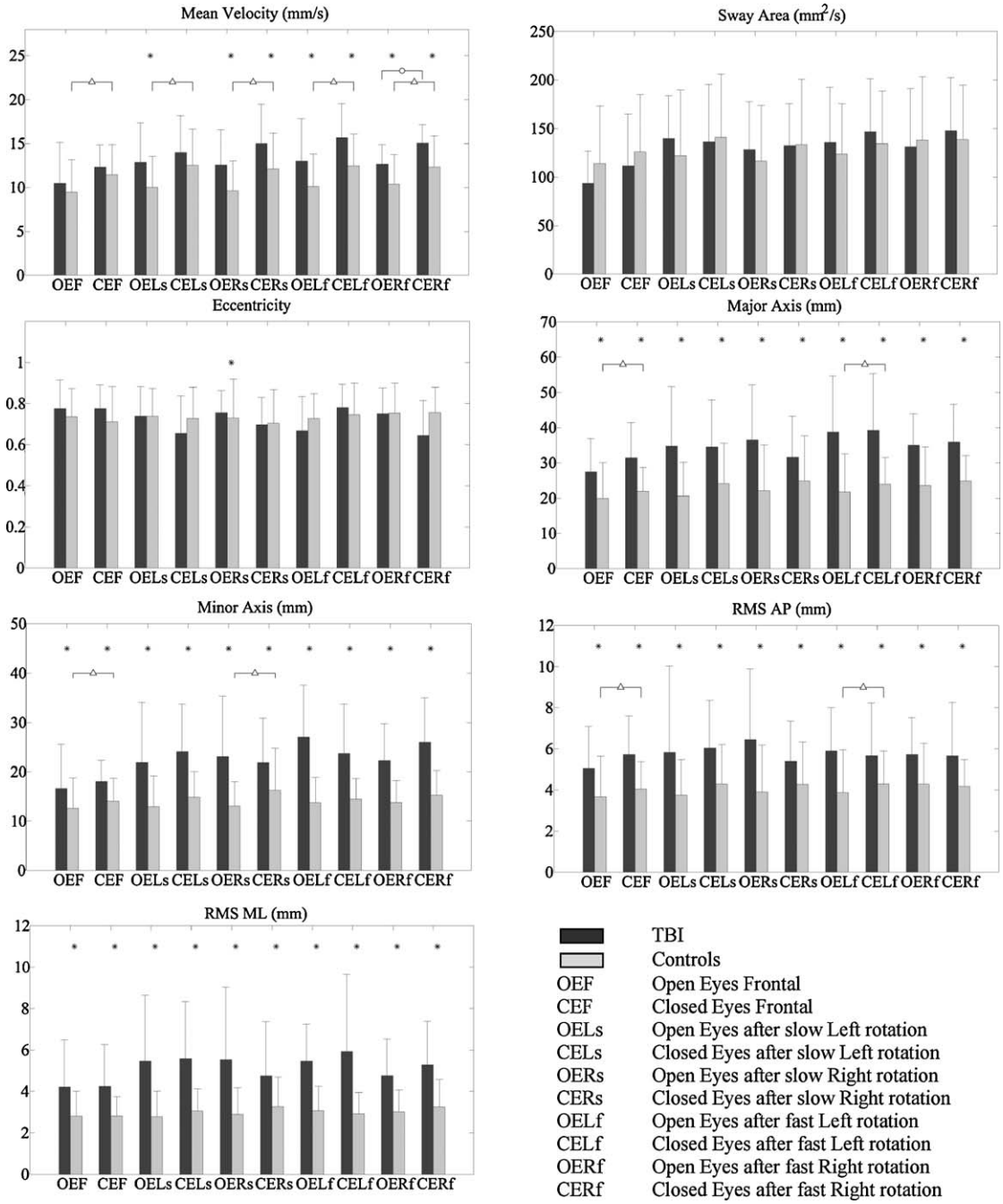

Figure 4.6: Comparison of posturographic parameters between TBI patients and controls: mean values and standard deviation are shown for each parameter and each trial condition listed in the legenda. * Significant difference between TBI and controls ($p \leq 0.05$); $^{\triangle}$ significant difference, in controls, between eyes open and closed ($p \leq 0.05$); $^{\circ}$ significant difference, in TBI, between eyes open and closed ($p \leq 0.05$).

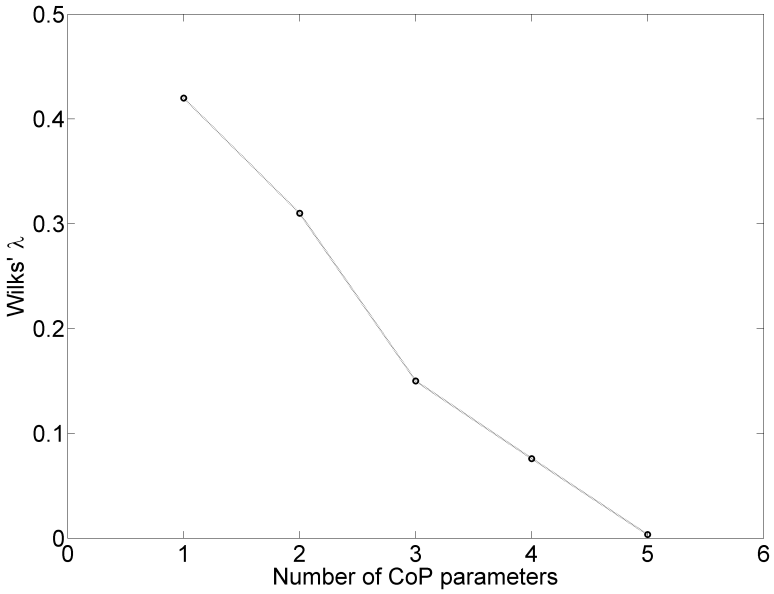

Figure 4.7: Wilks Lambda (λ) as a function of the number of CoP parameters. (1) The best single parameter (minor axis). (2) The best combination of two parameters (minor axis and major axis). (3) The best combination of three parameters (minor axis, major axis and RMS AP). (4) The best combination of four parameters (minor axis, major axis, RMS AP and eccentricity). (5) The best combination of five parameters (minor axis, major axis, RMS AP, eccentricity and sway area).

five parameters is minor axis, major axis, RMS AP, eccentricity, and sway area ($\lambda = 0.0035$). Therefore, the λ-value decreases remarkably each time a parameter is added to the set of the best CoP parameters and it falls below 0.05 when considering the best combination of five parameters. Hence, in the rest of the analysis, I consider only these five parameters. Note that eccentricity and sway area do not play a role in differentiating the two populations if they are considered as standalone parameters, but they become useful if they are considered in combination with the other parameters.

The parameter selection procedure was performed considering all the 10 trials. The effect of considering a smaller number of trials is evident from figure 4.8,which shows multivariate data from TBI patients and controls plotted against the first two canonical variables C1 and C2. Figure 4.8(a and b) shows the results of multivariate analysis to compare controls and TBI patients, while figure 4.8(c and d) shows the differences among the three sub-groups of TBI patients and controls. The procedure of parameter

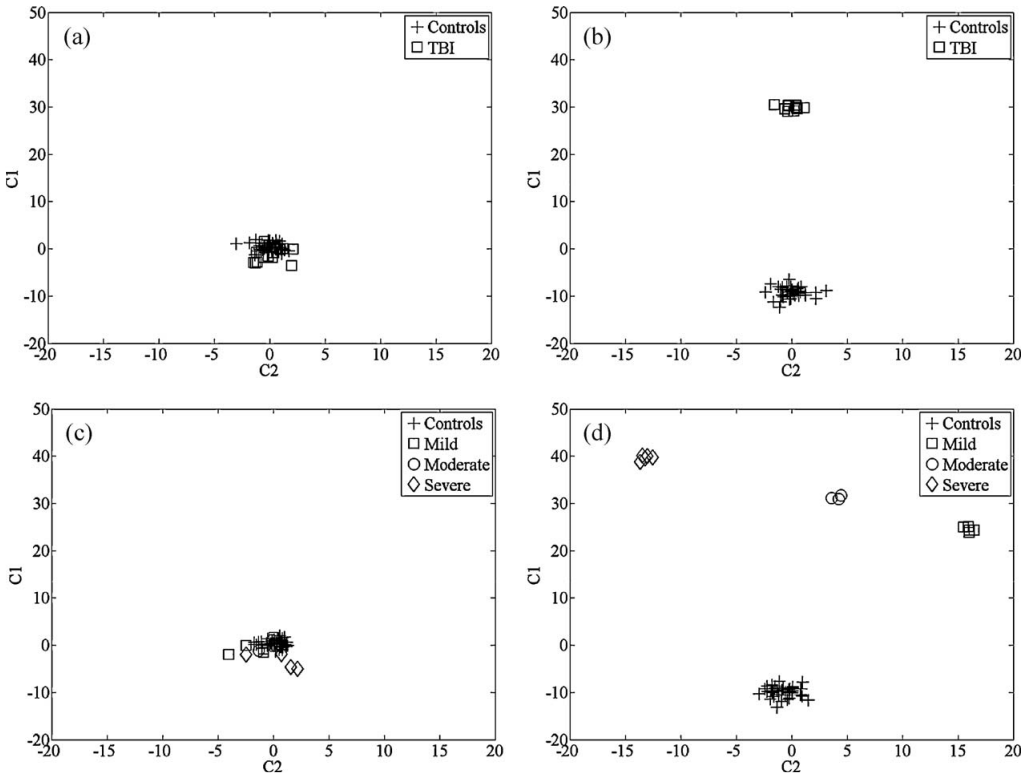

Figure 4.8: Scatter plots of the first (C1) vs. the second (C2) canonical variable for controls and TBI patients. (a) Two trials: open eyes frontal (OEF) and closed eyes frontal (CEF). (b) 10 trials: OEF, CEF, OELs, CELs, OERs, CERs, OELf, CELf, OERf, CERf. (c) Two trials: OEF and CEF. TBI patients with different levels of neuro-ophthalmic residual impairment (mild, moderate or severe) and controls. (d) 10 trials. TBI patients with different levels of neuro-ophthalmic residual impairment (mild, moderate or severe) and controls.

selection was not redone, while we recomputed the canonical variables for this specific case. Fig. 3(a) shows the results on two acquisition trials only (open eyes frontal and closed eyes frontal), while Fig. 3(b) refers to the complete set of 10 trials. In figure 4.8(a) TBI patients and controls are partially overlapped, even if some of the TBI patients fall outside the control group cloud (λ= 0.63,p = 0.014). In figure 4.8(b) the two populations are completely separated (λ= 0.0035, p = 3.3 x 10^{13}). Therefore, considering all the 10 trials, TBI patients are completely differentiated from controls.

Figure 4.8(c and d) shows controls and patients suffering from mild, moderate, and severe residual visual impairment, as reported by Table 4.4. When only two trials are

considered, the various groups are scarcely separated (figure 4.8(c)). On the contrary, when all the 10 trials are taken into account, not only the patients are well differentiated from controls, but also the three groups are completely separated among them (figure 4.8(d)). Moreover, the distance between controls and the three TBI groups increases with increasing level of visual impairment.

4.3.4 Discussion

The most widely used parameters in posturography are the total length of the CoP path (sway path length) and the mean velocity. They are essentially the same parameter, except that mean velocity is normalized with respect to the test duration and hence does not depend on it. They are usually evaluated with the subject in quiet stance on the platform with the head in frontal position, both with eyes open and closed. It is important to notice that velocity integrates both amplitude and frequency changes, thus a concomitant reduction in sway frequency can reduce the discriminant power of velocity. Dehail et al. [54] studied a group of 68 TBI patients (60 of which with a GCS score <8, and 33 with a residual neurological impairment) and found that sway path length was significantly increased, compared to controls, both with eyes open and closed. In my sample population, I found that mean velocity did not separate TBI patients from controls in the trials with the head in frontal position (both with eyes open and closed), while it separated the two populations in the newly proposed test conditions (after slow or fast head rotation). The difference between myr results and those reported in [54] may be explained by the fact that in this study patients reported, in general, less severe TBI and suffered from no vestibular or sensorimotor impairment.

I hypothesized that subjects with visual impairment rely less than controls on the information arising from the visual system. Geurts et al. [50], working with a group of TBI patients who complained of reduced gross motor skills without sensory-motor impairments, report that visual deprivation was most detrimental for TBI patients, particularly for the medio-lateral control. In my patients, differences between the open- and closed-eyes balance performances are almost never statistically significant, while they are significant in controls for the parameter mean velocity. These results are coherent with our hypothesis, since we found that visual deprivation is less detrimental for patients.

Among others, Visser et al. [51] pointed out that the poor discriminative ability (between health and disease) of posturography may relate to the substantial inter-subject and intra-subject variability. Given these uncertainties, many researchers record a broad range of different parameters and/or perform repeated tests in the same or in different test conditions. As a consequence, for each subject, many parameters and many test conditions are considered which are partially correlated among them.

To take into account all the information arising from the complete protocol, I used a multivariate approach. Multivariate analysis requires a prior variable selection, as described in [31]. The results of variables selection are often counterintuitive. In my study, I excluded the best combination of five parameters that were discriminative in univariate analysis. This is not surprising, since univariate analysis does not take into consideration the correlation among parameters.

Thanks to the representation of subjects in the plane of the first two canonical variables, I demonstrated (see figure 4.8) that it is possible to obtain a complete separation of patients from controls when all the 10-test conditions are considered and is also possible to discriminate among groups of patients with different residual visual impairment. Specifically, C1 discriminates patients from controls, while C2 summarizes the information needed to separate patients according to the degree of their residual visual impairment.

4.3.5 Conclusion

Using the proposed 10-trial protocol it was possible to clearly distinguish balance abnormalities of TBI patients with respect to controls. Moreover, I found that the severity of the residual neuro-ophthalmic deficit is correlated to the severity of the balance impairment. This is of paramount importance from a clinical perspective since it demonstrates that static posturography, associated to the presented protocol, can be applied to objectively evaluate the balance performances of a patient enrolled in a rehabilitation program and assess his/her progresses.

4.4 Conclusions

The use of geometrical parameters in studying postural control allowed to reach interesting results.

The proposed protocol and the evaluation of geometrical parameters allowed highlighting differences between groups of pathological and healthy subjects.

In particular, in the volleyball study, the starting hypothesis about different strategies in athletes compared to controls in using the visual information during mantainance of upright position was confirmed. Moreover, I was able to differentiate among different atheletes of different levels and different role in the game situation.

In TBI study, I was able to highlight differences between pathological and control subjects. Moreover, it was possible to evidence different difficulties in patients with different levels of residual visual impairments.

References

[1] V. Agostini, E. Chiaramello, L. Canavese, C. Bredariol, and M. Knaflitz, "Postural sway in volleyball players," *Human Movement Science*, (accepted).

[2] V. Agostini, E. Chiaramello, C. Bredariol, C. Cavallini, and M. Knaflitz, "Postural control after traumatic brain injury in patients with neuro-ophthalmic deficits.," *Gait Posture*, vol. 34, pp. 248–253, Jun 2011.

[3] M. Schmid, S. Conforto, V. Camomilla, A. Cappozzo, and T. D'Alessio, "The sensitivity of posturographic parameters to acquisition settings.," *Med Eng Phys*, vol. 24, pp. 623–631, Nov 2002.

[4] J. A. Raymakers, M. M. Samson, and H. J. J. Verhaar, "The assessment of body sway and the choice of the stability parameter(s)," *Gait Posture*, vol. 21, pp. 48–58, Jan 2005.

[5] T. McGuine and J. S. Keene, "The effect of a balance training program on the risk of ankle sprains in high school athletes," *Am J Sports Med*, vol. 34 (7), p. 11031111, 2006.

[6] W. Petersen, C. Braun, W. Bock, K. Schmidt, A. Weimann, W. Drescher, E. Eiling, R. Stange, T. Fuchs, J. Hedderich, and T. Zantop, "A controlled prospective case control study of a prevention training program in female team handball players: the german experience," *Arch Orthop Trauma Surg*, vol. 125, p. 614621, 2005.

[7] K. Sderman, S. Werner, T. Pietil, B. Engstrm, and H. Alfredson, "Balance board training: prevention of traumatic injuries of the lower extremities in female soccer players? a prospective randomized intervention study," *Knee Surg Sports Traumatol Arthrosc*, vol. 8, no. 6, pp. 356–363, 2000.

[8] E. Verhagen, A. van der Beek, J. Twisk, L. Bouter, and R. B. W. van Mechelen, "The effect of a proprioceptive balance board training program for the prevention of ankle sprains. a prospective controlled trial," *Am J Sports Med*, vol. 32 (6), p. 13851392, 2004.

[9] D. A. Winter, "Human balance and posture control during standing and walking," *Gait & Posture*, vol. 3, pp. 193–214, 1995.

[10] L. Baratto, P. Morasso, C. Re, and G. Spada, "A new look at posturographic analysis in the clinical context: sway-density vs. other parameterization techniques," *Motor Control*, vol. 6, p. 246270, 2002.

[11] A. Ruhe, R. Fejer, and B. Walker, "The test-retest reliability of centre of pressure measures in bipedal static task conditions–a systematic review of the literature," *Gait Posture*, vol. 32, pp. 436–445, Oct 2010.

[12] V. V. Arkov, T. F. Abramova, T. M. Nikitina, V. V. Ivanov, D. V. Suprun, M. U. Shkurnikov, and A. G. Tonevitskii, "Comparative study of stabilometric parameters in sportsmen of various disciplines.," *Bull Exp Biol Med*, vol. 147, pp. 233–235, Feb 2009.

[13] P. G. Gerbino, E. D. Griffin, and D. Zurakowski, "Comparison of standing balance between female collegiate dancers and soccer players.," *Gait Posture*, vol. 26, pp. 501–507, Oct 2007.

[14] P. Perrin, D. Deviterne, F. Hugel, and C. Perrot, "Judo, better than dance, develops sensorimotor adaptabilities involved in balance control," *Gait Posture*, vol. 15, pp. 187–194, Apr 2002.

[15] E. Golomer, J. Crmieux, P. Dupui, B. Isableu, and T. Ohlmann, "Visual contribution to self-induced body sway frequencies and visual perception of male professional dancers.," *Neurosci Lett*, vol. 267, pp. 189–192, Jun 1999.

[16] J. M. Schmit, D. I. Regis, and M. A. Riley, "Dynamic patterns of postural sway in ballet dancers and track athletes.," *Exp Brain Res*, vol. 163, pp. 370–378, Jun 2005.

[17] N. Vuillerme, F. Danion, L. Marin, A. Boyadjian, J. M. Prieur, I. Weise, and V. Nougier, "The effect of expertise in gymnastics on postural control.," *Neurosci Lett*, vol. 303, pp. 83–86, May 2001.

[18] E. Bie and M. Kuczyski, "Postural control in 13-year-old soccer players.," *Eur J Appl Physiol*, vol. 110, pp. 703–708, Nov 2010.

[19] M. Kuczyski, Z. Rektor, and D. Borzucka, "Postural control in quiet stance in the second league male volleyball players," *Human movement*, vol. 10(1), pp. 12–15, 2009.

[20] B. Dai, C. J. Sorensen, and J. C. Gillette, "The effects of postseason break on stabilometric performance in female volleyball players.," *Sports Biomech*, vol. 9, pp. 115–122, Jun 2010.

[21] E. Jafarzadehpur, N. Aazami, and B. Bolouri, "Comparison of saccadic eye movements and facility of ocular accommodation in female volleyball players and non-players.," *Scand J Med Sci Sports*, vol. 17, pp. 186–190, Apr 2007.

[22] T. Paillard and F. No, "Effect of expertise and visual contribution on postural control in soccer," *Scand J Med Sci Sports*, vol. 16, pp. 345–348, Oct 2006.

[23] A. Piras, R. Lobietti, and S. Squatrito, "A study of saccadic eye movement dynamics in volleyball: comparison between athletes and non-athletes," *J Sports Med Phys Fitness*, vol. 50, pp. 99–108, Mar 2010.

[24] H. Ishigaki and M. Miyao, "Differences in dynamic visual acuity between athletes and nonathletes.," *Percept Mot Skills*, vol. 77, pp. 835–839, Dec 1993.

[25] P. Rougier and M. Garin, "Performing saccadic eye movements or blinking improves postural control," *Motor Control*, vol. 11, pp. 213–223, Jul 2007.

[26] T. E. Prieto, J. B. Myklebust, R. G. Hoffmann, E. G. Lovett, and B. M. Myklebust, "Measures of postural steadiness: differences between healthy young and elderly adults," *IEEE Trans Biomed Eng*, vol. 43, pp. 956–966, Sep 1996.

[27] J. Tarantola, A. Nardone, E. Tacchini, and M. Schieppati, "Human stance stability improves with the repetition of the task: effect of foot position and visual condition," *Neurosci Lett*, vol. 228, pp. 75–78, Jun 1997.

[28] L. Chiari, L. Rocchi, and A. Cappello, "Stabilometric parameters are affected by anthropometry and foot placement.," *Clin Biomech (Bristol, Avon)*, vol. 17, no. 9-10, pp. 666–677, 2002.

[29] I. Guyon and A. Elisseeff, "An introduction to variable and feature selection," *Journal of Machine Learning Research*, vol. 3, p. 11571182, 2003.

[30] K. V. Mardia, J. T. Kent, and J. M. Bibby, *Multivariate Analysis*. Academic press, 1979.

[31] W. Krzanowski, *Principles of multivariate analysis: A users perspective*. Clarendon Press., 1988.

[32] R. Johnson and D. Wichern, *Applied multivariate statistical analysis*. Prentice Hall, 2002.

[33] C. A. Emery, "Is there a clinical standing balance measurement appropriate for use in sports medicine? a review of the literature," *J Sci Med Sport*, vol. 6 (4), p. 492504, 2003.

[34] R. J. Doyle, E. T. Hsiao-Wecksler, B. G. Ragan, and K. S. Rosengren, "Generalizability of center of pressure measures of quiet standing.," *Gait Posture*, vol. 25, pp. 166–171, Feb 2007.

[35] K. Stambolieva, V. Diafas, V. Bachev, L. Christova, and P. Gatev, "Postural stability of canoeing and kayaking young male athletes during quiet stance," *Eur J Appl Physiol*, vol. 112, pp. 1807–1815, May 2012.

[36] D. Alpini, V. Mattei, H. Schlecht, and R. Kohen-Raz, "Postural control modifications induced by synchronized ice skating," *Sport Sci Health*, vol. 2, p. 1117, 2008.

[37] M. C. Marques, R. van den Tillaar, T. J. Gabbett, V. M. Reis, and J. J. Gonz?lez-Badillo, "Physical fitness qualities of professional volleyball players: determination of positional differences," *J Strength Cond Res*, vol. 23, pp. 1106–1111, Jul 2009.

[38] J. A. Langlois, W. Rutland-Brown, and K. E. Thomas, "The incidence of traumatic brain injury among children in the united states: differences by race.," *J Head Trauma Rehabil*, vol. 20, no. 3, pp. 229–238, 2005.

[39] A. Maas, N. Stocchetti, and R. Bullock, "Moderate and severe traumatic brain injury in adults," *Lancet Neurol*, vol. 7, p. 72841, 2008.

[40] F. Tagliaferri, C. Compagnone, M. Korsic, F. Servadei, and J. Kraus, "A systematic review of brain injury epidemiology in europe.," *Acta Neurochir (Wien)*, vol. 148, pp. 255–68; discussion 268, Mar 2006.

[41] G. Teasdale and B. Jennett, "Assessment of coma and impaired consciousness. a practical scale.," *Lancet*, vol. 2, pp. 81–84, Jul 1974.

[42] L. Chamelian and A. Feinstein, "Outcome after mild to moderate traumatic brain injury: the role of dizziness.," *Arch Phys Med Rehabil*, vol. 85, pp. 1662–1666, Oct 2004.

[43] S. Thornhill, G. M. Teasdale, G. D. Murray, J. McEwen, C. W. Roy, and K. I. Penny, "Disability in young people and adults one year after head injury: prospective cohort study.," *BMJ*, vol. 320, pp. 1631–1635, Jun 2000.

[44] N. Kapoor and K. J. Ciuffreda, "Vision disturbances following traumatic brain injury.," *Curr Treat Options Neurol*, vol. 4, pp. 271–280, Jul 2002.

[45] I. B. Suchoff, N. Kapoor, K. J. Ciuffreda, D. Rutner, E. Han, and S. Craig, "The frequency of occurrence, types, and characteristics of visual field defects in acquired brain injury: a retrospective analysis.," *Optometry*, vol. 79, pp. 259–265, May 2008.

[46] G. P. VanStavern, V. Biousse, M. J. Lynn, D. J. Simon, and N. J. Newman, "Neuro-ophthalmic manifestations of head trauma.," *J Neuroophthalmol*, vol. 21, pp. 112–117, Jun 2001.

[47] A. R. Kulkarni, S. P. Aggarwal, R. R. Kulkarni, M. D. Deshpande, P. B. Walimbe, and A. S. Labhsetwar, "Ocular manifestations of head injury: a clinical study.," *Eye (Lond)*, vol. 19, pp. 1257–1263, Dec 2005.

[48] K. J. Ciuffreda, N. Kapoor, D. Rutner, I. B. Suchoff, M. E. Han, and S. Craig, "Occurrence of oculomotor dysfunctions in acquired brain injury: a retrospective analysis.," *Optometry*, vol. 78, pp. 155–161, Apr 2007.

[49] J. R. Basford, L.-S. Chou, K. R. Kaufman, R. H. Brey, A. Walker, J. F. Malec, A. M. Moessner, and A. W. Brown, "An assessment of gait and balance deficits after traumatic brain injury.," *Arch Phys Med Rehabil*, vol. 84, pp. 343–349, Mar 2003.

[50] A. C. Geurts, G. M. Ribbers, J. A. Knoop, and J. van Limbeek, "Identification of static and dynamic postural instability following traumatic brain injury.," *Arch Phys Med Rehabil*, vol. 77, pp. 639–644, Jul 1996.

[51] J. E. Visser, M. G. Carpenter, H. van der Kooij, and B. R. Bloem, "The clinical utility of posturography.," *Clin Neurophysiol*, vol. 119, pp. 2424–2436, Nov 2008.

[52] L. Rocchi, L. Chiari, and A. Cappello, "Feature selection of stabilometric parameters based on principal component analysis.," *Med Biol Eng Comput*, vol. 42, pp. 71–79, Jan 2004.

[53] M. Samson and A. Crowe, "Intra-subject inconsistencies in quantitative assessments of body sway," *Gait & Posture*, vol. 4, pp. 252–7, 1996.

[54] P. Dehail, H. Petit, P. Joseph, P. Vuadens, and J. Mazaux, "An assessment of postural instability in patients with traumatic brain injury upon enrolment in a vocational adjustment programme," *J Rehabil Med*, vol. 39, p. 5316, 2007.

[55] A. C. Geurts, J. A. Knoop, and J. van Limbeek, "Is postural control associated with mental functioning in the persistent postconcussion syndrome?," *Arch Phys Med Rehabil*, vol. 80, pp. 144–149, Feb 1999.

[56] K. R. Kaufman, R. H. Brey, L.-S. Chou, A. Rabatin, A. W. Brown, and J. R. Basford, "Comparison of subjective and objective measurements of balance disorders following traumatic brain injury.," *Med Eng Phys*, vol. 28, pp. 234–239, Apr 2006.

[57] E. Lahat, J. Barr, B. Klin, Z. Dvir, T. Bistrizer, and G. Eshel, "Postural stability by computerized posturography in minor head trauma.," *Pediatr Neurol*, vol. 15, pp. 299–301, Nov 1996.

[58] S. Slobounov, C. Cao, W. Sebastianelli, E. Slobounov, and K. Newell, "Residual deficits from concussion as revealed by virtual time-to-contact measures of postural stability.," *Clin Neurophysiol*, vol. 119, pp. 281–289, Feb 2008.

[59] L. D. Wade, C. G. Canning, V. Fowler, K. L. Felmingham, and I. J. Baguley, "Changes in postural sway and performance of functional tasks during rehabilitation after traumatic brain injury.," *Arch Phys Med Rehabil*, vol. 78, pp. 1107–1111, Oct 1997.

5

Rotational components in center of pressure signals

In this chapter, the rotary spectra analysis mathematically described in chapter 3 will be applied to center of pressure signals of a group of healthy subjects.

Both the stationary and non-stationary cases will be analyzed.

5.1 Stationary case[1]

Applications of the analysis of the CoP trajectory can be found in studies about the physiology of the human motor control (e.g. [2]), in the assessment of pathological conditions, e.g. Parkinsons disease [3], vestibular disorders [4], cerebral palsy [5], traumatic brain injury [6], as well as in the evaluation of athletes balance performances [7].

In an effort to interpret the CoP signal, several techniques were developed in different research fields. As an example, in the framework of statistical mechanics, Collins and De Luca [8] formulated a method based on fractional Brownian motion, analyzing the short- and long-term time intervals of the CoP signal. In the field of motor control, the study of Zatsiorsky and Duarte [9] considered the instant equilibrium point and its migration in the plane, introducing the rambling-trembling decomposition. This decomposition separates the low and high frequency components of the CoP signal. Recent advances in the study of postural control focused on the muscle synergies and strategies adopted during voluntary body sway [2, 10, 11].

[1] This study is described also in [1], a paper which passed the first stage of review to be published in Motor Control.

In the great majority of the clinical studies, it is widely accepted to extrapolate geometrical parameters from the CoP trajectory (e.g. sway path length, sway area, smallest ellipse containing the CoP trajectory) or statistical parameters from the antero-posterior (AP) and medio-lateral (ML) time series (e.g. root mean square). The decomposition of the CoP signal into the AP and ML timeseries was traditionally introduced to account for the plantarflexion/dorsiflexion about the ankle joint, and the abduction/adduction about the hip joint, respectively [12]. Baratto et al. [13] report the use of 38 different posturographic parameters. These parameters were defined in the time domain, in the frequency domain, or were based on diffusion plots and sway-density plots. Most of the parameters calculated according to these different approaches are affected by relevant intra- and inter-subject variability and/or do not have a clear physiological interpretation [14]. Furthermore, the traditional CoP decomposition into AP and ML time-series may hide some important information embodied in the combined signal, like the presence of loops around the instant equilibrium point [15].

In this study, the problem of characterizing the CoP signal is approached from a different point of view: my hypothesis is that the CoP signal contains rotational components. To extract the rotational components from the CoP signal I applied the rotary spectra analysis, already described from the mathematical point of view in chapter3.

The objective of this study is to verify the presence of rotational components in the CoP signal. Therefore, I applied the rotary spectra analysis to the CoP signal, demonstrated the presence of rotational components, and extracted information about the rotational characteristics of the body sway.

5.1.1 Application to static posturography

The described mathematical formulation is applied to the sway path of healthy subjects recorded by means of a force platform. In particular, the rotary spectra analysis is applied to the bivariate time series of the CoP trajectory:

$$\begin{aligned} x(t) &= CoP_x(t) \\ y(t) &= CoP_y(t), \end{aligned} \tag{5.1}$$

where CoP_x and CoP_y are the sway path orthogonal components on the force platform plane.

Sample population and experimental trials

The sway path was investigated on a group of 42 healthy volunteers, 25 females and 17 males (mean age 23.74.7 years), who did not suffer from orthopedic, neurological or visual problems.

Each subject was asked to stand quietly in upright position on the force platform, arms at the side, and to look straight ahead at a visual target. The target was a static black disk (diameter: 5 cm) located on the wall (2 m from the subject), at the subjects eye level. The inter-malleolar distance was fixed at 4 cm and the feet opening angle was 30°.

The acquisition protocol consisted of two trials with eyes open (OE) and closed (CE), respectively. Trials were randomized to avoid learning and fatigue effects.

The experimental protocol was approved by the local ethical committee and all participants gave their written informed consent to be included in the study.

Acquisition System and Signal Processing

The experimental setup consisted of a Kistler 9286A (Kistler, Switzerland) force platform and of an acquisition system STEP32 (DemItalia, Italy). Each acquisition lasted 60 seconds. The signals were recorded with a sampling frequency of 2 kHz and down-sampled to 20 Hz.

The mean value of CoPx and CoPy is subtracted from the respective time series. A high-pass filter with cut-off frequency equal to 0.05 Hz is then applied to the two time series in order to remove possible trends. We then compute the one-sided spectra S^+ and S^- for the two oppositely rotating components.

The amplitude and phases of the two Fourier components X(f) and Y(f) are obtained by applying the Welch method with signal epochs of length equal to 10 s, overlapped by 50%, and windowed by a Gaussian window.

5.1.2 Results

As an example of rotary spectra analysis applied to static posturography, Fig.5.1 shows the sway path of a representative subject and the corresponding decomposition into rotary spectra. The CoP trajectories and rotary spectra are reported for both experimental conditions with the subject keeping the eyes open and gazing at a target

((a) and (b)) and with the subject keeping the eyes closed ((c) and (d)). In both conditions we are able to extract rotational components, in CCW and CW directions. In both open and closed eye conditions we observe a main peak at low frequencies, for both CW and CCW components.

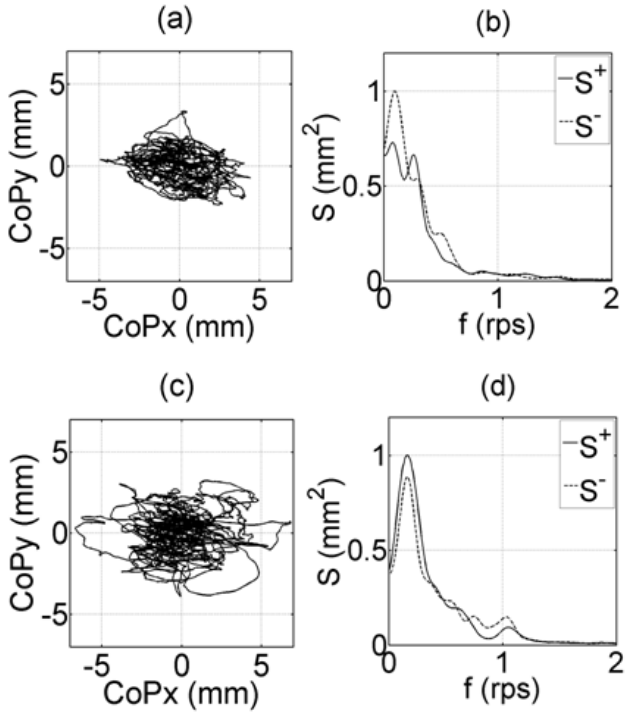

Figure 5.1: Sway path of a representative subject in (a) open and (c) closed eyes conditions. The plots (b) and (d) show the corresponding rotary spectra: S^+ = CCW component, S^- = CW component.

In order to characterize the detected rotational components of the sway path over the population of healthy subjects, we defined eight rotary spectral parameters. We considered the frequency at which is found the 25%, 50%, 75% and 95% of the power spectral density. They are indicated as f25, f50, f75 and f95, respectively. The parameter f50 is the median of the power spectral density distribution, and f25 and f75 represent the first and third quartiles of the distribution. We considered also the mean frequency, the skewness, the mode and the total power of the distribution.

The results of the rotary spectra analysis applied to the CoP signals of the population are summarized in Table 5.1. At low frequencies (f25) there are statistically

significant differences between open and closed eyes trials, both for the CCW and the CW components. The parameters f50, f75 and the mean frequency show a significant difference only for the CCW component. The parameter f95 is higher in the CE condition than in the OE, both for S^+ and S^-, but it shows a greater variability with respect to the other parameters and the difference between OE and CE results not to be significant.

Skewness is a measure of the asymmetry of a distribution. In all the analyzed test conditions the skewness is found to be positive, indicating that the right tail of the distribution is longer than the left tail. No significant differences are found for this parameter comparing OE and CE trials. Statistical mode is defined as the value that occurs more frequently in a distribution. In the data set, the average mode ranges between 0.14 rps and 0.17 rps (see Table 5.1). Also for this parameter no significant differences are found comparing OE and CE trials. In the last column of Table 5.1 I report the total power of the distribution which shows significant differences between OE and CE trials for both S^+ and S^-.

Descriptive statistics of a subset of rotary parameters is given in Fig. 5.3 by means of the boxplot representation of the sample population. The mean and median frequencies, bandwidth (corresponding to 95% of the total power) and total power of the distribution are considered. Differences between the open and closed eyes trials can be noticed both for the CW and the CCW components, as already mentioned. In particular, the median values obtained in closed-eyes trials are always greater than those obtained in open-eyes trials, although this difference is not always significant.

I calculated the IRC for each subject of the population (frequency band: 0-10 Hz). In open eyes trials, I found that IRC has positive values in 24 subjects, and negative in the remaining 18 subjects. In closed eyes trials, I observed that IRC has positive values in 23 subjects and negative in 19 subjects.

For each subject, I compared the spectral power of the CW and CCW components, by means of a two sample F-test for variances ($\sigma = 5\%$). I obtained that, in open eyes trials, differences between S^+ and S^+ are statistically significant in 40 subjects. For 23 of them S^+ has a larger spectral power than S^-, while in the remaining 17, S^+ is predominant. In closed eyes trials, I observed significant differences between S^+ and S^- in 39 subjects. For 20 of them S^+ is predominant, while in theremaining 19, prevails S^-. These results confirm what has been obtained with the IRC parameter: there is

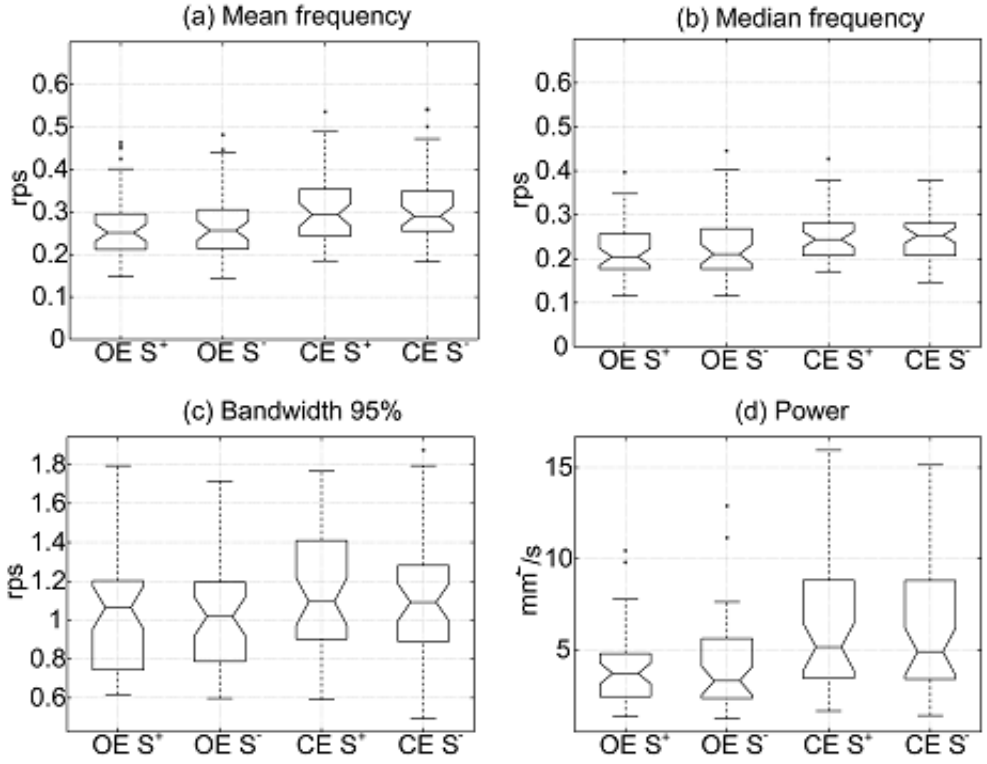

Figure 5.2: Boxplot representation of rotary spectral parameters related to the population of healthy subjects: (a) mean frequency, (b) median frequency, (c) bandwidth at 95% of the total power and (d) total power. OE = Open Eyes, CE = Closed Eyes, S^+ = CCW component, S^- = CW component. Each boxplot represents the median, first and third quartiles, minimum and maximum values of the empirical distribution. Possible outliers are depicted as a single cross.

not a clear preferential rotational direction in the sample of healthy subjects that I considered.

5.1.3 Discussion

In this study I hypothesized that the CoP signal shows inherent rotational characteristics. Applying rotary spectra analysis I was able to extract rotational components from the CoP signal. In literature, only few CoP parameters consider both the AP and ML components; one of the most commonly used is the mean velocity [16], which is the Euclidean norm of the AP and ML components normalized with respect to the test duration. The complex-valued representation of the CoP signal, which is the base

of the rotary spectra analysis, allows to consider not only the amplitude of the signal, but also its phase [17].

I investigated the presence of rotational components in CoP signals of a population of healthy subjects, and I obtained the clockwise and counter-clockwise rotary spectra for each subject. This approach was never used before to analyze posturographic signals.

I characterized each rotary spectrum calculating its bandwidth, mean and median frequency, skewness, mode, and power spectral density.

Spectral parameters calculated for the 42 subjects show a small inter-subject variability. This is an encouraging result, since traditional stabilometric parameters usually show high inter-subject variability [14].

In the population considered, I did not find significant differences between the parameters describing the clockwise and the counter-clockwise rotating components. This is not surprising, since there are no physiological reasons to hypothesize the prevalence of one component over the other. In agreement with this assertion, Experiment 2 of Balasubramaniam and Turvey [18] demonstrated that postural fluctuations are not influenced by handedness.

Comparing open and closed eyes conditions, I found that there are significant differences between the spectral powers, which show greater values with the subjects eyes closed. Differences between the power associated to the CoP trajectories with open and closed eyes are well documented in literature. As an example, Prieto et al. [16] demonstrated that the total power (entire CoP trajectory and AP time series) is higher with the subjects eyes closed with respect to eyes open, both in young and elderly adults. Furthermore, the presence of a condition effect (open vs. closed eyes) is important to check the sensitiveness of a posturographic parameter, as suggested by Baratto et al. [13].

An interesting result highlighted by this new approach is that the mode value of the rotary spectra falls in the range 0.14-0.17 rps. The peak that is observed in this frequency range probably has a physiologically explainable meaning that was never documented before. I hypothesize that the mode value is due to the sympathetic rhythm. In fact, experiments performed on the muscle sympathetic nerve activity (MSNA), recording the electrical activity on the peroneal nerve at the fibula head (microneurography), demonstrated that the neural activity is clustered in series of

bursts that tend to occur with a periodicity of approximately 10 s. This was found in subjects standing upright [19] or almost upright (in a 75 head-up tilt, provided with a footrest) [20]. It is known that the sympathetic system modulates the spindles properties that, in turns, affect the static and dynamic behavior of muscles. This could explain the observation of rotational motions with cycle duration close to the periodicity of sympathetic bursts in upright posture.

Moreover, it was demonstrated that the MSNA mirrors spontaneous low-frequency (LF) fluctuations of blood pressure (Mayer waves) [20]. Pressure fluctuations could be another cause of perturbation of quiet standing.

Further support to the hypothesis that the sympathetic nervous system modulates postural sway is provided by a recent study [21] that relies on phasic stimulation of the carotid baroceptors to demonstrate the influence of the autonomic nervous system on posture.

Since the issue of the influence of the autonomic nervous system in balance could play an important role, further research is needed to fully understand the interrelations between autonomic activity and posture.

5.1.4 Conclusion

I investigated the hypothesis of presence of rotational components in the postural sway signal. I was able to demonstrate rotational components by applying rotary spectra technique to CoP signals of a population of healthy subjects. This approach provides a better understanding of the physiological mechanisms underlying postural control, since it evidences the presence of rotational components in the CoP signal. This cannot be obtained with traditional approaches that considers AP and ML times series separately. I hypothesize that rotary spectra peaks obtained in the study of postural control during upright standing are strictly correlated to the bursts of muscle sympathetic nerve activity. More research is needed to investigate possible clinical applications of this methodology and to deeply understand the physiological control mechanisms involved in maintaining upright posture.

Table 5.1: Rotary spectral parameters

		f25 (rps)	f50 (rps)	f75 (rps)	f95 (rps)	Mean frequency (rps)	Skewness	Mode (rps)	Power (mm^2/s)
OE	S^+	0.12 ±0.03	0.22±0.06	0.39±0.13	1.05±0.30	0.27±0.08	1.4±0.4	0.15±0.08	4.2±2.3
	S^-	0.12 ±0.04	0.23±0.07	0.40±0.14	1.03±0.31	0.27±0.08	1.3±0.4	0.14±0.09	4.2±2.6
CE	S^+	0.14 ±0.03	0.25±0.05	0.45±0.15	1.13±0.32	0.31±0.08	1.3±0.4	0.17±0.05	6.1±3.6
	S^-	0.14 ±0.03	0.26±0.06	0.46±0.18	1.12±0.34	0.31±0.09	1.2±0.4	0.16±0.07	6.2±3.7
t-test OE	S^+	*	*	*	-	*	-	-	*
vs. CE	S^-	*	-	-	-	-	-	-	*

Significant differences among open eyes (OE) and closed eyes (CE) conditions are marked with an asterisk:
* $p \leq 0.05$

5.2 Non stationary case

It has been demonstrated that CoP trajectories are non-stationary signals [22, 23]. Different methods have been applied to CoP trajectories to evaluate time varying characteristics: short time Fourier transform (STFT) [24], methods based on bilinear distributions [25, 26], evolutionary spectrum theory [27, 28], wavelet decomposition [29].

In this section I will present results of the extension to non-stationary case of the rotary spectra analysis applied to the CoP signals. The time-frequency analysis is based of the Cohen's class. In particular I applied the Choi-Williams transform.

The experimental trials, sample populations and acquisition system are the same described for the stationary case. Therefore, each acquisition lasted 60 seconds. The signals were recorded with a sampling frequency for 2kHz and then down-sampled to 20 Hz.

5.2.1 Signal processing

The mean value of CoPx and CoPy is subtracted from the respective time series. A high-pass filter with cut-off frequency equal to 0.05 Hz is then applied to the two time series in order to remove possible trend.

The time-frequency distribution for the CoPx and CoPy time series and the cross time-frequency distribution among the two time-series were calculated using Choi-Williams transform. The instantaneous auto-correlation functions for the single time-series and the instantaneous cross-correlation function were calculated using the alias free formulation. I considered a value of $f_s * T/2$ for the maximum time delay to formulate the auto and cross correlation instantaneous functions, where fs is the sampling frequency of 20 Hz and T is the recording duration (60 s).

Concerning the kernel selectivity, I considered three different values of σ (equation 3.33), equal to 0.1, 0.5, and 1, in order to evaluate the correct σ value, not too low, to avoid removing signal components, but also not too high, to avoid considering inference terms as components of the signal.

The calculated time-frequency distribution have been used in equation 3.35 to obtain the time frequency rotary spectra.

In order to evaluate the coherence between the two rotating components in the time-frequency plane, I calculated the parameter described in chapter 3 as the "stability

of the ellipse" μ_k, extending the formulation of equation 3.15 to the time-frequency domain.

5.2.2 Results

Kernel dimension

All the analyzed data presented similar time-frequency distributions. The time-frequency distribution of the rotational components of the center of pressure signal of a typical subject during eyes open trials is shown in figure 5.3, for different values of kernel σ. In particular, figure 5.3a and figure 5.3b show time-frequency distribution of the counter-clockwise and clockwise rotating components, respectively, calculated with a value of σ of 0.1. Analogously, figure 5.3c and figure 5.3d show time-frequency distributions calculated with a value of σ of 0.5, and figure 5.3e and figure 5.3f show time-frequency distributions calculated with σ equal to 1. Results are normalized with respect to the major amplitude of the two distributions, in order to compare them. It is possible to notice that there are not great differences in time frequency distributions calculated with different kernel dimensions, as changing the value of σ no main components appears or disappears. Therefore, in the following analysis, an intermediate value of 0.5 was applied.

Time- frequency distribution for a representative subject

Figure 5.4 shows time-frequency distribution of CCW and CW rotating components of a representative subject recorded during open-eye and closed-eye trials. Results are normalized with respect to the major amplitude of the four distributions, in order to compare them.

The time-frequency distributions confirm the hypothesis about the non-stationarity of the CoP signal.

I observe that, in the open-eye condition, the majority of the rotational components have frequency lower than 0.5 rps. In closed-eye trial the bandwidth is a higher, but always lower than 1 rps. In all the distributions there are few frequency components, which have the same frequency for all the time, but change their power contribution. I do not observe any chirp component.

In Fig. 1a) and 1b) there are two main rotating components, with frequencies approximately equal to 0.1 rps and 0.3 rps, respectively. These components, with

different power contribution, are present in almost all the examined time-frequency distribution.

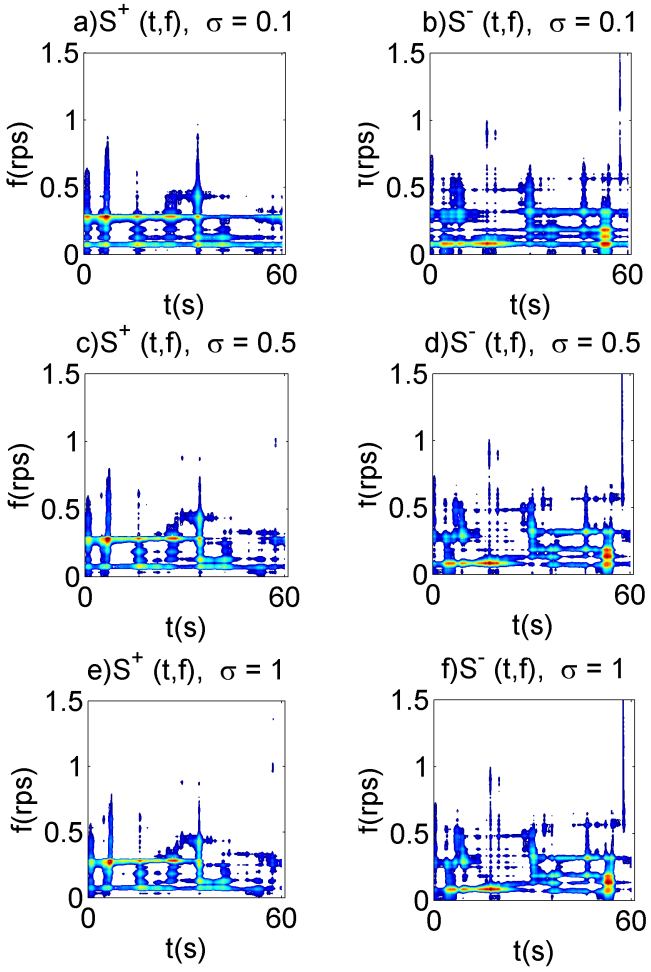

Figure 5.3: Time frequency distribution of rotating components in the CoP signal of a representative subject calculated with different dimensions of the Choi-Williams kernel. In particular: a) CCW components, σ equal to 0.1, b) CW components, σ equal to 0.1, c) CCW components, σ equal to 0.5, d) CW components, σ equal to 0.5, e) CCW components, σ equal to 1, f) CW components, σ equal to 1.

Stability of the ellipse

Figure 5.5 shows the contour plot of the parameter μ_k calculated in open eyes condition, for the same representative subject of previous figures. From the plot in the time-frequency domain I can notice that the common components are at low frequencies,

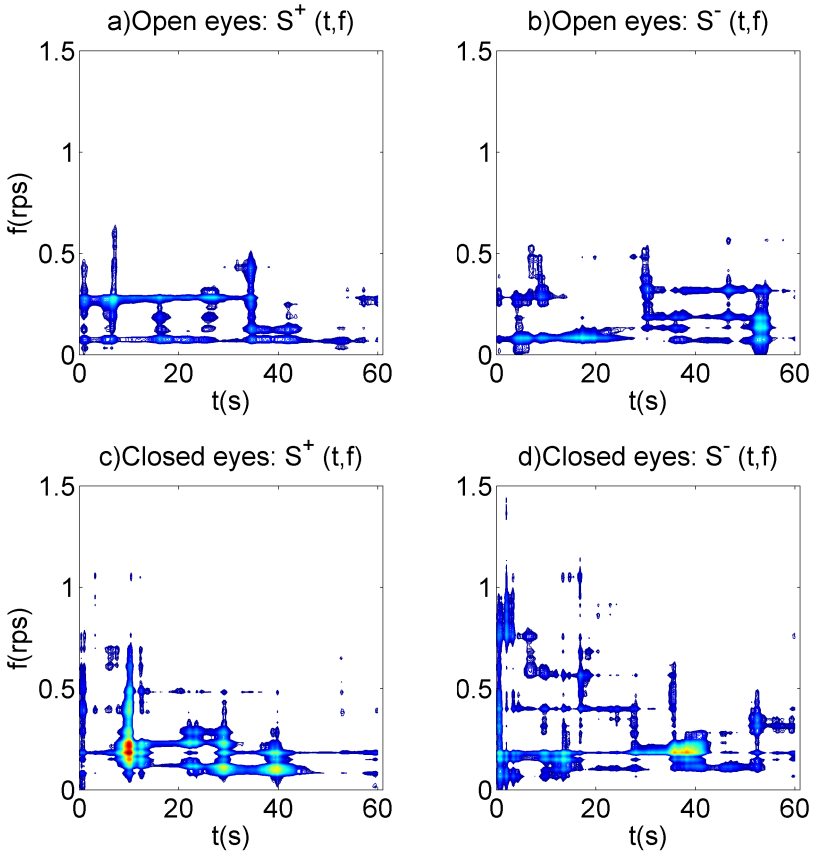

Figure 5.4: Time-frequency distribution of a) CCW rotary spectra in OE condition; b) CW rotary spectra in OE condition; c) CCW rotary spectra in CE condition; d) CW rotary spectra in CE condition.

and in particular at about 0.1 rps, for the first part of the acquisition (about from 0 to 30 seconds). Later in the acquisition it is still present, but not continuously as at the beginning.

Figure 5.6 shows the marginal of the time-frequency distribution of the stability of the ellipse. It is possible to notice that there are three main peaks, one at 0.08 rps, one at 0.13 rps, and another, smaller, one at 0.3 rps.

5.2.3 Discussion

All the described results on a single representative subject are similar considering the whole population. These results indicate that in most of the time-frequency

distributions there are few frequency components. No chirp components have been observed.

In almost all the time-frequency distributions it is possible to observe two main frequency components, not always continuous in time, one at about 0.1 rps and one at about 0.3 rps. As already described in the previous section in with marginals of the rotating components were evaluated, a possible explanation for the presence 0.1 rps component is a correlation with the sympathetic nervous activity. About the 0.3 rps contribute, it is possible to hypothesize that could be a breathing contribute [24]. Observing the marginal rotary spectra it was not possible to clearly identify this second frequency component.

In order to evaluate the frequency components simultaneously present in the CCW and CW rotary components, I calculated the stability of ellipse parameter. The findings confirm the presence of the previously described frequency components.

It is very difficult to analyse all the information arising from the time-frequency distribution of the CCW and CW components of a population of subjects. Therefore, I formulated an automatic method to interpret and classify time-frequency distribution, in order to better understand time-frequency characteristics of the rotational components of CoP signal.

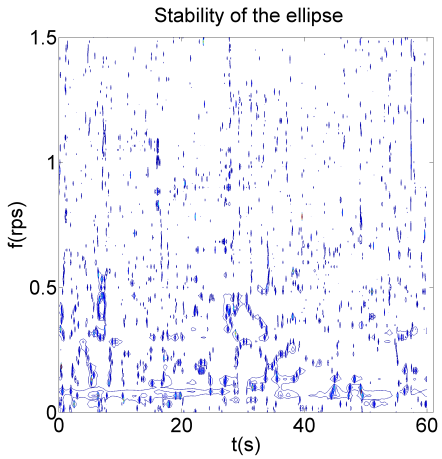

Figure 5.5: Time-frequency stability of the ellipse.

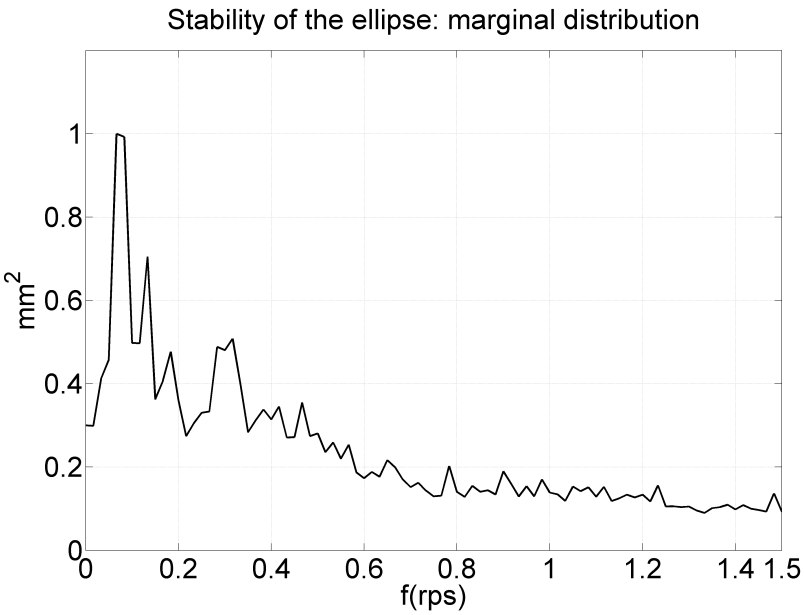

Figure 5.6: Marginal distribution of the stability of the ellipse.

5.3 Conclusions

I investigated the hypothesis of presence of rotational components in the postural sway signal, both considering the CoP signal to have a stationary and non-stationary behaviour. In both cases, the rotary spectra approach allowed to evidence the presence of rotational components in a population of healthy subjects. The importance of the method is that is provides a better understanding of the physiological mechanisms underlying postural control, considering the AP and ML series not separately but as components of a complex signal. Observing the marginals of the rotary spectra, I hypothesize that rotary spectra peaks are strictly correlated to the bursts of muscle sympathetic nerve activity.

The extension of the rotary spectra analysis to deal with the CoP as a non-stationary signal confirmed the previously obtained results. In addiction, the time-frequency approach indicated that in most of the time-frequency distributions there are few frequency components, which have the same frequency for all the time, but change their power contribution. No chirp components have been observed.

It is very difficult to analyse all the information arising from the time-frequency distribution of the CCW and CW components of a population of subjects. Therefore, in next chapter, I will apply unsupervised feature selection methods to better understand time-frequency characteristics of the rotational components of CoP signal.

References

[1] V. Agostini, E. Chiaramello, and M. Knaflitz, "Rotational components in center of pressure signals," *Motor Control*, (unpublished; passed the first stage of review).

[2] V. Krishnamoorthy, M. L. Latash, J. P. Scholz, and V. M. Zatsiorsky, "Muscle synergies during shifts of the center of pressure by standing persons.," *Exp Brain Res*, vol. 152, pp. 281–292, Oct 2003.

[3] J. W. Blaszczyk, R. Orawiec, D. Duda-K?odowska, and G. Opala, "Assessment of postural instability in patients with parkinson's disease.," *Exp Brain Res*, vol. 183, pp. 107–114, Oct 2007.

[4] H. Suarez, M. Arocena, A. Suarez, T. A. D. Artagaveytia, P. Muse, and J. Gil, "Changes in postural control parameters after vestibular rehabilitation in patients with central vestibular disorders.," *Acta Otolaryngol*, vol. 123, pp. 143–147, Jan 2003.

[5] M. Ferdjallah, G. F. Harris, P. Smith, and J. J. Wertsch, "Analysis of postural control synergies during quiet standing in healthy children and children with cerebral palsy.," *Clin Biomech (Bristol, Avon)*, vol. 17, pp. 203–210, Mar 2002.

[6] V. Agostini, E. Chiaramello, C. Bredariol, C. Cavallini, and M. Knaflitz, "Postural control after traumatic brain injury in patients with neuro-ophthalmic deficits.," *Gait Posture*, vol. 34, pp. 248–253, Jun 2011.

[7] P. Perrin, D. Deviterne, F. Hugel, and C. Perrot, "Judo, better than dance, develops sensorimotor adaptabilities involved in balance control," *Gait Posture*, vol. 15, pp. 187–194, Apr 2002.

[8] J. J. Collins and C. J. DeLuca, "Open-loop and closed-loop control of posture: a random-walk analysis of center-of-pressure trajectories.," *Exp Brain Res*, vol. 95, no. 2, pp. 308–318, 1993.

[9] V. M. Zatsiorsky and M. Duarte, "Rambling and trembling in quiet standing.," *Motor Control*, vol. 4, pp. 185–200, Apr 2000.

[10] A. Danna-Dos-Santos, K. Slomka, V. M. Zatsiorsky, and M. L. Latash, "Muscle modes and synergies during voluntary body sway.," *Exp Brain Res*, vol. 179, pp. 533–550, Jun 2007.

[11] G. Torres-Oviedo and L. H. Ting, "Muscle synergies characterizing human postural responses.," *J Neurophysiol*, vol. 98, pp. 2144–2156, Oct 2007.

[12] D. Winter, F. Prince, J. Frank, C. Powell, and K. Zabjek, "Unified theory regarding a/p and m/l balance in quiet stance.," *J Neurophysiol.*, vol. 75(6), pp. 2334–43., 1996.

[13] L. Baratto, P. G. Morasso, C. Re, and G. Spada, "A new look at posturographic analysis in the clinical context: sway-density versus other parameterization techniques.," *Motor Control*, vol. 6, pp. 246–270, Jul 2002.

[14] J. E. Visser, M. G. Carpenter, H. van der Kooij, and B. R. Bloem, "The clinical utility of posturography.," *Clin Neurophysiol*, vol. 119, pp. 2424–2436, Nov 2008.

[15] T. Robert, V. Zatsiorsky, M. Duarte, and M. Latash, "Rambling-trembling decomposition in two dimensions," in *Proceedings of the Annual Conference of the American Society of Biomechanics, Palo Alto, CA.*, 2007.

[16] T. E. Prieto, J. B. Myklebust, R. G. Hoffmann, E. G. Lovett, and B. M. Myklebust, "Measures of postural steadiness: differences between healthy young and elderly adults.," *IEEE Trans Biomed Eng*, vol. 43, pp. 956–966, Sep 1996.

[17] A. Bravi and A. M. Sabatini, "A multidimensional approach to postural sway modeling," in *Medical Measurements and Applications Proceedings (MeMeA), 2010 IEEE International Workshop on*, 2010.

[18] R. Balasubramaniam and M. Turvey, "The handedness of postural fluctuations," *Human Movement Science*, vol. 19(5), p. 667684, 2000.

[19] D. Burke, G. Sundlf, and G. Wallin, "Postural effects on muscle nerve sympathetic activity in man.," *J Physiol*, vol. 272, pp. 399–414, Nov 1977.

[20] R. Furlan, A. Porta, F. Costa, J. Tank, L. Baker, R. Schiavi, D. Robertson, A. Malliani, and R. Mosqueda-Garcia, "Oscillatory patterns in sympathetic neural

discharge and cardiovascular variables during orthostatic stimulus.," *Circulation*, vol. 101, pp. 886–892, Feb 2000.

[21] L. Bernardi, M. Bissa, G. DeBarbieri, A. Bharadwaj, and A. Nicotra, "Arterial baroreflex modulation influences postural sway.," *Clin Auton Res*, vol. 21, pp. 151–160, Jun 2011.

[22] J. P. Carroll and W. Freedman, "Nonstationary properties of postural sway.," *J Biomech*, vol. 26, no. 4-5, pp. 409–416, 1993.

[23] K. Newell, S. Slobounov, B. Slobounova, and P. Molenaar, "Short-term non-stationarity and the development of postural control," *Gait Posture*, vol. 6, pp. 56–62, 1997.

[24] S. Conforto, T. DAlessio, V. Camomilla, and A. Cappozzo, "Time-frequency analysis of postural signals," in *Abstracts from the 1st SIAMOC Congress, Ancona, Italy*, 2001.

[25] P. J. Loughlin and M. S. Redfern, "Spectral characteristics of visually induced postural sway in healthy elderly and healthy young subjects.," *IEEE Trans Neural Syst Rehabil Eng*, vol. 9, pp. 24–30, Mar 2001.

[26] Y.-J. Shin, D. Gobert, S.-H. Sung, E. J. Powers, and J. B. Park, "Application of cross time-frequency analysis to postural sway behavior: the effects of aging and visual systems.," *IEEE Trans Biomed Eng*, vol. 52, pp. 859–868, May 2005.

[27] T. Schumann, M. S. Redfern, J. M. Furman, A. el Jaroudi, and L. F. Chaparro, "Time-frequency analysis of postural sway.," *J Biomech*, vol. 28, pp. 603–607, May 1995.

[28] M. Ferdjallah, G. F. Harris, and J. J. Wertsch, "Instantaneous postural stability characterization using time-frequency analysis.," *Gait Posture*, vol. 10, pp. 129–134, Oct 1999.

[29] J. R. Chagdes, S. Rietdyk, J. M. Haddad, H. N. Zelaznik, A. Raman, C. K. Rhea, and T. A. Silver, "Multiple timescales in postural dynamics associated with vision and a secondary task are revealed by wavelet analysis.," *Exp Brain Res*, vol. 197, pp. 297–310, Aug 2009.

6

Automatic classification of CoP signals based on time-frequency distributions of rotational components

In this work I developed a method to automatically analyze TF properties of rotational components in the COP signals, and applied it to a population of healthy subjects.

Firstly, TF rotary spectra analysis is performed for each COP signal, obtaining two TF plots, one for the counter-clockwise and one for clockwise rotating components. Then, several features are extracted, identifying the main frequency components of the TF distributions. Finally, a clustering algorithm was applied to the whole data set to find similarities and dissimilarities in the population.

I obtained a classification in 5 different groups, each characterized by few features which described the TF plots of the group. I was able to identify 5 types of recurrent behaviors in terms of frequency components characteristics in the population of healthy subjects.

6.1 Introduction

In last chapters I proposed to analyze posturographic signals using the rotary spectra analysis technique, to assess rotational components in the Centre of Pressure (COP) signals [1].

6. AUTOMATIC CLASSIFICATION METHOD BASED ON TF DISTRIBUTIONS

As previously observed, the CoP signal is non-stationary [2]. To better understand the time-varying nature of the postural control system, it is interesting to analyze CoP signal considering temporal dynamics of postural sway [3, 4]. To analyze non-stationary characteristics of rotational components of the COP signal, I applied time-frequency analysis in the development of rotary spectra formulation (see chapter5). I obtained time-frequency distributions of rotating components of COP signals in a population of healthy subjects. To the best of my knowledge, no previous work in literature described these time-frequency distributions.

The rationale of this chapter is the problem of analyzing and interpreting information carried on by the calculated time-frequency distributions of the rotational components in the COP signals.

My interest is to describe each time-frequency plot according to some characteristics, defined starting from physiological observations about the maintenance of postural control in the upright position. In particular, I am interested in investigating about the presence of two frequency components, in the range of 0.1-0.2 rps and 0.3-0.4 rps, respectively. As observed in [1], the rotary spectra marginals peaks in the range of 0.1-0.2 rps could be strictly correlated to the bursts of muscle sympathetic nerve activity, as it was known to modulate postural sway [5]. Analogously, it was observed that respiration has a significant effect on the maintenance of equilibrium [6], therefore a rotational component with higher frequency values, around 0.3 rps, could be related to respiration effect. Examining these frequency components in time-frequency domain allows to evaluate their time duration, helping in better understanding of physiological mechanisms under postural control.

Starting from time-frequency plots of a population of healthy subjects, and their description in terms of frequency components, I am interested in clustering them, in order to find similarities and dissimilarities.

The task of examining each time-frequency distribution manually is challenging because of the huge amount of data and the great dependence on the researcher. Therefore, I created an automatic method to analyze and interpret information carried on by the whole group of time-frequency plots.

Many works in literature describe automatic methods of feature extraction and classification of signals based on time-frequency plots, in different fields e.g. seizure detection in EEG signals [7, 8], classification of myoelectric signals [9], automatic

speech recognition [10]. However, in all these works, the effort of the authors is to detect already known characteristics in time-frequency plots. My starting point is completely different, as I am interested not just in developing a method to recognize elements, but in automatically analyzing time-frequency plots in order to extract information without a priori knowledge.

In this work I developed a method to automatically analyze time-frequency properties of rotational components in the COP signals. Firstly, time-frequency rotary spectra analysis is performed for each COP signal, obtaining two time-frequency plots, one for the counter-clockwise and one for clockwise rotating components. Then, several features are extracted, identifying the main frequency components of the time-frequency distributions. Finally, a clustering algorithm was applied to the whole data set to find similarities and dissimilarities in the population.

6.2 Materials and methods

Fig.6.1 shows a scheme of the proposed method. Below the three main steps, i.e. time frequency analysis, feature extraction, and clustering, are described. Moreover, the data set of COP signals is illustrated.

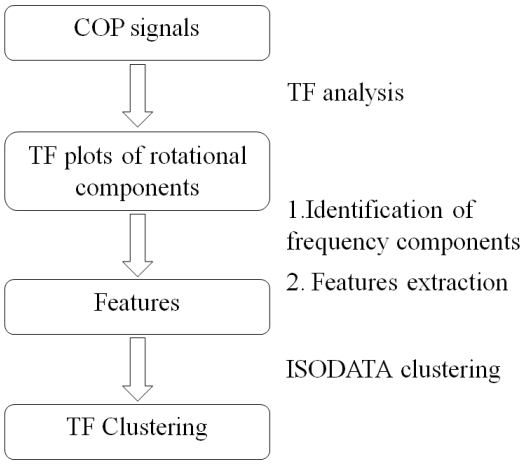

Figure 6.1: Flow chart of the proposed method

Time Frequency Analysis of rotational components

The description about time frequency analysis of rotational components of COP signals have been previously explained in chapter 3 and 4.

Feature Extraction

The first step to describe time-frequency plot in terms of its frequency components is to automatically identify them. The method I applied, similarly to the one proposed in [11], was based on region growing [12], an image processing technique to obtain segmentation. The first step in the technique is to select a set of seed points. Seed points selection is based on a first amplitude threshold, T1. The initial region begins as the exact location of these seeds. The regions are then grown from these seed points to adjacent points depending on a second amplitude threshold, T2. Both amplitude thresholds have been defined starting from the histogram of the pixels amplitudes, after normalizing the distribution values between 0 and 1. More specifically, if the statistical mode of the histogram was lower than 0.3, T1 and T2 were set equal to 0.35 and 0.28, respectively. If the mode of the histogram was between 0.3 and 0.5, T1 and T2 were set equal to 0.68 and 0.35, respectively. Finally, if the mode of the histogram was higher than 0.7, T1 and T2 were set equal to 0.85 and 0.45, respectively. These values of threshold were defined in order to segment as best as possible all the frequency components. Figure 6.2 exemplifies the three cases.

Figure 6.3 shows a representative case of the time-frequency distribution segmentation. Segmenting each frequency component, we were able to automatically find its characteristics of frequency, amplitude and time duration.

The second step is the definition of a set of features. As I am interested in investigating about presence and characteristics of components with frequency in the range of 0.1-0.2 rps and 0.3-0.4 rps, I divided the time-frequency plane in 3 different frequency bands of interest, one from 0 to 0.2 rps, one from 0.21 rps to 0.3 rps, and the last one from 0.31 to 0.5 rps. In each of these bands, I explored how many frequency components were present, how long did they last and what was their energy. The time duration of the frequency components have been divided in 3 classes, short, if shorter than 30 s, medium if longer than 30 s and shorter than 50 s, and long if present for at least 50 s. Analogously, the amplitude of the component is low, medium, or high if it

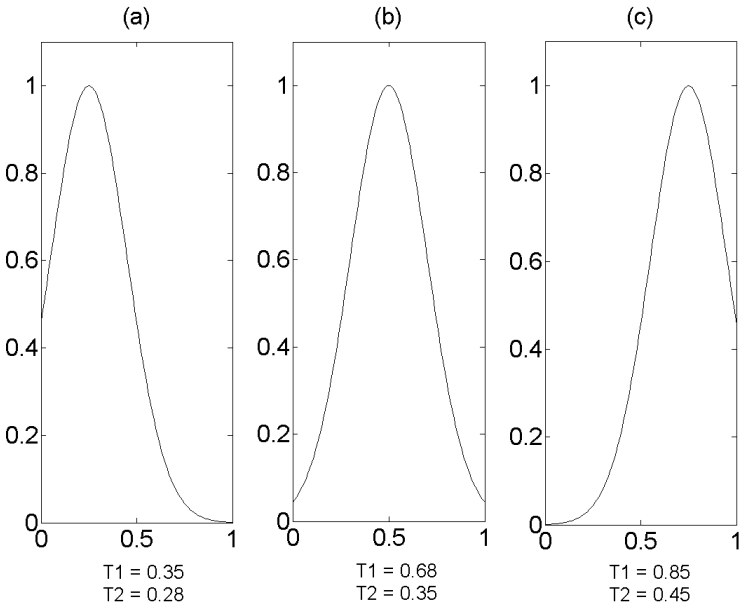

Figure 6.2: Amplitude thresholds for region growing, depending on the statistical mode of the pixel amplitude histogram. I differentiated three cases: (a) representative of histograms with mode lower than 0.3, (b) representative of histograms with mode between 0.3 and 0.5, and (c) representative of histograms with mode higher than 0.7.

contains, respectively, less than 30%, between 30% and 60%, or more than 60% of the total energy of the signal.

It is important to notice that the information about the energy of each components is considered as a fractional part of the whole energy of the signal. In this way, information about the absolute value of energy of each time-frequency distribution is discarded, as I am interested to describe each time-frequency in terms of frequency components and not in terms of absolute amplitude.

Therefore, I defined 27 different features, summarized in table 6.1.

Clustering

The clustering algorithm we applied is Iterative Self-Organizing Data Analysis Technique (Algorithm) (ISODATA) [13]. ISODATA is an unsupervised iterative algorithm of classification. Firstly it performs a k-means clustering [14], then splits any cluster whose samples are sufficiently dissimilar and merges any two clusters which are sufficient close. The procedure is iterative, and requires the user to define a number of

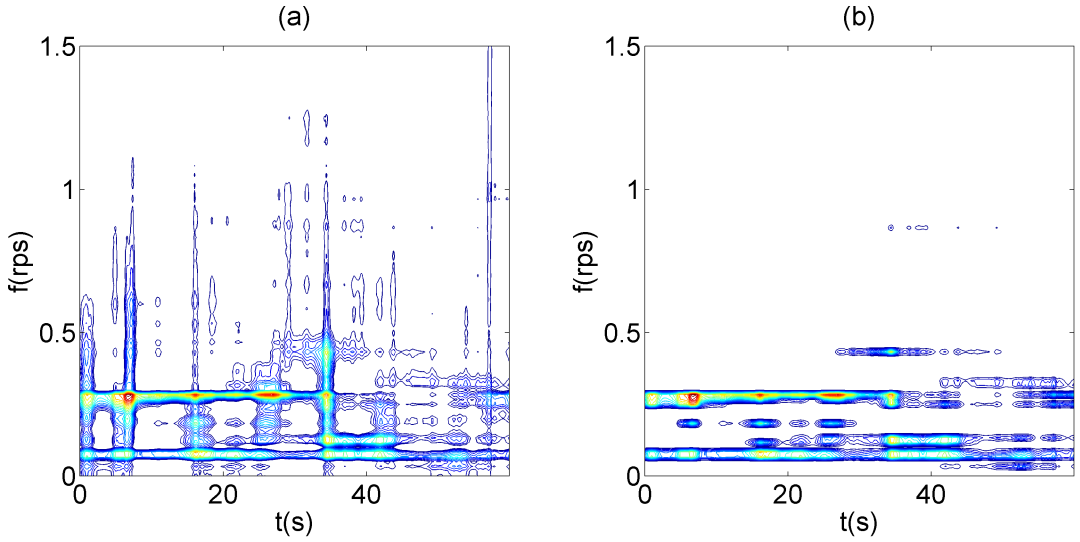

Figure 6.3: Contour plot of the time-frequency distribution of a representative subject (a) before and (b) after the segmentation of the main frequency components.

parameter, listed below.

- N_{min_EX}: minimum number of examples for each cluster. I set it equal to 8.
- N_D: approximately, desired number of clusters. I set it equal to 4.
- σ_S^2: maximum spread parameter for splitting. I set it equal to 4.
- D_{merge}: maximum distance separation for merging. I set it equal to 8.
- N_{merge}: maximum number of clusters that can be merged. I set it equal to 3.

A quick description of the main steps of the ISODATA algorithm is:

1. Select an initial number of clusters N_C and use the first N_c examples as clusters centers μ_k, k =1,...,N_C
2. Assign each example to the closest cluster
   (a) Exit the algorithm if the classification of examples has not changed
3. Eliminate clusters that contain less than N_{min_EX} examples and assigning their examples to the remaining clusters based on the minimum distance. Decrease N_C accordingly.

Table 6.1: List of features

Frequency	Amplitude	Time duration	Features
$0 \leq f < 0.2$ rps	High amplitude	$t \geq 50$ s	F1
		$30 \leq t < 50$ s	F2
		$t < 30$ s	F3
	Medium amplitude	$t \geq 50$ s	F4
		$30 \leq t < 50$ s	F5
		$t < 30$ s	F6
	Low amplitude	$t \geq 50$ s	F7
		$30 \leq t < 50$ s	F8
		$t < 30$ s	F9
$0.2 \leq f < 0.5$ rps	High amplitude	$t \geq 50$ s	F10
		$30 \leq t < 50$ s	F11
		$t < 30$ s	F12
	Medium amplitude	$t \geq 50$ s	F13
		$30 \leq t < 50$ s	F14
		$t < 30$ s	F15
	Low amplitude	$t \geq 50$ s	F16
		$30 \leq t < 50$ s	F17
		$t < 30$ s	F18
$0.5 \leq f$ rps	High amplitude	$t \geq 50$ s	F19
		$30 \leq t < 50$ s	F20
		$t < 30$ s	F21
	Medium amplitude	$t \geq 50$ s	F22
		$30 \leq t < 50$ s	F23
		$t < 30$ s	F24
	Low amplitude	$t \geq 50$ s	F25
		$30 \leq t < 50$ s	F26
		$t < 30$ s	F27

4. For each cluster:

   (a) Compute the center μ_k as the sample mean of all the examples assigned to the cluster

(b) Compute the average distance between examples and clusters centers

(c) For each cluster, compute the variance of each axis and find the axis n* with maximum variance $\sigma_k^2(n*)$

5. Split clusters with $\sigma_k^2(n*) > \sigma_S^2$, if their average distance is higher than the medium of distances or if $N_c < N_D$. Increment N_C accordingly and reassign the cluster's examples to one of the new clusters based on the minimum distance to cluster centers.

6. If $N_C > 2N_D$, merge clusters that with reciprocal distance lower than D_{merge}. Decrement N_C accordingly and compute the new cluster center.

7. Go to step 2.

It is important to notice that in the defined parameter I indicated a desired number of clusters that is not the exact number of clusters that the algorithm has to reach, but it is only an indication about the order of magnitude.

Each example of my population of time-frequency distributions was a vector with 27 elements, each for one feature.

Data set

The sway path was investigated on a group of 42 healthy volunteers, who did not suffer from orthopedic, neurological or visual problems. Subjects were asked to stand quietly, in upright position, over a force platime-frequencyorm. The acquisition protocol consisted of two randomized conditions with eyes open (OE) and closed (CE), respectively. The experimental setup consisted of a Kistler 9286A (Kistler, Switzerland) force platime-frequencyorm and of an acquisition system STEP32 (DemItalia, Italy). Each acquisition lasted 60 s. The signals were recorded with a sampling frequency of 2 kHz and down-sampled to 20 Hz.

Signal Processing

The rotary spectra analysis is applied to the sway path orthogonal components on the force platime-frequencyorm plane COPx and COPy. The mean value of COPx and COPy is subtracted from the respective time series. A high-pass filter with cut-off frequency equal to 0.05 Hz is than applied to the two time series in order to remove

possible trends. I extended the rotary analysis to time-frequency domain, applying a Choi-Williams kernel with σ equal to 0.5, to obtain the time-frequency rotary spectra S^{+}(t,f) and S^{-}(t,f). I applied the method to all the calculated time-frequency distribution. I examined both the clustering obtained from the whole group of time-frequency plots, and the classifications obtained considering OE and CE acquisition separately.

6.3 Results

Applying the time-frequency analysis to the COP signals of the whole population of healthy subjects, I obtained a total of 168 time-frequency plots.

After extracting features and clustering the whole set of time-frequency, I obtained 5 groups. The first group contains 15 time-frequency plots, the second 57 time-frequency plots, the third 33 elements, the fourth 27 elements, and the fifth 36 elements. Fig.6.4 shows how the features (columns) are distributed in the 5 groups (rows). Each cell shows the number of times in which the feature is present in the group normalized on the number of elements. The lighter the cell, the more frequent the feature in the group.

Each group has few features which are representative of the characteristics of the cluster, and these main features are never in common between different groups. The first group shows a strong presence of features F5 and F18. The second group is represented by features F1 and F2. The third group is characterized by feature F3. The fourth group is characterized by features F4 and F17. The last group is characterized by features F6, F14 and F15. There are no groups in which features from F19 to F27, representative of components with frequency higher than 0.5 rps, show a strong presence.

Table 6.2 shows the distribution of time frequency plots of CoP signals recorded in OE and CE conditions in the 5 groups obtained with the ISODATA clustering. Applying a Pearson's χ^2 test, I obtained a probability of $p = 0.68$, so it is not possible to reject the null hypothesis. Therefore it is possible to say that in the described 5 groups the time-frequency plots of COP signals recorded in OE and CE condition are equally distributed.

Figure 6.5 shows results of clustering of time-frequency plots recorded in OE (fig.6.5a) and CE (fig.6.5b) conditions. In both cases I obtained 4 clusters. In OE condition, the groups contains 20, 22, 18, and 24 elements, respectively. In CE condition, the groups

a

Table 6.2: Distribution of OE and CE conditions in the obtained clustered

	Group 1	Group 2	Group 3	Group 4	Group 5
OE	8	30	18	14	14
CE	7	27	15	13	22

contains 21, 22, 9, and 32 elements, respectively. Analogously to figure 6.4, each group is characterized by few features, and there are not groups described by the same main feature. The distributions of the features in the four groups in OE and CE conditions look very similar. In OE condition the main features for each group are: F3, F6 and F15 for the first group, F2 for the second group, F4, F5, and F14 for the third group, and F1 for the fourth group. Analogously, in CE condition the main features for each group are: F6 and F15 for the first group, F2 for the second group, F14 for the third group, and F1 for the fourth group. Both in OE and CE conditions there are not groups with a strong presence of features from F19 to F27.

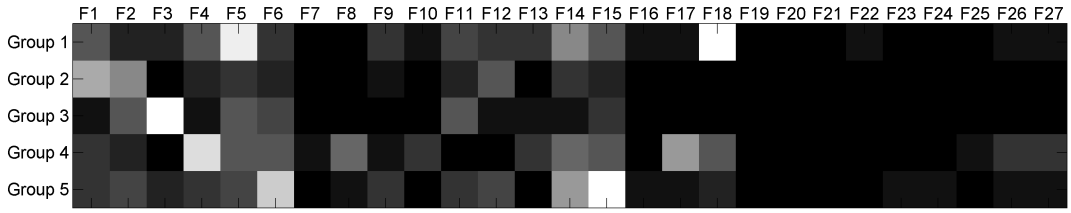

Figure 6.4: Results of the clustering algorithm applied to time-frequency distributions of the whole population. Each row shows a group, each column shows a feature. Each cell displaces the number of times in which the feature is present in the group, normalized on the number of element of the group. There are 16 gray levels.

6.4 Discussion

Rotary components in the time-frequency domain could be considered as multi-component separable signals, as their components are clearly separated in the time-frequency domain, accordingly to the definition described by Rankine et al. in [11]. Therefore, I defined 27 features to describe each time-frequency plot in terms of its

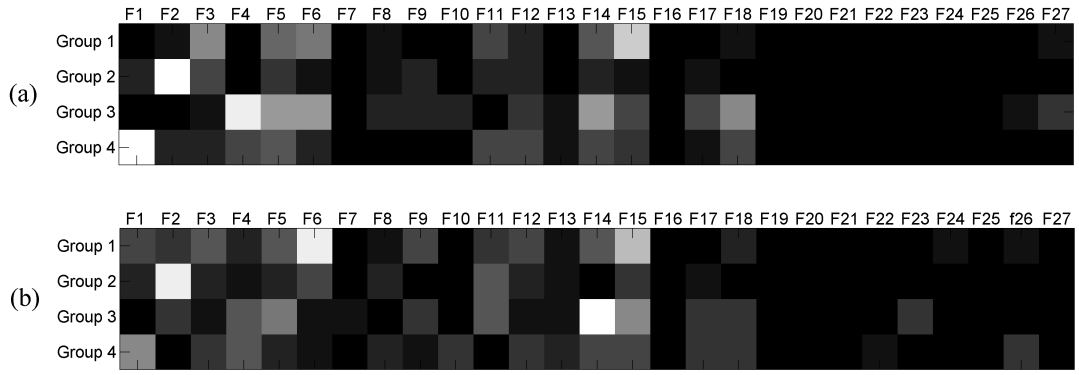

Figure 6.5: Results of the clustering algorithm applied to TF distribution of the COP signals recorded in (a) OE condition and (b) CE condition. Each row shows a group, each column shows a feature. Each cell displaces the number of times in which the feature is present in the group, normalized on the number of element of the group. There are 16 gray levels.

frequency components. These features were formulated to individuate the presence of rotational components with a physiological meaning.

Clustering all the 168 time-frequency plots calculated on the whole population of healthy subjects I found 5 well separated groups. Each of them was characterized by a few number of features. The time-frequency distributions were separated according to these features, so I can consider them as main characteristics of each group. This means that I am able to identify 5 types of recurrent behaviors in terms of frequency components characteristics in the population of healthy subjects.

All the detected groups have a strong characterization in terms of low frequency components. This result is coherent to the findings previously described in [1]. My hypothesis about the presence of this rotational components is a strictly correlation between rotational components of the COP signal and the bursts of muscle sympathetic nerve activity.

Examining the time-frequency distribution of the rotation components I was able to investigate how long this low frequency component was. In both groups 2 and 3 the characterizing features are those representing the presence of components with frequency between 0 and 0.2 rps, high amplitude, and time duration longer than 30 s, for group 2, and shorter than 30 s, for group 3. Therefore, the main characteristic of

50% of the time-frequency plots is the presence of a low frequency component, but for group 2 the most frequent behavior is a continuous component, while in group 3 there are shorter components. This can distinguish two different patterns of activation of the muscle sympathetic nerve.

In the other groups the characterization in terms of low frequency components still exists, but I also observed higher frequency components, in the range of 0.2-0.5 rps. Group 1, 4 and 5 appear similar as they have a low frequency component with medium amplitude and different time duration which can highlight different patterns of activation of the muscle sympathetic nerve, and a higher frequency component, with medium or low time duration.

It is well known that visual deprivation influences postural sway, and that the total path of the COP is longer in CE than in OE conditions [15, 16]. This means that the energy of the COP signal in CE condition is higher than in OE conditions. However, in the described 5 groups the time-frequency plots of COP signals recorded in OE and CE condition are equally distributed. This is not surprising, as in my description I considered the energy of each components as a fractional part of the whole energy of the signal, discarding information about the absolute value of energy of each time-frequency distribution. The reason for this choice was that we were interested in finding similarities and dissimilarities between time-frequency plots in terms of frequency components, and there were no reasons to hypothesize differences in rotational components between OE and CE conditions.

In OE and CE conditions I found 4 groups, while considering the whole data set of time frequency distributions I obtained 5 groups. This is not surprising, as ISODATA algorithm merges and splits clusters based on the number of their examples, and based on the desired number of groups. Considering OE and CE conditions separately, I clustered a lower number of time frequency distributions, therefore I obtained a lower number of groups. However, in both conditions, I observed that the four are characterized by the same features. In particular, in OE condition the second and the fourth groups are characterized by the presence of a low frequency component with long time duration and high amplitude. Analogously, the first and the third groups show both a low frequency component and another component in the range 0.2-0.5 rps. In CE condition the results are quite similar.

The results are very similar, confirming the results obtained considering the whole data set together.

I obtained no groups, both examining the whole population and considering OE and CE separately, in which there are components with frequency higher than 0.5 rps. This confirm my hypothesis about the importance of components with frequency lower than 0.5 rps in describing rotational characteristics of the CoP signals.

6.5 Conclusion

I developed an automatic method to analyze and classify COP signals based on a time-frequency distribution of their rotational components and applied it to a population of healthy subjects. This automatic method allowed to analyze in quick and repeatable way a high number of time-frequency plots, extracting useful information to better highlight time-frequency characteristics of COP rotational components.

However, the proposed method is strictly based on the analyzed problem, as the set of features was defined starting from physiological observations about postural control. A different definition of the features could allow to face different time-frequency distribution related to other signals, with similar characteristics to the described one.

References

[1] E. Chiaramello, M. Knaflitz, and V. Agostini, "Rotary spectra analysis applied to static stabilometry.," *Conf Proc IEEE Eng Med Biol Soc*, vol. 2011, pp. 4939–4952, 2011.

[2] J. P. Carroll and W. Freedman, "Nonstationary properties of postural sway.," *J Biomech*, vol. 26, no. 4-5, pp. 409–416, 1993.

[3] T. Schumann, M. S. Redfern, J. M. Furman, A. el Jaroudi, and L. F. Chaparro, "Time-frequency analysis of postural sway.," *J Biomech*, vol. 28, pp. 603–607, May 1995.

[4] S. Conforto, T. DAlessio, V. Camomilla, and A. Cappozzo, "Time-frequency analysis of postural signals," in *Abstracts from the 1st SIAMOC Congress, Ancona, Italy*, 2001.

[5] L. Bernardi, M. Bissa, G. DeBarbieri, A. Bharadwaj, and A. Nicotra, "Arterial baroreflex modulation influences postural sway.," *Clin Auton Res*, vol. 21, pp. 151–160, Jun 2011.

[6] M. Schmid, S. Conforto, D. Bibbo, and T. D'Alessio, "Respiration and postural sway: detection of phase synchronizations and interactions.," *Hum Mov Sci*, vol. 23, pp. 105–119, Sep 2004.

[7] A. T. Tzallas, M. G. Tsipouras, and D. I. Fotiadis, "Automatic seizure detection based on time-frequency analysis and artificial neural networks.," *Comput Intell Neurosci*, p. 80510, 2007.

[8] H. Hassanpour, M. Mesbah, and B. Boashash, "Time-frequency feature extraction of newborn eeg seizure using svd-based techniques," *EURASIP Journal on Applied Signal Processing*, vol. 16, p. 25442554, 2004.

[9] K. Englehart, B. Hudgins, P. A. Parker, and M. Stevenson, "Classification of the myoelectric signal using time-frequency based representations.," *Med Eng Phys*, vol. 21, no. 6-7, pp. 431–438, 1999.

[10] A. Potamianos and P. Maragos, "Time-frequency distributions for automatic speech recognition," *IEEE Trans on Speech and Audio Processing*, vol. 196-200, p. 2001, 9(3).

[11] L. Rankine, M. Mesbah, and B. Boashash, "If estimation for multicomponent signals using image processing techniques in the timefrequency domain," *Signal Processing*, vol. 87(6), p. 12341250, 2007.

[12] R. Adams and L. Bischof, "Seeded region growing," *IEEE Trans on pattern analysis and machine intelligence*, vol. 16(6), pp. 641– 647, 1994.

[13] G. H. Ball and D. J. Hall, "A clustering technique for summarizing multivariate data.," *Behav Sci*, vol. 12, pp. 153–155, Mar 1967.

[14] T. Liao, "Clustering of time series dataa survey," *Pattern recognition*, vol. 38, p. 1857 1874, 2005.

[15] L. Baratto, P. G. Morasso, C. Re, and G. Spada, "A new look at posturographic analysis in the clinical context: sway-density versus other parameterization techniques.," *Motor Control*, vol. 6, pp. 246–270, Jul 2002.

[16] T. E. Prieto, J. B. Myklebust, R. G. Hoffmann, E. G. Lovett, and B. M. Myklebust, "Measures of postural steadiness: differences between healthy young and elderly adults.," *IEEE Trans Biomed Eng*, vol. 43, pp. 956–966, Sep 1996.

7

Conclusions

In this dissertation I faced the problem of analyzing CoP signals recorded in quiet standing with different strategies.

I applied geometrical parameters in describing the CoP signals to analyze differences between groups of pathological and healthy subjects. A new acquisition protocol was proposed, and it was demonstrated that it could help in highlighting specific characteristics of each subject.

I proposed a new approach to analyze posturographic signals, based on the hypothesis that the CoP signal contains rotational components. To verify this hypothesis and to extract rotational components from the CoP signal I applied the rotary spectra analysis, a technique firstly developed in the oceanographic field, but which was never applied in analyzing biological signals. This method demonstrated the presence of rotational components in CoP signals of a population of healthy subjects. Moreover an interesting result was that the mode value of the rotary spectra fell in the range 0.14-0.17 rps. The peak that was observed in this frequency range probably has a physiologically explainable meaning that was never documented before. I hypothesized that rotary spectra peaks obtained in the study of postural control during upright standing are strictly correlated to the bursts of muscle sympathetic nerve activity.

Since the CoP signal is not strictly stationary, the classical rotary spectra theory was extended to deal with non-stationary signals. In particular, I applied bilinear Choi-Williams time-frequency distribution to obtain time-frequency analysis of rotating components. This allowed evaluating rotational characteristics of the CoP signal in the time-frequency plane.

As interpretation and classification of a large number of time-frequency distributions could be difficult, time expensive, and highly depending on the researcher, I developed an automatic analysis method, which allowed to obtain a fast and repeatable description of each distribution in terms of frequency components. Applying a clustering algorithm, I was able to find similarities and dissimilarities among the time-frequency plots of the healthy population, individuating main characteristics.

In conclusion, all the followed strategies gave satisfactory results. The proposed protocol and the evaluation of geometrical parameters allowed highlighting differences between groups of pathological and healthy subjects. I proposed a new approach in analyzing CoP signal in terms of rotational components, which gave interesting results on a group of healthy subjects. The technique was extended to time-frequency domain and an automatic analysis method of time-frequency distribution was developed.

The most innovative aspect of this work, the rotary spectra analysis, both in stationary and non-stationary cases, is complementary to other approaches described in literature to study the CoP signal, and could contribute in reaching better understanding of the physiological mechanisms underlying postural control.

An interesting future work will be required to investigate the hypothesis about the correlation between characteristics of the rotational components in the CoP signal and the muscle sympathetic nerve activity. The analysis could be carried on examining both CoP signals and electrocardiographic signals recorded simultaneously on a subject during quiet standing. It would be interesting to analyze the correlation between heart rate variability and rotary spectra of the CoP signals in the time-frequency domain.